

# A Self-Consistent Theory of Steady-State Lamellar Solidification in Binary Eutectic Systems

G. E. NASH

*Transformations and Kinetics Branch  
Material Sciences Division*

February 9, 1976



**NAVAL RESEARCH LABORATORY**  
**Washington, D.C.**

Approved for public release; distribution unlimited.





20. Abstract (Continued)

Using the information obtained from the analysis, an approximate theory of the lamellar-rod transition is formulated. The predictions of the theory are shown to be in qualitative agreement with experimental observations of this transition. In addition a simplified version of the general integro-differential equations is developed and used both to assess the effect of interface curvature on the interfacial solute concentrations and to check the new theory for consistency with experiment.

## CONTENTS

1.	INTRODUCTION	1
2.	MATHEMATICAL FORMULATION	8
	2.1 Formulation of the Boundary-Value Problem	8
	2.2 Some Comments on the Analysis	17
3.	A FORMAL SOLUTION OF THE FREE BOUNDARY PROBLEM	21
	3.1 Chemical Diffusion	21
	3.1.1 The potential theoretic method	21
	3.1.2 Implementation of the potential theoretic method	24
	3.2 Thermal Diffusion	36
	3.2.1 The "fictitious source" method	37
	3.2.2 Implementation of the fictitious source method	39
	3.3 Construction of the Formal Solution	48
4.	SOME ASPECTS OF THE BEHAVIOR OF SYSTEM I	55
	4.1 A Qualitative Analysis of System I and Its Implications	55
	4.1.1 The torque at the triple point	55
	4.1.2 A qualitative examination of System I	56
	4.1.3 The implications of the analysis	62
	4.2 Asymptotic Estimates as $\omega \rightarrow 0$	64
	4.3 On the Existence or Nonexistence of Solutions to System I for $\omega_{\infty} = 0$	68

4.3.1	Integration of equation (75) for large values of $\mu$	69
4.3.2	Integration of equation (75) for arbitrary values of $\mu$	73
4.3.3	A physical interpretation of the results	79
4.4	An Approximate Version of System I	82
4.4.1	The approximate equations	82
4.4.2	An important property of System II	88
5.	NUMERICAL RESULTS AND COMPARISON WITH EXPERIMENTAL DATA	90
5.1	Numerical Procedures and Results	90
5.1.1	A procedure for solving System II	90
5.1.2	Validation of the numerical procedures	92
5.1.3	Sensitivity of the solution of equation (73) to interface shape changes and comparison to the Jackson-Hunt solution	94
5.1.4	Some typical numerical results	101
5.2	Comparison with Experimental Data and Previous Theoretical Results	101
5.2.1	A procedure for assessing the theory	104
5.2.2	Estimation of $\alpha_1$ , $\alpha_3$ , $\alpha_4$ , and $\psi_{op}$	105
5.2.3	Comparison of theory with experiment	109
5.2.4	Comparison with the theory of Jackson and Hunt	114
	SUMMARY AND CONCLUSIONS	116
	REFERENCES	120

APPENDIX A - Derivation of the Explicit Form of the Single-Layer Potential	123
APPENDIX B - The Indeterminacy Associated with the Solute Concentration Field	132
APPENDIX C - Derivation of Equation (62)	137
APPENDIX D - A description of the Computer Program for Solving System II	145



A SELF-CONSISTENT THEORY OF STEADY-STATE LAMELLAR  
SOLIDIFICATION IN BINARY EUTECTIC SYSTEMS

UNCLASSIFIED

I. INTRODUCTION

It has been known for some time that many binary eutectic alloys, when solidified unidirectionally, develop a lamellar microstructure consisting of alternate layers of  $\alpha$  and  $\beta$  phase crystals with the lamellar phases aligned parallel to the solidification direction. Because of the fine-scale distribution of these aligned eutectic structures and their inherent stability at elevated temperatures, these alloys possess excellent high-temperature load-bearing capabilities and show great promise for supplementing and/or replacing the conventional nickel-based super alloys currently being used in naval aircraft engine components.

Although the feasibility of producing a wide variety of technically interesting eutectic systems has been amply demonstrated, no satisfactory theory has been available for rationally predicting the characteristic structures produced by unidirectional solidification.

The first systematic theoretical investigation of lamellar solidification in binary eutectic systems was that of Tiller [1]. Tiller went

---

Manuscript submitted November 13, 1975.

through a rather careful dimensional analysis and concluded that a freezing rate-lamellar spacing relation of the form  $V\lambda^2 = \text{const.} = C$  ( $V$  being the freezing rate and  $\lambda$  the lamellar spacing) should apply. His solution, however, was incomplete in the sense that unknown shape factors were involved in the calculation of the constant  $C$ . Somewhat later Jackson and Hunt [2] attempted to eliminate the unknown shape factors in Tiller's analysis by utilizing an exact solution of the chemical diffusion equation for a planar solid/liquid interface. Since, in general, the solid/liquid interface is non-planar, the Jackson-Hunt approach was not entirely successful in remedying the deficiency in Tiller's analysis.

The aforementioned investigators were severely hampered in their efforts by the lack of a suitable method for solving the diffusion equation in a domain bounded by an arbitrarily shaped solid/liquid interface. Colin, et al. [3], in an attempt to resolve this difficulty, proposed a method for obtaining the required solutions based on eigenfunction expansion techniques. Such methods,

however, usually work well only when the boundaries coincide with the coordinate lines. When the boundary is of arbitrary shape, the eigenfunction expansions tend either to converge very slowly, or not at all [4]. Therefore, their solution was not entirely satisfactory.

Strässler and Schneider [5] also investigated this problem and, with the aid of certain classical results in potential theory, obtained both an integral representation for the solution in terms of an unknown potential, and an integral equation from which the potential could be determined. Their approach was superior to that of Colin, et al.; being far more general and less cumbersome, and yet having none of the attendant difficulties.

Strässler and Schneider also utilized their solution to the diffusion equation to investigate the lamellar eutectic freezing problem, and developed an iterative scheme for obtaining both the solid/liquid interface shapes and a definitive freezing rate-lamellar spacing relation. Although this work constituted an admirable attempt to rigorously treat the problem, it fell short in two respects;

namely, the convergence of the iteration scheme was not demonstrated, either analytically or numerically, and the thermodynamic equilibrium at the  $\alpha/\beta$ /liquid triple point was not accounted for properly.

It is the purpose of this report to attempt to remedy these difficulties by carefully reconsidering some of the essential physics involved in steady-state lamellar freezing, and to develop a theory which is as self-consistent as possible, thereby providing a first step in understanding the formation of the characteristic microstructures produced by directional solidification.

In Sections 2 and 3, the problem is formulated as a boundary-value problem for the thermal and solute diffusion equations, and is subsequently reduced to a system of ordinary nonlinear integro-differential equations for the shape of the solid/liquid interface and the solute concentration on the interface. The analysis makes use of the potential theoretic methods developed at NRL over the last several years for solving various free-boundary problems associated with the diffusion equation [6,7], and is noteworthy because the quantities of interest, namely the quantities defined on the

interface, may be determined without calculating the bulk temperature and solute distributions. In this respect, the analysis is similar to that of Strässler and Schneider; however certain of the resulting integro-differential equations are somewhat simpler in form than those derived in the aforementioned study, primarily because no intermediate potentials are involved.

The behavior of the integro-differential equations is critically examined in Section 4, and simplified versions of these equations are derived by assuming that (1) the solute diffusion length is large compared to the lamellar spacing and (2) the interface is approximately isothermal. In particular, it is shown that:

- The thermodynamic equilibrium requirements at the  $\alpha/\beta$ /liquid triple point must be compatible with constraints imposed by the diffusion equation in order for lamellar solutions to exist.

- When lamellar solutions are possible, the solutions generally admit to a relatively narrow range of possible crystallographic orientation relationships between the two solid phases.

• For a given alloy system, the solutions to the simplified integro-differential equations are functions of a single non-dimensional parameter which is proportional to  $V \lambda^2$ . This result has the important ramification that the use of virtually any subsidiary condition for the selection of the system operating point must lead to a relation of the form  $V \lambda^2 = \text{const.}$

• Lamellar growth may not be possible when the ratio of thermal gradient to freezing rate is less than some critical value which depends on the phase properties and the volume phase fraction. This result can be used to explain the lamellar-rod transition.

In Section 5, various preliminary numerical results are presented, and, in particular, the new theory is utilized to assess the effect of interface curvature on the interfacial solute concentration distribution. Specifically, it is shown that the planar interface model can lead to considerable errors in the calculated concentration distributions, particularly in nonsymmetric systems.

Finally, the theory is checked for consistency with experimental data for a number of alloy systems, and the theoretically predicted  $V-\lambda$  relations are compared with those predicted by the Jackson-Hunt analysis.

## 2. MATHEMATICAL FORMULATION

### 2.1 Formulation of the Boundary-Value Problem

In this section we formulate the boundary value problem which describes the growth of a lamellar eutectic solid in its melt under the influence of an imposed temperature gradient. The geometry of the system under consideration is illustrated in Figures 1 and 2.

In systems which do not facet (systems in which the effects of interfacial molecular attachment kinetics are negligible), the solidification kinetics are controlled primarily by the rate at which solute can diffuse into the liquid, which in turn depends on the temperature distribution at the solid/liquid interface. Quantitative information pertaining to both the solute and temperature distributions is therefore required in order to completely characterize the solidification process.

Because  $D_s$  is generally much smaller than  $D_l$  (by several orders of magnitude), where  $D_s$  and  $D_l$  are the chemical diffusivities of the solid and liquid phases, respectively, solute diffusion in

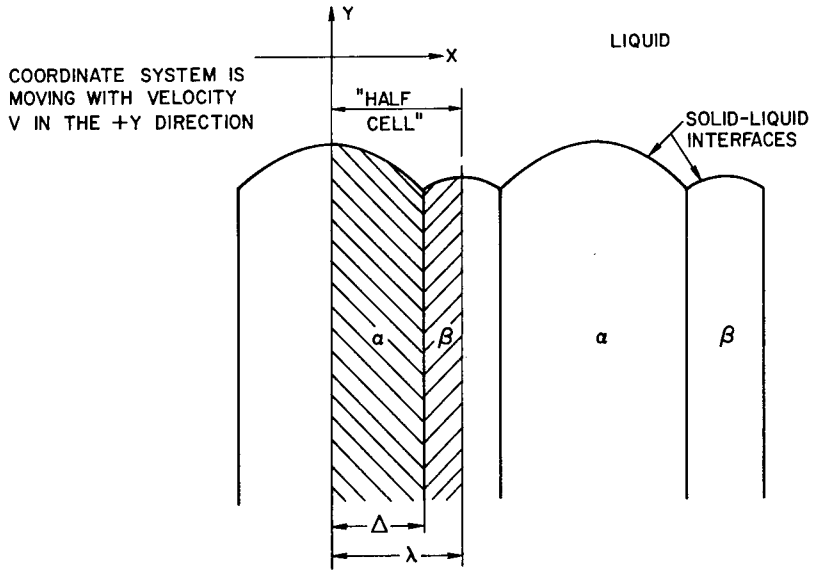


Fig. 1 — Schematic representation of the model used to simulate lamellar solidification

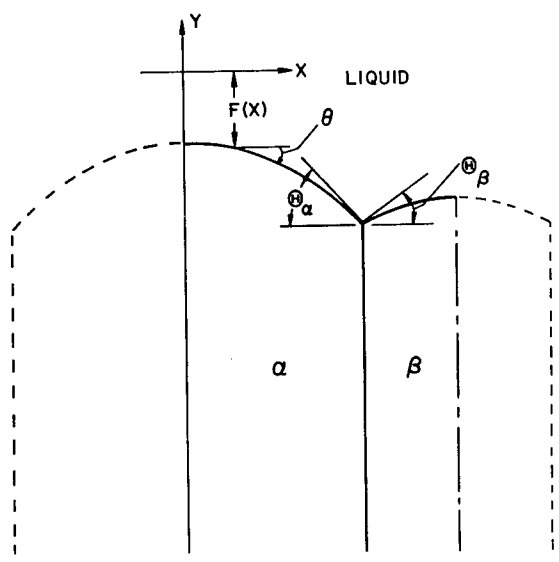


Fig. 2 — Schematic representation of the solid/liquid interface

the solid may be safely neglected. Hence, the solute distribution in the solid,<sup>†</sup>  $c_s$ , is independent of  $Y$  and is given simply by  $c_s(X) = \hat{c}_{s\alpha}(X)$  (in the  $\alpha$  phase),  $c_s(X) = \hat{c}_{s\beta}(X)$  (in the  $\beta$  phase), where  $\hat{c}_{s\alpha}(X)$  and  $\hat{c}_{s\beta}(X)$  are the solute concentrations on the solid side of the solid/liquid interface and are as yet unknown.

The solute distribution in the liquid,  $c_l$ , and the temperature distribution in the solid and liquid,  $T$ , on the other hand, are determined by solving the appropriate diffusion equation. Thus, assuming that the freezing process proceeds in a steady-state manner, i.e., assuming that the prescribed solidification velocity,  $V$ , is constant and that the solid-liquid interface shape,  $F(X)$ , is invariant with time,  $c_l$  can be found by solving

$$\nabla^2 c_l + \frac{V}{D_l} \frac{\partial c_l}{\partial Y} = 0 \quad (\text{in the liquid}) \quad (1)$$

in the "half-cell" in Fig. 1, where equation (1) is the steady-state diffusion equation written in the moving coordinate system  $(X, Y)$ . Similarly, assuming that the ratio of chemical to thermal

---

<sup>†</sup> All concentrations are in units of mass fraction.

diffusivity,  $D_l/D_t$ , is sufficiently small, an estimate of the temperature distribution which is asymptotically valid as  $D_l/D_t \rightarrow 0$  may be obtained by solving Laplace's equation

$$\nabla^2 T = 0 \quad (\text{in the solid and liquid}) \quad (2)$$

in the half-cell.

Finally, in addition to equations (1) and (2),  $c_l$  and  $T$  must also satisfy the following far-field, boundary and interface conditions:

$$\lim_{Y \rightarrow -\infty} \frac{\partial T}{\partial Y} = G_s \quad (3a)$$

$$\lim_{Y \rightarrow \infty} \frac{\partial T}{\partial Y} = G_l \quad (3b)$$

(far-field conditions),

$$\lim_{Y \rightarrow \infty} c_l = c_\infty \quad (4)$$

where  $G_s$  and  $G_l$  are the far-field temperature

gradients in the solid and liquid, respectively  
(only one of which may be prescribed independently),  
and  $c_\infty$  is the specified bulk composition;

$$\frac{\partial T}{\partial X} = \frac{\partial E_2}{\partial X} = 0, \quad (X=0, \lambda), \quad (5)$$

where satisfaction of equation (5) guarantees that  
the symmetry and periodicity requirements are met,  
and  $\lambda$  is the width of the half-cell;

$$-g_x^c = \frac{V}{D_2} \cos \theta \left( \hat{C}_2 - \frac{P_\alpha}{P_2} \hat{C}_{S\alpha} \right) \quad (6a)$$

$(X \in [0, \Delta))$

$$-g_x^c = \frac{V}{D_2} \cos \theta \left( \hat{C}_2 - \frac{P_\beta}{P_2} \hat{C}_{S\beta} \right) \quad (6b)$$

$(X \in (\Delta, \lambda])$

(on the solid/liquid interface)

$$k_2 g_x^t = k_\alpha g_s^t \quad (7a)$$

$(X \in [0, \Delta))$

$$k_2 g_x^t = k_\beta g_s^t \quad (7b)$$

$(X \in (\Delta, \lambda])$

(on the solid/liquid interface),

where equations (6) and (7) represent local conservation of mass and heat flux, respectively, across the solid/liquid interface (equation (7) does not contain a latent heat term, because the latent heat effect is  $O(D_l/D_t)$  and can therefore be neglected as  $D_l/D_t \rightarrow 0$ ),  $g_l^c$  and  $g_l^t$  denote the normal derivatives  $\frac{\partial c_l}{\partial n}$  and  $\frac{\partial T}{\partial n}$ , respectively, evaluated on the liquid side of the solid/liquid interface,  $g_s^t$  denotes  $\frac{\partial T}{\partial n}$ , evaluated on the solid side of the solid/liquid interface,  $\hat{c}_l$  is the solute distribution in the liquid, evaluated at the solid/liquid interface,  $k_\varepsilon$  ( $\varepsilon = \alpha, \beta$ ) are the thermal conductivities in the appropriate phase,  $\rho_\varepsilon$  are the corresponding densities,  $\Delta$  is the width of the  $\alpha$  region, and  $\theta = \tan^{-1}(-F')$ ;

$$T = T_E - (\hat{c}_l - c_E) m_\alpha + a_\alpha K \quad (8a)$$

$$(X \in [0, \Delta])$$

$$T = T_E + (\hat{c}_l - c_E) m_\beta + a_\beta K \quad (8b)$$

$$(X \in (\Delta, \lambda])$$

(on the solid/liquid interface)

$$\hat{C}_{S\alpha} = C_{\alpha E} + \frac{m_{\alpha}}{n_{\alpha}} (\hat{C}_1 - C_E) + b_{\alpha} K$$

(X ∈ [0, Δ])

(9a)

$$\hat{C}_{S\beta} = C_{\beta E} + \frac{m_{\beta}}{n_{\beta}} (\hat{C}_2 - C_E) + b_{\beta} K ;$$

(X ∈ (Δ, λ])

(9b)

(on the solid/liquid interface),

where equations (8) and (9) are the constitutive equations relating the interface temperature and concentrations and are obtained from the phase diagram as modified by curvature effects (equation (8) provides the coupling between the temperature and solute distributions),  $\hat{T}$  is the temperature on the solid/liquid interface;  $T_E$  is the eutectic temperature,  $c_E$  is the eutectic composition;  $c_{\epsilon E}$  ( $\epsilon = \alpha, \beta$ ) are the terminal solid solubilities (see Fig. 3),  $m_{\epsilon}$  and  $n_{\epsilon}$  are the absolute values of the slopes of the liquidus and solidus lines evaluated at  $T_E$ ,  $a_{\epsilon}$  is a Gibbs-Thomson coefficient ( $a_{\epsilon} = \gamma_{\epsilon l} / \Delta S_{f\epsilon}$ );  $\gamma_{\epsilon l}$  is the appropriate solid/liquid interfacial free energy;  $\Delta S_{f\epsilon}$  is the entropy of fusion per unit volume,  $b_{\epsilon}$  is a second Gibbs-Thomson coefficient which is

generally small and will be neglected

henceforth, and  $\kappa$  is the solid/liquid interface curvature ( $\kappa = F''/(1+F'^2)^{3/2}$ );

$$k_{\alpha} g_{\alpha}^t = k_{\beta} g_{\beta}^t \quad (\text{on the } \alpha/\beta \text{ interface}), \quad (10)$$

where equation (10) represents local conservation of heat flux across the  $\alpha/\beta$  interface, and  $g_E^t$  ( $E = \alpha, \beta$ ) denotes  $\frac{\partial T}{\partial n}$ , evaluated on the  $\alpha$  or  $\beta$  side of the  $\alpha/\beta$  interface;

$$\rho_l c_{\infty} \lambda = \rho_{\alpha} \int_0^{\Delta} \hat{c}_{s\alpha}(z) dz + \rho_{\beta} \int_{\Delta}^{\lambda} \hat{c}_{s\beta}(z) dz \quad (11a)$$

$$\lambda \rho_l = \Delta \rho_{\alpha} + (\lambda - \Delta) \rho_{\beta} \quad (11b)$$

$$[k_{\alpha} \Delta + k_{\beta} (\lambda - \Delta)] G_S = \lambda k_l G_L, \quad (12)$$

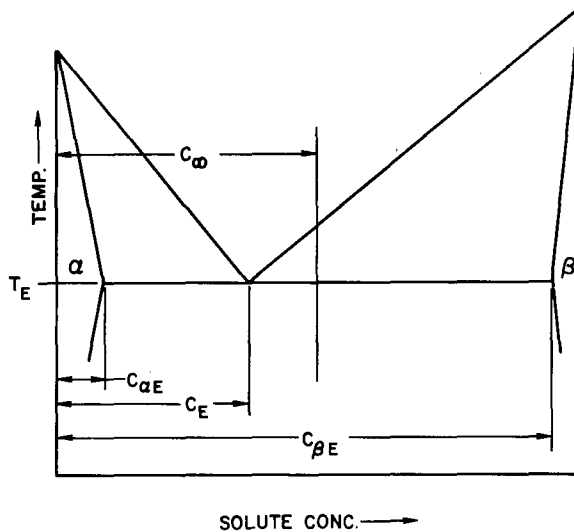


Fig. 3 — Schematic representation of a binary eutectic phase diagram

where equations (11) and (12) represent global conservation of mass and heat flux, respectively; and, finally,

$$\gamma_{\alpha l} \sin \Theta_{\alpha} + \gamma_{\beta l} \sin \Theta_{\beta} = \gamma_{\alpha\beta} \quad (13a)$$

$$\gamma_{\alpha l} \cos \Theta_{\alpha} - \gamma_{\beta l} \cos \Theta_{\beta} = \text{torque terms} \quad (13b)$$

$$F(\Delta_-) = F(\Delta_+) \quad (13c)$$

$$F'(0) = F'(\lambda) = 0, \quad (13d)$$

where equations (13a) and (13b) are statements of thermodynamic equilibrium at the  $\alpha/\beta/\text{liquid}$  triple point (assuming the solid/liquid interfacial energies to be isotropic and admitting an as yet unspecified torque term due to possible anisotropy in the solid/solid interfacial energy,  $\gamma_{\alpha\beta}$ ), equations (13c) and (13d) are statements of interface continuity at the triple point and symmetry, respectively; and

$$\Theta_{\alpha} = \lim_{x \rightarrow \Delta_-} |\tan^{-1} F'(x)|,$$

$$\Theta_{\beta} = \lim_{x \rightarrow \Delta_+} |\tan^{-1} F'(x)|.$$

The system of equations (1)-(13) is a mathematical statement of the boundary-value problem which describes the lamellar solidification process. Of primary interest is the determination of the interface quantities  $\hat{c}_i$  and  $\hat{T}$ , the volume phase fractions  $\Delta/\lambda$ , and the interface shapes,  $F(X)$ , which are compatible with a specified solidification rate (or lamellar spacing) and thermal gradient.

## 2.2 Some Comments on the Analysis

Before proceeding any further, it is worthwhile to comment briefly on several aspects of the analysis. First, the problem is a free-boundary problem in the sense that the domains over which equations (1) and (2) are to be solved are not specified completely at the outset, because  $F(X)$  and  $\Delta/\lambda$  are a priori unknown. Rather, these quantities must be found in the course of the solution. Such problems are generally nonlinear and do not usually yield to classical methods of solution.

Second, even when  $F(X)$ ,  $V$ , and  $\lambda$  are specified, the system composed of equations (1), (4)-(6), (9), and (11) does not necessarily admit to a unique

solution. Rather, the concentration fields associated with this system contain a term of the form

$$I(Y, \lambda, V) = \int_0^\lambda A(Z, \lambda, V) e^{-\frac{V}{D_s} (Y - F(Z))} dz, \quad (14)$$

where the function  $A(Z, \lambda, V)$  is indeterminate from diffusional considerations alone. This is a rather subtle point and is considered in more detail in Appendix B. It suffices to say here that the determination of  $I(Y, \lambda, V)$  is intimately related to the triple-point equilibrium conditions, equations (13a) and (13b).

Thirdly, as will become apparent later, multiple families of solutions may exist for a prescribed lamellar spacing and thermal gradient. Thus, a one-parameter family of solutions may exist for fixed values of  $\lambda$ ,  $G_s$  (or  $G_\beta$ ), and  $V$ , with each member of the family corresponding to a different crystallographic orientation relationship between the two solid phases. Moreover, when  $\lambda$ ,  $G_s$  (or  $G_\beta$ ); and the orientation relationship are fixed, a second family of solutions exists and can be generated simply by varying the freezing rate,  $V$ .

It is probable that the solutions belonging to the second family represent possible physical states when the correct orientation relationship is prescribed. Indeed, Hunt and Jackson [8], in their work on transparent organic systems, demonstrated that a lamellar morphology could be maintained over a range of freezing rates, even when the changes in lamellar spacing which would normally take place were suppressed (this was accomplished by using thin specimens to grow a fault-free structure). It has also been observed that a lamellar morphology can persist when the orientation relationship is varied (by forcing the lamellae to curve, for instance), provided that the orientation relationship does not deviate too far from the preferred one (see ref. [9] for a comprehensive summary of these results). Hence, it is conceivable that solutions belonging to the first family can also be realized physically.

Finally, it should be noted that the aforementioned experimental results are highly atypical. In the vast majority of experimental situations, it is observed that (1) the lamellar spacing is

a single-valued function of the freezing rate, and (2) a preferred orientation relationship invariably develops as solidification proceeds. Therefore, it is evident that the steady-state theory does not provide complete predictive capability.

The point of view adopted in this report is that the selection of the preferred lamellar spacing and orientation relationship is essentially a time-dependent phenomenon, and is therefore outside the purview of steady-state theory. The most that a steady-state theory can provide are candidates for the favored solutions. Only by introducing additional information via a stability analysis or a variational principle can the appropriate steady-state solution be selected.

### 3. A FORMAL SOLUTION TO THE FREE-BOUNDARY PROBLEM

To solve the free-boundary problem defined by equations (1)-(13), it is necessary to both solve the chemical and thermal diffusion equations, and determine the shape of the solid/liquid interface. It proves convenient to consider each diffusion process separately in the initial stages of the analysis, and then introduce the coupling via the interfacial constitutive relations in the final stage. Hence, we begin our investigation by examining the chemical diffusion equation.

#### 3.1 Chemical Diffusion

The solute diffusion portion of the problem consists of obtaining solutions to equation (1) which also satisfy the subsidiary conditions (4)-(6), (9), and (11). The required solutions will be constructed in this section using a potential theoretic method very similar to that described in reference [6].

##### 3.1.1 The potential theoretic method

The potential theoretic method developed in reference [6] was devised to treat a general class of free-boundary problems associated with

the diffusion equation and essentially consists of utilizing the jump properties of the single and double layer potentials associated with the diffusion equation to transform the original boundary-value problem into an equivalent (and hopefully simpler) problem involving only the determination of the solid/liquid interface shape and certain quantities defined on the interface. Because the procedure yields integral representations for the bulk solute concentrations in terms of the interfacial quantities, the original free-boundary problem may be regarded as solved once these quantities are determined. A detailed discussion of this method is presented below:

Denoting the portion of the half-cell occupied by the liquid as  $\mathcal{D}_l$  and that occupied by the solid as  $\mathcal{D}_s$ , the potential theoretic method may be outlined as follows:

1. A solution,  $\tilde{\Phi}_2(X, Y)$ , to equation (1) is constructed throughout the entire half-cell,  $\mathcal{D}_2 \cup \mathcal{D}_S$ , such that condition (5) is satisfied and

$$\lim_{Y \rightarrow +\infty} \tilde{\Phi}_2 = \lim_{Y \rightarrow -\infty} \tilde{\Phi}_2 = 0$$

$$[\tilde{\Phi}_2] \equiv \lim_{\substack{P \rightarrow S \\ P \in \mathcal{D}_2}} \tilde{\Phi}_2 - \lim_{\substack{P \rightarrow S \\ P \in \mathcal{D}_S}} \tilde{\Phi}_2 \equiv \tilde{\Phi}_2^+ - \tilde{\Phi}_2^- = \tilde{C}_2$$

$$\left[ \frac{d\tilde{\Phi}_2}{dn} \right] \equiv \lim_{\substack{P \rightarrow S \\ P \in \mathcal{D}_2}} \frac{d\tilde{\Phi}_2}{dn} - \lim_{\substack{P \rightarrow S \\ P \in \mathcal{D}_S}} \frac{d\tilde{\Phi}_2}{dn} \equiv \frac{d\tilde{\Phi}_2^+}{dn} - \frac{d\tilde{\Phi}_2^-}{dn} = \tilde{f}_2,$$

where P is a generic spatial point (X, Y), S is a point on the solid/liquid interface, and  $\tilde{C}_2$  and  $\tilde{f}_2$  are prescribed jumps in  $\tilde{\Phi}_2$  and its normal derivative across the interface.

2.  $\tilde{\Phi}_2^-$  is set equal to zero.

This step insures that  $\tilde{\Phi}_2(P) = 0$  for  $P \in \mathcal{D}_S$ , and hence guarantees that  $\tilde{\Phi}_2^+ = \tilde{C}_2$  and  $\frac{d\tilde{\Phi}_2^+}{dn} = \tilde{f}_2$ .

In addition, this step provides a compatibility

relation in the form of an integral equation involving  $\tilde{c}_x$ ,  $\tilde{f}_x$ , and  $F(X)$ .

3. A second solution,  $\phi_x(P)$ , is constructed such that  $\phi_x = \tilde{\phi}_x + c_{\infty} + I(y, \lambda, \nu)$ , where  $I(Y, \lambda, \nu)$  is given by equation (14).  $\phi_x(P)$  satisfies both equation (1) and conditions (4) and (5); moreover,  $\phi_x(P) = c_x(P)$  for  $P \in \mathcal{D}_x$ , provided that conditions (6), (9), (11), and the compatibility relation are satisfied.

4. The compatibility equation is used in conjunction with the relation  $\hat{c}_x = \tilde{c}_x + c_{\infty} + I(F(X), \lambda, \nu)$ , equations (6), (8), (9), (11), (13), and additional equations arising from thermal diffusion considerations to form a system of equations from which the quantities  $\Delta/\lambda$ ,  $\tilde{c}_x$ ,  $\hat{T}$ , and  $F(X)$  are obtained. These quantities may then be used to determine the bulk concentration and temperature distributions, if desired.

### 3.1.2 Implementation of the potential theoretic procedure

In this section we shall examine the properties of the single and double layer potentials associated with equation (1) in the strip  $[0, \lambda]$ , and then employ these potentials in the procedure just outlined to obtain explicit expressions for the solute concentration and the compatibility relation.

It is convenient to introduce the following nondimensional variables:

$$\begin{aligned} x &= X/\lambda, \quad y = Y/\lambda, \\ f &= F/\lambda, \quad \omega = V\lambda/2D_e. \end{aligned} \quad (15)$$

Then, in terms of these variables, the appropriate single and double layer potentials,  $U_\omega^v [h](x, y)$  and  $W_\omega^v [p](x, y)$ , respectively, are given by

$$U_\omega^v [h](x, y) = \frac{1}{2\omega} \int_0^1 \tilde{K}(x, z, y, v(z), \omega) h(z) \frac{dz}{\cos \theta(z)} \quad (16a)$$

and

$$W_\omega^v [p](x, y) = \frac{1}{2\omega} \int_0^1 \frac{d}{dn_\lambda} \left\{ \tilde{K}(x, z, y, v(z), \omega) \right\} p(z) \frac{dz}{\cos \theta(z)}, \quad (16b)$$

where  $h(z)$  and  $p(z)$  are the density functions for the appropriate potential,

$$\frac{d}{dn_\lambda} = \sin \theta(z) \frac{\partial}{\partial z} + \cos \theta(z) \frac{\partial}{\partial v(z)}; \quad (17)$$

$$\begin{aligned}
\tilde{K}(x, z, y, v(z), \omega) = & -\frac{\omega}{2\pi} \ln [2 \cosh \pi (y - v(z)) - 2 \cos \pi (x - z)] \\
& - \frac{\omega}{2\pi} \ln [2 \cosh \pi (y - v(z)) - 2 \cos \pi (x + z)] + 1 \\
& + \omega |y - v(z)| + H(y - v(z)) [e^{-2\omega (y - v(z))} - 1] \\
& + 2\omega \sum_{n=1}^{\infty} \cos n\pi x \cos n\pi z [(\omega^2 + n^2\pi^2)^{-1/2} \\
& \cdot \exp\{- (\omega^2 + n^2\pi^2)^{1/2} |y - v(z)| - \omega (y - v(z))\} \\
& - (n\pi)^{-1} \exp\{- n\pi |y - v(z)|\}] ,
\end{aligned} \tag{18}$$

$H(x)$  denotes the Heaviside unit step function, and  $v(x)$  is a single-valued function of  $x$  in the strip  $x \in [0, 1]$ . A detailed derivation of the expression for  $U_{\omega}^v[h](x, y)$  is given in Appendix A.

The potentials  $U_{\omega}^v[h](x, y)$  and  $W_{\omega}^v[p](x, y)$  are known to have the following properties:

1. They satisfy the nondimensional version of equation (1),

$$\nabla^2 c_e + 2\omega \frac{\partial c_e}{\partial y} = 0,$$

at all points in the strip  $[0,1]$  except for points on the surface  $y = v(x)$ .

2.

$$\frac{\partial}{\partial x} U_{\omega}^v[h] = \frac{\partial}{\partial x} W_{\omega}^v[p] = 0, \quad (x=0,1)$$

$$\lim_{y \rightarrow \infty} U_{\omega}^v[h](x,y) = 0,$$

$$\lim_{y \rightarrow -\infty} U_{\omega}^v[h](x,y) = \frac{1}{2\omega} \int_0^1 h(z) \frac{dz}{\cos \theta(z)},$$

$$\lim_{y \rightarrow \infty} W_{\omega}^v[p](x,y) = \lim_{y \rightarrow -\infty} W_{\omega}^v[p](x,y) = 0.$$

3.

$$\begin{aligned} \lim_{\substack{(\eta, \zeta) \rightarrow (x, v(x)) \\ (\eta, \zeta) \in \mathcal{R}_2}} U_{\omega}^v[h](\eta, \zeta) &= \lim_{\substack{(\eta, \zeta) \rightarrow (x, v(x)) \\ (\eta, \zeta) \in \mathcal{R}_5}} U_{\omega}^v[h](\eta, \zeta) = U_{\omega}^{v*}[h](x), \end{aligned}$$

where

$$U_{\omega}^{v*}[h](x) = \frac{1}{2\omega} \int_0^1 \tilde{K}(x, z, v(x), v(z), \omega) h(z) \frac{dz}{\cos \theta(z)}; \quad (19)$$

$(\eta, \zeta)$  is a generic spatial point;  $(x, v(x))$  is a point on the surface  $v(x)$ ;  $\mathcal{R}_2$  is the portion of the strip  $[0,1]$  consisting of the points  $(x, y)$  such that  $y > v(x)$ ; and  $\mathcal{R}_5$  is the complementary portion of the strip.

4.

$$\lim_{(\eta, \xi) \rightarrow (x, v(x))} \frac{d}{d\eta_x} U_{\omega}^v [h] (\eta, \xi) = -\frac{i}{2} h(x) + X_{\omega}^{v*} [h] (x),$$

$(\eta, \xi) \in \mathbb{R}_2$

$$\lim_{(\eta, \xi) \rightarrow (x, v(x))} \frac{d}{d\eta_x} U_{\omega}^v [h] (\eta, \xi) = +\frac{i}{2} h(x) + X_{\omega}^{v*} [h] (x),$$

$(\eta, \xi) \in \mathbb{R}_5$

where

$$\frac{d}{d\eta_x} = \sin \theta(x) \frac{\partial}{\partial \eta} + \cos \theta(x) \frac{\partial}{\partial \xi} \quad (20)$$

and where  $X_{\omega}^{v*} [h] (x)$  is a well-behaved function of  $x$ .

5.

$$\lim_{(\eta, \xi) \rightarrow (x, v(x))} W_{\omega}^v [f] (\eta, \xi) = +\frac{1}{2} f(x) + W_{\omega}^{v*} [f] (x),$$

$(\eta, \xi) \in \mathbb{R}_2$

$$\lim_{(\eta, \xi) \rightarrow (x, v(x))} W_{\omega}^v [f] (\eta, \xi) = -\frac{i}{2} f(x) + W_{\omega}^{v*} [f] (x),$$

$(\eta, \xi) \in \mathbb{R}_5$

where

$$W_{\omega}^{\nu*}[f](x) = \frac{1}{2\omega} \int_0^1 \frac{d}{dn_3} \left\{ \tilde{K}(x, z, \nu(x), \nu(z), \omega) \right\} f(z) \frac{dz}{\cos\theta(z)}, \quad (21)$$

6.

$$\begin{aligned} \frac{d}{dn_x} W_{\omega}^{\nu}[f](\eta, \xi) &= \frac{d}{dn_x} U_{\omega}^{\nu}[2\omega p \cos\theta](\eta, \xi) \\ &+ Y_{\omega}^{\nu}[f](\eta, \xi), \end{aligned}$$

where  $Y_{\omega}^{\nu}[f](\eta, \xi)$  is continuous across  $\nu(x)$ .

¶ It is now a relatively simple matter to implement the procedure described in the previous section.

Using the properties of the potentials  $U_{\omega}^{\nu}[h](x, y)$  and  $W_{\omega}^{\nu}[f](x, y)$ , it is readily verified that the solution

$$\tilde{\Phi}_2(x, y) = W_{\omega}^{\nu}[\tilde{c}_2](x, y) - U_{\omega}^{\nu}[\tilde{g}_2 + 2\omega \tilde{c}_2 \cos\theta](x, y) \quad (22)$$

satisfies all of the conditions set forth in step 1, provided that

$$\frac{1}{2\omega} \int_0^1 [\tilde{g}_2(z) + 2\omega \tilde{c}_2(z) \cos \theta(z)] \frac{dz}{\cos \theta(z)} = 0, \quad (23)$$

where  $\tilde{g}_2$  now denotes the nondimensional normal derivative of  $\tilde{\phi}_2$  evaluated on the liquid side of the interface. Assuming for the moment that equation (23) is satisfied (it will be shown shortly that equation (23) is identically satisfied as a consequence of global mass conservation), step 2 can now be implemented and the compatibility relation obtained by setting  $\tilde{\phi}_2^- = 0$ . With the aid of properties 3 and 5, this results in

$$-\frac{1}{2} \tilde{c}_2(x) + W_\omega^{f*} [\tilde{c}_2](x) - U_\omega^{f*} [\tilde{g}_2 + 2\omega \tilde{c}_2 \cos \theta](x) = 0. \quad (24)$$

¶ Finally, the interfacial and bulk solute concentrations,  $\hat{c}_2(x)$  and  $c(x, y)$  respectively, are constructed as in step 3. Thus, provided that equation (24) and the nondimensional versions of equations (6) and (11), i.e.,

$$-g_2^A(x) = 2\omega \cos \theta(x) (\hat{c}_2(x) - g_2(x)), \quad (25)$$

$$c_{\infty} = \frac{f_{\alpha}}{f_2} \int_0^{\delta} \hat{c}_{s\alpha}(z) dz + \frac{f_{\beta}}{f_2} \int_{\delta}^1 \hat{c}_{s\beta}(z) dz, \quad (26a)$$

$$\delta \frac{f_{\alpha}}{f_2} + (1-\delta) \frac{f_{\beta}}{f_2} = 1, \quad (26b)$$

are satisfied,  $c_2(x, y)$  and  $\hat{c}_2(x)$  are given by<sup>†</sup>

$$\begin{aligned} c_2(x, y) &= \tilde{\Phi}_2(x, y) + c_{\infty} + \int_0^1 A(\tilde{z}, \omega) e^{-2\omega(y-f(\tilde{z}))} d\tilde{z} \\ &= W_{\omega}^{\dagger}[\tilde{c}_2](x, y) - U_{\omega}^{\dagger}[\tilde{g}_1 + 2\omega\tilde{c}_2 \cos \theta](x, y) \\ &\quad + \int_0^1 A(\tilde{z}, \omega) e^{-2\omega(y-f(\tilde{z}))} d\tilde{z} + c_{\infty} \end{aligned} \quad (27)$$

and

$$\hat{c}_2(x) = \tilde{c}_2(x) + c_{\infty} + \int_0^1 A(\tilde{z}, \omega) e^{-2\omega(f(x)-f(\tilde{z}))} d\tilde{z}, \quad (28)$$

---

<sup>†</sup> Strictly speaking,  $A(\tilde{z}, \omega)$  is a function of the nondimensional half-cell width, as well as  $\tilde{z}$  and  $\omega$ . We have chosen here not to display this relationship explicitly.

where

$$j = \Delta/\lambda,$$

$$q(x) = \begin{cases} \frac{\rho_\alpha}{\rho_\beta} \hat{c}_{s\alpha}, & x \in [0, j) \\ \frac{\rho_\beta}{\rho_\alpha} \hat{c}_{s\beta}, & x \in (j, 1] \end{cases}, \quad (29)$$

$g_1^c$  is the nondimensional normal derivative of the solute field evaluated at the interface, and  $\hat{c}_{s\epsilon}$  ( $\epsilon = \alpha, \beta$ ) is given by equation (9).

It only remains to verify the condition expressed by equation (23) and to obtain integral representations for equations (24) and (27).

Consider the expression

$$\tilde{f}_1(x) + 2\omega \tilde{c}_2(x) \cos \theta(x).$$

Since

$$\tilde{f}_1 \equiv \frac{d}{dx} \tilde{\Phi}_2(x, y) \Big|_{\substack{y \rightarrow f(x) \\ y \in \mathcal{D}_2}}$$

by definition and

$$c_2(x, y) = \tilde{\Phi}_2(x, y) + c_\infty + \int_0^1 A(\beta, \omega) e^{-2\omega(y-f(\beta))} d\beta$$

by equation (27),

$$\left. \frac{d}{dx} C_2(x, y) \right|_{\substack{y \rightarrow f(x) \\ y \in \mathcal{D}_x}} \equiv g_x^c$$

$$= \tilde{g}_2 - 2\omega \cos \theta \int_0^1 A(z, \omega) e^{-2\omega(f(x)-f(z))} dz. \quad (30)$$

Substituting equations (28) and (30) into equation (25)

gives

$$\tilde{g}_2(x) = -2\omega \cos \theta(x) (\tilde{C}_2(x) + c_\infty - g(x));$$

hence,

$$\tilde{g}_2(x) + 2\omega \cos \theta(x) \tilde{C}_2(x) = 2\omega \cos \theta(x) (g(x) - c_\infty). \quad (31)$$

If, now, equation (31) is substituted into the integrand in equation (23), the result

$$\frac{1}{2\omega} \int_0^1 \left[ \tilde{g}_2(z) + 2\omega \tilde{C}_2(z) \cos \theta(z) \right] \frac{dz}{\cos \theta(z)} =$$

$$\frac{\rho_x}{\rho_1} \int_0^d \hat{C}_{su}(z) dz + \frac{\rho_0}{\rho_2} \int_0^1 \hat{C}_{sp}(z) dz - c_\infty = 0$$

(by equations (26a))

is obtained, thus confirming equation (23).

Equation (31) is also of use in obtaining the required integral representations for the solute field and the compatibility relation from equations (27) and (24). Thus, with the aid of equations (16)-(19), (21), (26a), and (31),  $c_2(x, y)$  and the compatibility relation can be written as

$$\begin{aligned}
 c_2(x, y) = & c_{\infty} + \int_0^1 K_1(x, z, y, f(z), \omega) \tilde{C}_2(z) dz \\
 & + \int_0^1 K_2(x, z, y, f(z), \omega) S_1(z) dz \\
 & + \int_0^1 A(z, \omega) e^{-2\omega(y-f(z))} dz
 \end{aligned} \tag{32}$$

and

$$\begin{aligned}
 -\frac{1}{2} \tilde{C}_2(x) + \int_0^1 K_1(x, z, f(x), f(z), \omega) \tilde{C}_2(z) dz \\
 + \int_0^1 K_2(x, z, f(x), f(z), \omega) S_1(z) dz = 0,
 \end{aligned} \tag{33}$$

respectively, where

$$S_1(x) = c_{\infty} - q(x) = \begin{cases} c_{\infty} - \frac{f_{\alpha}}{f_2} \hat{C}_{s\alpha} & , x \in [0, \delta), \\ c_{\infty} - \frac{f_{\beta}}{f_2} \hat{C}_{s\beta} & , x \in (\delta, 1] , \end{cases} \tag{34}$$

$$\begin{aligned}
 K_1(x, z, y, f(z), \omega) &= \frac{1}{2\omega} \frac{d}{dn_z} \tilde{K}(x, z, y, f(z), \omega) \cdot \frac{1}{\cos \theta(z)} \\
 &= \frac{\sinh \pi(y-f(z)) - \tan \theta(z) \sin \pi(x+z)}{4 [\cosh \pi(y-f(z)) - \cos \pi(x+z)]} \\
 &+ \frac{\sinh \pi(y-f(z)) + \tan \theta(z) \sin \pi(x-z)}{4 [\cosh \pi(y-f(z)) - \cos \pi(x-z)]} \\
 &+ \frac{1}{2} H(y-f(z)) [e^{-2\omega(y-f(z))} - 1] \\
 &- \tan \theta(z) \sum_{n=1}^{\infty} \cos n\pi x \sin n\pi z \\
 &\cdot \left( \frac{n\pi}{(\omega^2 + n^2\pi^2)^{1/2}} \exp \left\{ -(\omega^2 + n^2\pi^2)^{1/2} |y-f(z)| - \omega(y-f(z)) \right\} \right. \\
 &\left. - \exp \left\{ -n\pi |y-f(z)| \right\} \right) + \frac{1}{2} \tilde{K}(x, z, y, f(z), \omega) \\
 &+ [1 - 2H(y-f(z))] \sum_{n=1}^{\infty} \cos n\pi x \cos n\pi z \\
 &\cdot \left( \exp \left\{ -n\pi |y-f(z)| \right\} - \exp \left\{ -(\omega^2 + n^2\pi^2)^{1/2} |y-f(z)| \right. \right. \\
 &\left. \left. - \omega(y-f(z)) \right\} \right),
 \end{aligned}$$

(35a)

and

$$K_2(x, z, y, f(z), \omega) = \tilde{K}(x, z, y, f(z), \omega) - 1. \quad (35b)$$

The free-boundary problem can now be regarded as partially solved in the sense that an integral representation for the solution to equation (1) is known in terms of the unknown quantities  $\tilde{C}_p(x)$ ,  $f(x)$ , and  $\mathcal{J}$ , and that a compatibility equation relating these quantities is available. However, the compatibility equation, together with equations (26), (28), and the interfacial constitutive relations, do not contain sufficient information to uniquely determine  $\tilde{C}_p(x)$ ,  $f(x)$ , and  $\mathcal{J}$ ; in order to proceed further, thermal diffusion effects must be considered.

### 3.2 Thermal Diffusion

The thermal diffusion portion of the problem consists of obtaining solutions to equation (2) which also satisfy the subsidiary conditions (3), (5), (7), (10), and (12). The required solutions will be constructed in this section using a method very similar to that used in reference [7].

### 3.2.1 The "fictitious source" method

The method to be employed here is more classical in nature and is conceptually simpler than the technique previously described. Essentially, the method consists of employing fictitious heat source distributions to introduce arbitrary discontinuities in the normal derivatives of the temperature field across the solid/liquid and  $\alpha/\beta$  interfaces, and then adjusting the strength of these discontinuities so as to satisfy conditions (7) and (10). Specifically, this procedure results in both an integral representation of the temperature field in terms of two unknown discontinuity density functions  $\psi_1$ , and  $\psi_2$ , and a set of coupled integral equations for  $\psi_1$  and  $\psi_2$ . These relations, together with the interfacial constitutive relations, provide just the information required to complete the solution to the entire free-boundary problem. A systematic outline of the method follows:

1. A solution,  $\vartheta(x, y)$ , to the nondimensional version of equation (2),

$$\frac{\partial^2 \vartheta}{\partial x^2} + \frac{\partial^2 \vartheta}{\partial y^2} = 0, \quad (36)$$

is constructed throughout the strip,  $\mathcal{D}_2 \cup \mathcal{D}_5$ , such that the nondimensional version of condition (5) is satisfied and

$$\lim_{y \rightarrow -\infty} \frac{\partial \vartheta}{\partial y} = 1,$$

$$\lim_{y \rightarrow +\infty} \frac{\partial \vartheta}{\partial y} = G_L / G_S,$$

$$\left[ \frac{d\vartheta}{dn_x} \right]_{s\ell} = \psi_1,$$

$$\left[ \frac{d\vartheta}{dn} \right]_{\alpha\beta} = \psi_2,$$

where  $\vartheta$  is a nondimensional temperature ( $\vartheta = T / \lambda G_S$ );  $\left[ \frac{d\vartheta}{dn_x} \right]_{s\ell}$  and  $\left[ \frac{d\vartheta}{dn} \right]_{\alpha\beta}$  denote jumps in the normal derivative of  $\vartheta$  across the solid/liquid and  $\alpha/\beta$  interfaces, respectively, and  $\psi_1$  and  $\psi_2$  denote the prescribed values of the aforementioned jumps.

2. With  $G_S$  regarded as specified,  $G_L$  is obtained in terms of  $\psi_1$  and  $\psi_2$  so as to guarantee satisfaction of equation (12).

3. The normal derivatives of  $v$  are evaluated on either side of each interface and equations (7) and (10) are applied. This step leads to a set of two coupled integral equations for the discontinuity functions  $\psi_1$  and  $\psi_2$ , thus assuring that heat flux is conserved at all points on each interface.

4. The representation for  $v$  and the integral equations for  $\psi_1$  and  $\psi_2$  are used to provide the remaining information required in step 4 of the procedure described in Section 3.1.1, thus completing the solution of the free-boundary problem.

### 3.2.2 Implementation of the fictitious source method

The implementation of the fictitious source method is facilitated by the introduction of two particular solutions to equation (36),  $V_1^v[h](x, y)$  and  $V_2^{c_2/c_1}[p](x, y)$ , in the strip  $[0, 1]$ . These solutions are given by

$$V_1^v[h](x, y) = \int_0^1 K_3(x, z, y, v(z)) h(z) \frac{dz}{\cos \theta(z)} \quad (37)$$

and

$$V_{2c_2}^{c_1}[p](x, y) = \int_{c_1}^{-\infty} K_4(x, y, u) p(u) du, \quad (38)$$

where  $h(z)$  and  $p(z)$  are the density functions for the appropriate solution,  $c_1$  and  $c_2$  are constants,

$$\begin{aligned} K_3(x, z, y, v(z)) &= -\frac{1}{2}(y - v(z)) \\ &- \frac{1}{4\pi} \ln [2 \cosh \pi(y - v(z)) - 2 \cos \pi(x - z)] \\ &- \frac{1}{4\pi} \ln [2 \cosh \pi(y - v(z)) - 2 \cos \pi(x + z)]; \end{aligned} \quad (39)$$

$$\begin{aligned} K_4(x, y, u) &= -\frac{1}{2}(y - u) - \frac{1}{4\pi} \ln [2 \cosh \pi(y - u) - 2 \cos \pi(x - c_2)] \\ &- \frac{1}{4\pi} \ln [2 \cosh \pi(y - u) - 2 \cos \pi(x + c_2)], \end{aligned} \quad (40)$$

and  $v(x)$  is defined as in Section 3.1.2. The solutions  $V_1^v[h](x, y)$  and  $V_{2c_1}^{c_2}[p](x, y)$  also have a simple physical interpretation; namely, they represent the temperature fields due to distributions of heat sources acting on the surfaces  $y = v(x)$  and  $(c_2, y)$ ,  $y \in (-\infty, c_1)$ .

The solutions  $V_1^v[h](x, y)$  and  $V_{2c_1}^{c_2}[p](x, y)$  have the following properties:

1. They satisfy equation (36) at all points in the strip  $[0, 1]$  except at selected one-dimensional sets of points ( $y = v(x)$  for  $V_1^v[h]$  and  $(c_2, y), y \in (-\infty, c_1)$  for  $V_{2c_1}^{c_2}[p]$ ).

2.

$$\frac{\partial}{\partial x} V_1^v[h] = \frac{\partial}{\partial x} V_{2c_1}^{c_2}[p] = 0 \quad (x=0, 1)$$

$$\lim_{y \rightarrow -\infty} \frac{\partial}{\partial y} V_1^v[h] = \lim_{y \rightarrow -\infty} \frac{\partial}{\partial y} V_{2c_1}^{c_2}[p] = 0$$

(provided that  $\lim_{u \rightarrow -\infty} p(u) = 0$ ),

$$\lim_{y \rightarrow \infty} \frac{\partial}{\partial y} V_1^v[h] = - \int_0^1 h(\xi) \frac{d\xi}{\cos \theta(\xi)},$$

$$\lim_{y \rightarrow \infty} \frac{\partial}{\partial y} V_{2c_1}^{c_2}[p] = - \int_{c_1}^{-\infty} p(u) du.$$

3. They are continuous and have continuous first derivatives at all points in the strip except on the selected one-dimensional sets mentioned in item 1. In particular,  $\frac{d}{d\eta_x} V_1^v [h]$  undergoes a jump across the surface  $y = v(x)$ , and  $\frac{\partial}{\partial x} V_{2c_1}^{c_2} [p]$  undergoes a jump across the surface  $(c_2, y)$ ,  $y \in (-\infty, c_1)$ . The limiting values of these derivatives are given by

$$\lim_{\substack{(\eta, \zeta) \rightarrow (x, v(x)) \\ (\eta, \zeta) \in \mathbb{R}_2}} \frac{d}{d\eta_x} V_1^v [h] (\eta, \zeta) = -\frac{1}{2} h(x) + \cos \theta(x) Z_1^{v*} [h] (x),$$

$$\lim_{\substack{(\eta, \zeta) \rightarrow (x, v(x)) \\ (\eta, \zeta) \in \mathbb{R}_5}} \frac{d}{d\eta_x} V_1^v [h] (\eta, \zeta) = +\frac{1}{2} h(x) + \cos \theta(x) Z_1^{v*} [h] (x),$$

$$\lim_{\substack{(\eta, \zeta) \rightarrow (c_2, y) \\ (\eta, \zeta) \in (0, c_2) \times (-\infty, c_1)}} \frac{\partial}{\partial x} V_{2c_1}^{c_2} [p] (\eta, \zeta) = +\frac{1}{2} p(y) + Z_{2c_1}^{c_2*} [p] (y),$$

$$\lim_{\substack{(\eta, \zeta) \rightarrow (c_2, y) \\ (\eta, \zeta) \in (c_2, 1) \times (-\infty, c_1)}} \frac{\partial}{\partial x} V_{2c_1}^{c_2} [p] (\eta, \zeta) = -\frac{1}{2} p(y) + Z_{2c_1}^{c_2*} [p] (y),$$

where  $(\eta, \zeta)$ ,  $\mathcal{R}_\eta$ , and  $\mathcal{R}_\zeta$  have the same meanings as in Section 3.1.2,

$$Z_1^{v*}[h](x) = \int_0^1 K_5(x, z, v(x), v(z)) h(z) \frac{dz}{\cos \theta(z)}, \quad (41a)$$

$$Z_{2c_1}^{c_2*}[p](y) = \int_{c_1}^{-\infty} K_6(y, u) p(u) du, \quad (41b)$$

$$K_5(x, z, v(x), v(z)) = -\frac{1}{2} \frac{\sinh \pi(v(x) - v(z)) + \tan \theta(x) \sin \pi(x+z)}{4[\cosh \pi(v(x) - v(z)) - \cos \pi(x+z)]} - \frac{\sinh \pi(v(x) - v(z)) + \tan \theta(x) \sin \pi(x-z)}{4[\cosh \pi(v(x) - v(z)) - \cos \pi(x-z)]}, \quad (42)$$

and

$$K_6(y, u) = -\frac{\sin 2\pi c_2}{4[\cosh \pi(y-u) - \cos 2\pi c_2]}. \quad (43)$$

With the aid of these properties, the required solution to equation (36) can be constructed almost by inspection.

It is readily verified that the temperature field

$$\begin{aligned} \psi(x,y) = & \text{const.} + \gamma \\ & + V_1^f[\psi_2](x,y) + V_2^{\delta}(s)[\psi_2](x,y) \end{aligned} \quad (44)$$

satisfies equation (36) and all of the subsidiary conditions listed in step 1 of the fictitious source procedure, provided that

$$1. \lim_{u \rightarrow -\infty} \psi_2(u) \rightarrow 0,$$

$$2. \frac{G_2}{G_5} = 1 - \int_0^1 \psi_1(\beta) \frac{d\beta}{\cos \theta(\beta)} - \int_{f(\theta)}^{-\infty} \psi_2(u) du, \quad (45)$$

where the constant in equation (44) is arbitrary.

¶ It will be assumed henceforth that the first of these conditions is always satisfied. The second of these conditions can always be satisfied by adjusting  $G_2$ ; moreover, it can be shown that satisfaction of this condition automatically guarantees the satisfaction of the nondimensional version of equation (12). In view of these considerations, all that remains is to determine the discontinuity functions  $\psi_1$  and  $\psi_2$  such that equations (7) and (10) are satisfied.

To accomplish this task, the normal derivatives of  $\mathcal{V}$  on either side of the solid/liquid and  $\alpha/\beta$  interfaces are expressed in terms of  $\psi_1$  and  $\psi_2$  using the jump properties listed earlier, and the results are substituted into equations (7) and (10). This procedure results in the following set of integral equations for  $\psi_1$  and  $\psi_2$ :

$$S_2(x) \psi_1(x) + S_3(x) \left\{ \cos \theta(x) Z_1^{f*}[\psi_2](x) + \frac{d}{dn_x} V_{2+f(\delta)}^\delta[\psi_2](x, f(x)) + \cos \theta(x) \right\} = 0 \quad (46)$$

and

$$\frac{1}{2} \left( \frac{k_\alpha}{k_\beta} + 1 \right) \psi_2(y) + \left( \frac{k_\alpha}{k_\beta} - 1 \right) \cdot \left\{ \frac{\partial}{\partial x} V_1^f[\psi_2](\delta, y) + Z_{2+f(\delta)}^{\delta*}[\psi_2](y) \right\} = 0, \quad (47)$$

where

$$S_2(x) = \begin{cases} \frac{1}{2} \left( 1 + \frac{k_\alpha}{k_\beta} \right), & x \in [0, \delta), \\ \frac{1}{2} \left( 1 + \frac{k_\beta}{k_\alpha} \right), & x \in (\delta, 1], \end{cases} \quad (48a)$$

and

$$S_3(x) = \begin{cases} \frac{k_{\alpha}}{k_1} - 1 & , \quad x \in [0, \delta), \\ \frac{k_{\beta}}{k_1} - 1 & , \quad x \in (\delta, 1] . \end{cases} \quad (48b)$$

Once these equations are solved,  $\mathcal{V}(x, y)$  is completely determined for a given interface shape,  $f(x)$  (at least to within an arbitrary constant).

As a final result, we can employ equations (20) and (37)-(41) to obtain the explicit forms of equations (44), (46), and (47). Thus,

$\mathcal{V}(x, y)$  is given by

$$\begin{aligned} \mathcal{V}(x, y) = & \text{const.} + y + \int_0^1 K_3(x, z, y, f(z)) \phi_1(z) dz \\ & + \int_{f(\delta)}^{-\infty} K_4(x, y, u) \phi_2(u) du, \end{aligned} \quad (49)$$

and the integral equations assume the form

$$\begin{aligned} S_2(x) \phi_1(x) + S_3(x) \int_0^1 K_5(x, z, f(x), f(z)) \phi_1(z) dz \\ + S_3(x) \int_{f(\delta)}^{-\infty} K_7(x, f(x), u) \phi_2(u) du + S_3(x) = 0, \end{aligned} \quad (50)$$

$$\frac{1}{2} \left( \frac{k_\alpha}{k_\beta} + 1 \right) \Phi_2(y) + \left( \frac{k_\alpha}{k_\beta} - 1 \right) \int_{f(\delta)}^{-\infty} K_6(y, u) \Phi_2(u) du$$

$$+ \left( \frac{k_\alpha}{k_\beta} - 1 \right) \int_0^1 K_8(\xi, y, f(\xi)) \Phi_1(\xi) d\xi = 0 \quad (51)$$

$$\left\{ \begin{array}{l} x, \xi \in [0, 1] \\ y, u \in (-\infty, f(\delta)) \end{array} \right\},$$

where

$$K_7(x, f(x), u) = \frac{d}{dn_x} K_+(x, f(x), u)$$

$$= -\frac{1}{2} - \frac{\sinh \pi (f(x) - u) + \tan \theta(x) \sin \pi (x - \delta)}{4 [\cosh \pi (f(x) - u) - \cos \pi (x - \delta)]}$$

$$- \frac{\sinh \pi (f(x) - u) + \tan \theta(x) \sin \pi (x + \delta)}{4 [\cosh \pi (f(x) - u) - \cos \pi (x + \delta)]}, \quad (52)$$

$$K_8(\xi, y, f(\xi)) = \frac{\partial}{\partial x} K_3(\delta, \xi, y, f(\xi))$$

$$= \frac{-\sin \pi (\delta + \xi)}{4 [\cosh \pi (y - f(\xi)) - \cos \pi (\delta + \xi)]}$$

$$- \frac{\sin \pi (\delta - \xi)}{4 [\cosh \pi (y - f(\xi)) - \cos \pi (\delta - \xi)]}, \quad (53)$$

and where  $\Phi_1 = \psi_1 / \cos \theta$  and  $\Phi_2 = \psi_2$ .

As in the case of chemical diffusion, equations (49)-(51) provide only partial solutions to the free-boundary problem. In order to complete the solution, the interfacial coupling conditions must be considered.

### 3.3 Construction of the Formal Solution

Equations (9), (26), (28), (33), (45), (50), and (51) comprise a system of nine equations in the eleven unknowns  $\hat{c}_2(x)$ ,  $\tilde{c}_2(x)$ ,  $A(x, \omega)$ ,  $\hat{c}_{S\alpha}(x)$ ,  $\hat{c}_{S\beta}(x)$ ,  $f(x)$ ,  $\phi_1(x)$ ,  $\phi_2(y)$ ,  $\rho_\lambda$ ,  $G_\lambda$ , and  $\delta$ ; with  $\lambda$ ,  $\omega$ , and the torque term acting as parameters. Hence, two additional equations must be obtained in order to complete the analysis. It will be shown in this section that the required equations are provided by the interfacial constitutive relation (equation (8)), and the triple-point conditions, equations (13).

We begin by considering the first of these conditions, namely equation (8). Using the relations  $f = F/\lambda$  and  $\psi = T/G_S \lambda$ , equation (8) can be written as

$$\frac{1}{\kappa} (\hat{\psi} - \psi_E) = -\frac{m_\alpha \lambda}{2\alpha} (\hat{c}_2 - c_E) + \kappa \quad (\lambda \in [0, \delta]) \quad (54a)$$

$$\frac{1}{\mu} (\hat{v} - v_E) = \frac{m\beta\lambda}{a\alpha} (\hat{c}_2 - c_E) + \left(\frac{a\beta}{a\alpha}\right) \kappa, \quad (x \in (0, 1)) \quad (54b)$$

where  $\kappa$  is now given by  $f''/(1+f'^2)^{3/2}$  and  $\mu = \gamma_{\mu\sigma} / \lambda^2 G_S \Delta S_{f\alpha}$ . Setting the constant in equation (49) equal to  $v_E$  and substituting equations (49) and (28) into equation (54) then results in

$$\begin{aligned} \frac{f''}{(1+f'^2)^{3/2}} - \frac{f}{\mu} &= \frac{1}{\mu} \int_0^1 K_3(x, z, f(x), f(z)) \phi_1(z) dz \\ &+ \frac{1}{\mu} \int_{f(\delta)}^{-\infty} K_4(x, f(x), u) \phi_2(u) du \quad \left\{ \begin{array}{l} x \in [0, \delta) \\ z \in [0, 1] \\ u \in (-\infty, f(\delta)) \end{array} \right\} \quad (55a) \end{aligned}$$

$$+ \frac{m\alpha\lambda}{a\alpha} \left[ \tilde{c}_2(x) + (c_\infty - c_E) + \int_0^1 A(z, u) e^{-2\omega(f(x) - f(z))} dz \right],$$

$$\begin{aligned} \alpha_1 \frac{f''}{(1+f'^2)^{3/2}} - \frac{f}{\mu} &= \frac{1}{\mu} \int_0^1 K_3(x, z, f(x), f(z)) \phi_1(z) dz \\ &+ \frac{1}{\mu} \int_{f(\delta)}^{-\infty} K_4(x, f(x), u) \phi_2(u) du \quad \left\{ \begin{array}{l} x \in (\delta, 1] \\ z \in [0, 1] \\ u \in (-\infty, f(\delta)) \end{array} \right\} \quad (55b) \end{aligned}$$

$$- \alpha_2 \frac{m\alpha\lambda}{a\alpha} \left[ \tilde{c}_2(x) + (c_\infty - c_E) + \int_0^1 A(z, u) e^{-2\omega(f(x) - f(z))} dz \right],$$

where  $\alpha_1 = a_\beta / a_\alpha$  and  $\alpha_2 = m_\beta / m_\alpha$  .

Equation(55) essentially provides the coupling between the two diffusion processes, and in conjunction with the boundary and triple point conditions

$$\sin \Theta_\alpha + \alpha_3 \sin \Theta_\beta = \alpha_4 \quad (56a)$$

$$\cos \Theta_\alpha - \alpha_3 \cos \Theta_\beta = (\text{torque terms}) \quad (56b)$$

$$f(d_-) = f(d_+) \quad (56c)$$

$$f'(0) = f'(1) = 0, \quad (56d)$$

where  $\alpha_3 = \gamma_{\beta 2} / \gamma_{\alpha 2}$  and  $\alpha_4 = \gamma_{\alpha \beta} / \gamma_{\alpha 2}$  , constitutes one of the sought-after equations.

The second equation results from the fact that equations (56) are in general inconsistent with respect to equation (55) when the torque term is specified. This inconsistency arises because only second-order derivatives with respect to  $f(x)$  appear in equation (55), thus implying that equations (56a) and (56b) cannot be prescribed independently. Rather, only one of these conditions can be prescribed a priori; the remaining condition must be satisfied a posteriori.

The heretofore undetermined term  $A(\lambda, \omega)$  provides the system with the flexibility necessary to resolve this inconsistency. Thus, when one of the triple-point conditions is prescribed,  $A(\lambda, \omega)$  can usually be adjusted in such a way as to assure satisfaction of the remaining condition. This procedure leads to an additional relation (henceforth denoted as(\*)) between  $A(\lambda, \omega)$  and the remaining unknowns, thereby providing the second soughtafter equation.†

The completed system consisting of equations (9), (26), (28), (33), (45), (50), (51), (55), (56), and (\*) can be simplified somewhat by using equations (9), (26b), and (28) to eliminate the quantities  $\hat{c}_\lambda(\lambda)$ ,  $\hat{c}_{sa}(\lambda)$ ,  $\hat{c}_{sp}(\lambda)$ , and  $\beta_\lambda$ . Thus, with the aid of the aforementioned equations, equation (26a) can be written as

---

† We have not, as yet, been able to express relation (\*) explicitly for the general case considered here. However, in the next section it will be shown that a definitive expression for (\*) can be obtained when several reasonable approximations are made.

$$c_{\infty} [\delta p_{\alpha} + (1-\delta) p_{\beta}] = c_{\alpha E} \delta p_{\alpha} + c_{\beta E} (1-\delta) p_{\beta}$$

$$+ p_{\alpha} \int_0^{\delta} \frac{m_{\alpha}}{n_{\alpha}} \left[ \tilde{C}_2(t) + (c_{\infty} - c_E) + \int_0^1 A(z, \omega) e^{-2\omega(f(t)-f(z))} dz \right] dt$$

(57)

$$+ p_{\beta} \int_{\delta}^1 \frac{m_{\beta}}{n_{\beta}} \left[ \tilde{C}_2(t) + (c_{\infty} - c_E) + \int_0^1 A(z, \omega) e^{-2\omega(f(t)-f(z))} dz \right] dt,$$

and equation (33) assumes the form

$$-\frac{1}{2} \tilde{C}_2(x) + \int_0^1 K_1(x, z, f(x), f(z), \omega) \tilde{C}_2(z) dz$$

(33)

$$+ \int_0^1 K_2(x, z, f(x), f(z), \omega) S_1(z) dz = 0 \quad (x, z \in [0, 1])$$

with

$$S_1(x) = c_{\infty} - \frac{p_{\alpha}}{\delta p_{\alpha} + (1-\delta) p_{\beta}} \left\{ c_{\alpha E}$$

$$+ \frac{m_{\alpha}}{n_{\alpha}} \left[ \tilde{C}_2(x) + (c_{\infty} - c_E) + \int_0^1 A(z, \omega) e^{-2\omega(f(x)-f(z))} dz \right] \right\} \quad (58a)$$

$$(x \in [0, \delta])$$

$$S_1(x) = c_{\infty} - \frac{p_{\beta}}{\delta p_{\alpha} + (1-\delta)p_{\beta}} \left\{ c_{\beta E} + \frac{m_{\beta}}{n_{\beta}} \left[ \tilde{c}_2(x) + (c_{\infty} - c_E) + \int_0^1 A(z, \omega) e^{-\lambda \omega (f(x) - f(z))} dz \right] \right\}$$

( $x \in (\delta, 1]$ ).

(58b)

Equations (55), (56), (57), (33), and (\*), together with equations (45), (50), and (51), i.e.,

$$\frac{G_1}{G_5} = 1 - \int_0^1 \phi_1(z) dz - \int_{f(\delta)}^{-\infty} \phi_2(u) du, \quad (59)$$

(obtained from eq. (45)),

$$S_2(x) \phi_1 + S_3(x) \int_0^1 K_5(x, z, f(x), f(z)) \phi_1(z) dz + S_3(x) \int_{f(\delta)}^{-\infty} K_7(x, f(x), u) \phi_2(u) du + S_3(x) = 0, \quad (50)$$

and

$$\frac{1}{2} \left( \frac{k_{\alpha}}{k_{\beta}} + 1 \right) \phi_2(y) + \left( \frac{k_{\alpha}}{k_{\beta}} - 1 \right) \int_{f(\delta)}^{-\infty} K_6(y, u) \phi_2(u) du + \left( \frac{k_{\alpha}}{k_{\beta}} - 1 \right) \int_0^1 K_8(z, y, f(z)) \phi_1(z) dz = 0 \quad (51)$$

$$\left\{ \begin{array}{l} x, z \in [0, 1] \\ u, y \in (-\infty, f(\delta)) \end{array} \right\},$$

now form a system of equations (hereafter denoted as System I) in the unknowns  $\tilde{C}_2(x)$ ,  $f(x)$ ,  $\phi_1(x)$ ,  $\phi_2(y)$ ,  $A(x, \omega)$ ,  $\mathcal{J}$ , and  $G_{\mathcal{L}}$ . Once these quantities have been determined, the bulk temperature and solute distributions can be calculated from equations (49) and (32), and the problem is solved.

#### 4. SOME ASPECTS OF THE BEHAVIOR OF SYSTEM I

Since obtaining solutions to System I is tantamount to solving the original boundary-value problem, the remainder of this report will focus almost exclusively on that task. We begin, in the first part of this section, by examining the nature of the torque term in equation (56b), and utilizing the information thus obtained to qualitatively analyze the behavior of the solutions to System I. In the remaining parts of the section, several approximations are introduced, which are then used to develop both a quantitative theory of the lamellar-rod transition, and a numerically tractable version of System I.

##### 4.1 A Qualitative Analysis of System I and Its Implications

###### 4.1.1 The torque at the triple point

As discussed at the end of Section 2, the results of Hunt and Jackson [8] indicate that it is possible to maintain a lamellar morphology over a range of freezing rates for a fixed lamellar spacing. Because it is difficult to envision a mechanism by which the crystallographic orientation

relationship between the two solid phases could have varied during these experiments, and because there is a one-to-one relationship between the relative orientations and the torque at the triple point, the torque term in equation (56b) will henceforth be regarded as independent of  $\omega$  for given values of  $\lambda$  and  $G_s$ .

#### 4.1.2 A qualitative examination of System I

A considerable amount of insight into the behavior of System I can be gained by qualitatively examining the interaction between the surface energy and diffusion effects at the  $\alpha/\beta$ /liquid triple point.

It suffices to consider the limiting case  $k_\alpha = k_\beta = k_\lambda$  and  $n_\alpha = n_\beta = \infty$ . This choice greatly simplifies the analysis, but in no way affects its generality. When  $k_\alpha = k_\beta = k_\lambda$  and  $n_\alpha = n_\beta = \infty$ , it follows from equations (50), (51), (57), and (59) that  $G_s = G_\lambda$ ,  $\phi_1(x) = \phi_2(x) = 0$ , and  $J$  is a known constant. It therefore remains only to examine the behavior of equations (33), (\*), and equation (55) with  $\phi_1(x) = \phi_2(x) = 0$ .

Equation (33) is a linear Fredholm equation of the second kind with respect to  $\tilde{\xi}_2(x)$ , and it is always possible (at least in theory) to obtain an explicit solution for  $\tilde{\xi}_2(x)$  in terms of the resolvent kernel. Assuming this were actually carried out, the resulting expression for  $\tilde{\xi}_2(x)$  could be substituted into equation (55), thereby yielding the following equation for  $f(x)$  :

$$\frac{f''}{(1+f'^2)^{3/2}} - \frac{f}{\mu} = G_1(x, f(x), A(x, \omega), \omega, \dots) \quad (x \in [0, \delta]) \quad (60a)$$

$$\alpha_1 \frac{f''}{(1+f'^2)^{3/2}} - \frac{f}{\mu} = G_2(x, f(x), A(x, \omega), \omega, \dots) \quad (x \in (\delta, 1]), \quad (60b)$$

where  $G_1$  and  $G_2$  are known functionals.

Now suppose that equations (60a) and (60b) could be explicitly integrated, subject to the boundary conditions

$$f'(0) = 0, \quad f'(\delta) = -\tan \Theta_\omega \quad (\text{for equation (60a)})$$

$$f'(1) = 0, \quad f'(\delta) = \tan \Theta_\beta \quad (\text{for equation (60b)})$$

Then, it should always be possible to obtain relations of the form

$$F_1(f(d), \Theta_\alpha, A, \omega, \dots) = 0 \quad (\text{for equation (60a)})$$

$$F_2(f(d), \Theta_\beta, A, \omega, \dots) = 0, \quad (\text{for equation (60b)}),$$

which, upon the elimination of  $f(d)$ , can be reduced to an expression relating  $\Theta_\alpha$  and  $\Theta_\beta$ , i.e.,

$$F_3(\Theta_\alpha, \Theta_\beta, A, \omega, \dots) = 0. \quad (61)$$

In principle, equations (56a), (56b), and the requirement that  $\Theta_\alpha$  and  $\Theta_\beta$  be independent of  $\omega$  (again,  $\lambda$  and  $G_S$  are regarded as fixed) should provide sufficient information to determine  $\Theta_\alpha$ ,  $\Theta_\beta$ , and  $A(\chi, \omega)$  for any relative orientation relationship (henceforth denoted by the five-dimensional vector  $\underline{\xi}$ ) for which equations (56a) and (56b) admit to real solutions. Indeed, expanding equation (61) with respect to  $\omega$  about the point  $\omega = 0$  results in

$$F_3(\Theta_\alpha, \Theta_\beta, A(\chi, \omega), \omega, \dots) = \\ F_3(\Theta_\alpha, \Theta_\beta, A(\chi, 0), \dots) + O(\omega) = 0,$$

which can be satisfied by solving  $F_3(\Theta_\alpha, \Theta_\beta, A(\lambda, \omega), \dots) = 0$  for  $A(\lambda, \omega)$  and then adjusting the higher order terms in  $A(\lambda, \omega)$  to ensure that the  $O(\omega)$  terms in  $F_3$  vanish. Once  $\Theta_\alpha$ ,  $\Theta_\beta$ , and  $A(\lambda, \omega)$  have been determined, there should be no difficulty in completing the solution by obtaining  $f(\lambda)$  and  $\hat{c}_2(\lambda)$  by a simple integration procedure. Hence, it can be inferred that lamellar solutions (with  $\lambda$  and  $G_s$  regarded as fixed) should exist as a function of  $\omega$  in the range  $\omega \in (0, \infty)$  for all values of  $\xi$  corresponding to real values of the angles  $\Theta_\alpha$  and  $\Theta_\beta$ .

All such solutions thus obtained, however, might not have particularly desirable properties. For instance, it is shown in Appendix C that the solutions associated with the preceding analysis generally imply that the interfacial solute concentration,  $\hat{c}_2(\lambda)$ , is of the form

$$\hat{c}_2(\lambda) = c_0(\lambda) + c_E + O(\omega), \quad (62a)$$

where

$$\lim_{\lambda \rightarrow \infty} c_0(\lambda) = \text{const. (planar interface limit)} \quad (62b)$$

and

$$\lim_{\lambda \rightarrow 0} c_0(\lambda) = \infty. \quad (62c)$$

But equation (62b) implies that  $\hat{c}_2(\lambda) \neq c_E$  as  $\omega \rightarrow 0$  and  $\lambda \rightarrow \infty$  (the planar interface equilibrium limit), which is clearly undesirable because  $\hat{c}_2(\lambda)$  should equal  $c_E$  in this limit. Moreover, equation (62c) implies that lamellar solutions are possible only when  $\lambda > \lambda_{min}$ , where  $\lambda_{min}$  is the value of  $\lambda$  such that  $\hat{c}_2 \notin [0, 1]$ . This, again, is bothersome because it is reasonable to expect that, under certain conditions, lamellar solutions should be possible for arbitrarily small values of  $\lambda$ . Hence, it appears that a restriction of the form

$$\begin{aligned} \hat{c}_2(\lambda) &= \tilde{c}_2(\lambda) + c_\infty + \int_0^1 A(z, \omega) e^{-2\omega(f(z) - f(zi))} dz \\ &= c_E + O(\omega) \end{aligned} \quad (63)$$

should be imposed on the solutions to System I.

Inclusion of the above restriction necessitates a modification of the preceding analysis, because, as will be shown in Section 4.2, the result of applying equation (63) is to preset the term  $A(\chi, 0)$ .

Rather than expand  $F_3$  in equation (61) about the point  $\omega = 0$ , let us now expand  $F_3$  about some point  $\omega_{loc\omega}$ , where  $\omega_{loc\omega}$  is in general a function of  $\xi$ . The resulting expression, i.e.,

$$F_3(\Theta_\alpha, \Theta_\beta, A(\chi, \omega), \omega, \dots) =$$

$$F_3(\Theta_\alpha, \Theta_\beta, A(\chi, \omega_{loc\omega}), \dots) + O(\omega - \omega_{loc\omega}) = 0$$

(which, by the way, is precisely that (\*) relation mentioned in Section 3.3), can be satisfied by solving  $F(\Theta_\alpha, \Theta_\beta, A(\chi, \omega_{loc\omega}), \dots) = 0$  for  $\omega_{loc\omega}$  and  $A(\chi, \omega_{loc\omega})$  such that equation (63) is satisfied, and then adjusting the higher order terms in  $A(\chi, \omega)$  in such a way as to make the  $O(\omega - \omega_{loc\omega})$  terms in  $F_3$  vanish. It then follows by reasoning similar to that employed in the previous analysis that lamellar solutions, parametrized with respect to  $\omega$ , should exist for  $\omega$  in the range  $(\omega_{loc\omega}, \infty)$  for

all values of  $\xi$  which correspond to real values of  $\Theta_{\alpha}$  and  $\Theta_{\beta}$ .†

Finally, reference should be made to the end of Section 2, where it was mentioned that lamellar freezing generally proceeds at a rate which is uniquely related to the lamellar spacing. This fact implies that the system selects an operating point,  $\omega_{op}$ , which is a function of  $\lambda$ ,  $G_S$ , and  $\delta$ . Hence, as a practical matter, we need only be concerned with solutions to System I for which  $\omega_{low} \leq \omega_{op}$ .

#### 4.1.3 The implications of the analysis

The results just discussed have some interesting physical implications. For instance, in view of these considerations, the following three modes of behavior are possible in binary eutectic alloy systems:

Case 1.  $\omega_{low} > \omega_{op}$  for all values of  $\lambda$ ,  $G_S$ ,  $\xi$ , and volume fraction,  $\delta$ . This is the case in which lamellar growth is never possible, and is most likely realized in systems which exhibit "abnormal" microstructures.

† The quantity  $\omega_{low}$  could conceivably be infinite, in which case it is simply impossible to satisfy the (\*) relation.

Case 2.  $\omega_{l.o.v} \leq \omega_{op}$  for all values of  $\lambda$ ,  $G_S$ ,  $\xi$ , and  $f$ . This is the case in which lamellar growth is always possible.

Case 3.  $\omega_{l.o.v} \leq \omega_{op}$  for some values of  $\lambda$ ,  $G_S$ ,  $\xi$ , and  $f$ . This case is frequently encountered in systems capable of cooperative growth. In these systems, the occurrence of lamellar growth is favored by either high  $G/V$  ratios or volume fractions sufficiently close to 0.5. When these conditions are not met, a rod-like morphology is usually observed.

Given the required thermodynamic and transport data, the theory should yield quantitative results regarding these modes of behavior for any non-faceting eutectic system.

As a final remark, it should be mentioned that there is reason to believe that  $\omega_{l.o.v}$  is a very sensitive function of  $\xi$ , particularly when the system operates near a cusp in a generalized  $\lambda_{\alpha\beta}$  - plot. If this is indeed the case, then it may be inferred that the range of admissible orientation relationships during lamellar growth (i.e. those values of  $\xi$  for which  $\omega_{l.o.v} < \omega_{op}$ )

is quite limited. This result is in accord with the majority of experimental observations.

#### 4.2 Asymptotic Estimates as $\omega \rightarrow 0$

In order to proceed further, it is necessary to have available certain asymptotic estimates for System I as  $\omega \rightarrow 0$ .

With the aid of equation (63), the required estimates may be ascertained in a relatively straightforward manner. Thus, substituting equation (63) into equations (55), (57), and (58) gives

$$\alpha(x) \frac{f''}{(1+f'^2)^{3/2}} - \frac{f}{\mu} = \frac{1}{\mu} \int_0^1 K_3(x, z, f(x), f(z)) \phi_1(z) dz \quad (64)$$

$$+ \frac{1}{\mu} \int_{f(\delta)}^{-\infty} K_4(x, f(x), u) \phi_2(u) du + O(\omega) \quad \left. \begin{array}{l} x, z \in [0, 1] \\ u \in (-\infty, f(\delta)) \end{array} \right\},$$

where

$$\alpha(x) = \begin{cases} 1, & x \in [0, \delta) \\ \alpha_1, & x \in (\delta, 1] \end{cases}; \quad (65)$$

$$J = J^* + O(\omega),$$

where

$$J^* = \frac{(C_{\beta E} - C_{\infty})\rho_{\beta}}{\rho_{\beta}(C_{\beta E} - C_{\infty}) + \rho_{\alpha}(C_{\infty} - C_{\alpha E})}; \quad (66)$$

and

$$S_1(x) = C_{\infty} - \frac{\rho_{\alpha} C_{\alpha E}}{\rho_{\alpha} + (1-\delta)\rho_{\beta}} + O(\omega) \quad (x \in [0, \delta]) \quad (67a)$$

$$S_1(x) = C_{\infty} - \frac{\rho_{\beta} C_{\beta E}}{\rho_{\alpha} + (1-\delta)\rho_{\beta}} + O(\omega) \quad (x \in (\delta, 1]). \quad (67b)$$

Also, (1) expanding the kernels in equation (33) in a Taylor series with respect to  $\omega$ , i.e.,

$$K_1(x, z, f(x), f(z), \omega) = C_1(x, z, f(x), f(z)) + O(\omega) \quad (68a)$$

and

$$K_2(x, z, f(x), f(z), \omega) = \omega C_2(x, z, f(x), f(z)) + O(\omega^2), \quad (68b)$$

where

$$C_1(x, z, f(x), f(z)) = \frac{\sinh \pi (f(x) - f(z)) - \tan \theta(z) \sin \pi (x+z)}{4 [\cosh \pi (f(x) - f(z)) - \cos \pi (x+z)]}$$

$$+ \frac{\tan \theta(z) \sin \pi (x-z) + \sinh \pi (f(x) - f(z))}{4 [\cosh \pi (f(x) - f(z)) - \cos \pi (x-z)]} + \frac{1}{2} \quad (69)$$

and

$$C_2(x, z, f(x), f(z)) = -\frac{1}{2\pi} \left\{ \ln [2 \cosh \pi (f(x) - f(z)) - 2 \cos \pi (x-z)] \right.$$

$$+ \ln [2 \cosh \pi (f(x) - f(z)) - 2 \cos \pi (x+z)] \left. \right\} \quad (70)$$

$$- (f(x) - f(z)),$$

and (2) utilizing equations (63)-(65) along with the relations

$$C_{\infty} - \frac{\rho_{\alpha} C_{\alpha E}}{\delta^* \rho_{\alpha} + (1 - \delta^*) \rho_{\beta}} = (1 - \delta^*) \left[ \frac{C_{\beta E} \rho_{\beta} - C_{\alpha E} \rho_{\alpha}}{\delta^* \rho_{\alpha} + (1 - \delta^*) \rho_{\beta}} \right] \quad (71a)$$

and

$$C_{\infty} - \frac{\rho_{\beta} C_{\beta E}}{\delta^* \rho_{\alpha} + (1 - \delta^*) \rho_{\beta}} = - \delta^* \left[ \frac{C_{\beta E} \rho_{\beta} - C_{\alpha E} \rho_{\alpha}}{\delta^* \rho_{\alpha} + (1 - \delta^*) \rho_{\beta}} \right] \quad (71b)$$

gives for  $\tilde{C}_2(x)$  (via a perturbation analysis of equation (33)):

$$\tilde{C}_2(x) = \omega \left[ \frac{C_{\beta E} \rho_{\beta} - C_{\alpha E} \rho_{\alpha}}{\delta^* \rho_{\alpha} + (1 - \delta^*) \rho_{\beta}} \right] C_2^*(x) + O(\omega^2), \quad (72)$$

where  $C_2^*(x)$  is the solution to the equation

$$\begin{aligned} & -\frac{1}{2} C_2^*(x) + \int_0^1 C_1(x, z, f(x), f(z)) C_2^*(z) dz \\ & + (1 - \delta^*) \int_0^{\delta^*} C_2(x, z, f(x), f(z)) dz - \delta^* \int_{\delta^*}^1 C_2(x, z, f(x), f(z)) dz \\ & = 0. \end{aligned} \quad (73)$$

Finally, an explicit statement of the restriction on  $A(x, \omega)$  mentioned in Section 4.1.2 may be obtained by substituting equation (72) into

equation (63) and taking the limit as  $\omega \rightarrow 0$  .

Thus,  $A(x, \omega)$  must always satisfy the constraint

$$\int_0^1 A(\xi, 0) d\xi = c_E - c_{\infty} . \quad (74)$$

#### 4.3 On the Existence or Nonexistence of Solutions to System I for $\omega_{l, c, \omega} = 0$ .

In order to gain additional insight into the behavior of System I, it is worthwhile to examine the constraints at the triple point for a class of solutions for which specific results can be obtained by relatively elementary methods; namely the solutions corresponding to  $\omega_{l, c, \omega} = 0$  for

$$\kappa_{\alpha} = \kappa_{\beta} = \kappa_{\gamma} .$$

It will be assumed that a particular orientation  $\vec{\xi}$  can always be selected such that equation (56b) is satisfied. Therefore, the problem is to determine the conditions under which the constraints on the triple-point angles due to diffusion effects are compatible with the requirements of equation (56a).

It is evident from the discussion in Section 4.1.2 that we need only investigate the  $\mathbf{O}(1)$  (with respect to  $\omega$  ) terms in System I, because once compatibility is attained to  $\mathbf{O}(1)$ , it can be maintained to any

order simply by adjusting the higher order terms in  $A(x, \omega)$ .

When  $k_\alpha = k_\beta = k_\lambda$ , it follows from the considerations discussed in Section 4.1.2 that  $\phi_1 = \phi_2 = 0$  and  $G_S = G_\lambda = G$ . Moreover, setting  $\omega = 0$  in equations (66) and (72) results in  $f = f^*$  and  $\tilde{c}_\lambda(x) = 0$ . Hence, it remains only to consider the limiting form of equation (64) with  $\omega = \phi_1 = \phi_2 = 0$ , i.e.,

$$\frac{f''}{(1+f'^2)^{3/2}} - \frac{f}{\mu} \quad (\lambda \in [0, \delta]) \quad (75a)$$

and

$$\alpha_1 \frac{f''}{(1+f'^2)^{3/2}} - \frac{f}{\mu} \quad (\lambda \in [\delta, 1]), \quad (75b)$$

and, in particular, implement a procedure similar to that described in Section 4.1.2 to obtain explicit expression<sup>5</sup> for the triple-point angles.

#### 4.3.1 Integration of equation (75) for large values of $\mu$

When the parameter,  $\mu$ , is sufficiently large, it can be shown that

$$f(\delta) \gg \max_{[0, 1]} |f(x) - f(\delta)|,$$

which implies that

$$\int_0^\delta f(z) dz \cong \delta f(\delta) \quad \text{and} \quad \int_\delta^1 f(z) dz \cong (1-\delta) f(\delta). \quad (76)$$

# With the aid of equations (76), the relation

$$\frac{f''}{(1+f'^2)^{3/2}} = \frac{d}{dx} \left( \frac{f'}{(1+f'^2)^{1/2}} \right) = -\frac{d}{dx} \sin \theta,$$

and the boundary conditions  $f'(0) = f'(1) = 0$ , equations (75a) and (75b) can now be integrated out from the triple point to their respective end-points in a routine manner, thereby providing the following expressions for  $\Theta_\alpha$  and  $\Theta_\beta$  in terms of  $f(\delta)$ :

$$\sin \Theta_\alpha = -\frac{\delta f(\delta)}{\mu} \quad (77a)$$

and

$$\sin \Theta_\beta = \frac{-(1-\delta) f(\delta)}{\mu}. \quad (77b)$$

Eliminating  $f(\delta)$  from equations (77) then gives

$$\alpha_1 \delta \sin \Theta_\beta - (1-\delta) \sin \Theta_\alpha = 0, \quad (78)$$

which, when combined with equation (56a), yields the following expressions for  $\Theta_\alpha$  and  $\Theta_\beta$  :

$$\sin \Theta_\alpha = \frac{\alpha_1 \alpha_4(\xi) \delta}{\alpha_1 \delta + \alpha_3 (1-\delta)} \quad (79a)$$

and

$$\sin \Theta_\beta = \frac{\alpha_4(\xi) (1-\delta)}{\alpha_1 \delta + \alpha_3 (1-\delta)}. \quad (79b)$$

Equations (79) provide the required angles; however, it soon becomes apparent that certain conditions must be met in order for the values of  $\sin \Theta_\alpha$  and  $\sin \Theta_\beta$  to be less than unity. For example, if  $\alpha_1$  is set equal to unity (this will be shown in Section 5 to be reasonable approximation for most systems), then a little algebra reveals that:

1. If  $|\alpha_4(\xi) - \alpha_3| > 1$ , then  $\sin \Theta_\alpha$  and  $\sin \Theta_\beta$ , as given by equation (79), can never be less than unity.

2. If  $|\alpha_4(\bar{\xi}) - \alpha_3| < 1$ , then

$\sin \Theta_\alpha$  and  $\sin \Theta_\beta$  can be less than unity only when  $\delta \in [\delta_{low}, \delta_{up}]$ ,

where

$$\delta_{low} = \begin{cases} 0 & \text{if } \alpha_3 \geq \alpha_4(\bar{\xi}) \\ \frac{\alpha_4(\bar{\xi}) - \alpha_3}{1 + \alpha_4(\bar{\xi}) - \alpha_3} & \text{if } \alpha_3 \leq \alpha_4(\bar{\xi}) \end{cases} \quad (80a)$$

and

$$\delta_{up} = \begin{cases} 1 & \text{if } \alpha_4(\bar{\xi}) \leq 1 \\ \frac{\alpha_3}{\alpha_4(\bar{\xi}) + \alpha_3 - 1} & \text{if } \alpha_4(\bar{\xi}) \geq 1, \end{cases} \quad (80b)$$

and where  $\delta_{low} \in [0, 0.5]$  and  $\delta_{up} \in [0.5, 1]$ .

The nonexistence condition  $|\alpha_4 - \alpha_3| > 1$  is not particularly interesting and merely represents a condition under which equation (56a) (and hence the triple-point equilibrium conditions) can never be satisfied. On the other hand, the second condition essentially states that even when

it is possible to attain triple-point equilibrium, solutions to System I corresponding to  $\omega_{low} = 0$  may not exist for large values of  $\mu$  if the volume fraction deviates sufficiently far from a value of 0.5. This condition has interesting physical ramifications which will be considered shortly.

As a final item, it should be mentioned that the results just obtained are asymptotically valid even when  $R_\alpha \neq R_\beta \neq R_c$ , because the terms involving  $\phi_1$  and  $\phi_2$  in equation (64) approach zero as  $\mu$  becomes large.

#### 4.3.2 Integration of equation (75) for arbitrary values of $\mu$

When the magnitude of  $\mu$  is arbitrary, equations (75a) and (75b) can still be reduced to quadratures; however the procedure is considerably more involved than that for large values of  $\mu$ .

Without going into details, it can be shown (e.g., ref [10]) that when equations (75) are integrated out from the triple point to their respective end-points (with  $\alpha_1 = 1$ ), the following expressions are obtained for  $\Theta_\alpha$  and  $\Theta_\beta$  in terms of  $f(f)$ :

$$\delta = (1 - \xi_\alpha^2/2) \frac{2\mu^{1/2}}{\xi_\alpha} \left[ K(\xi_\alpha) - F\left(\xi_\alpha, \frac{\pi - \Theta_\alpha}{2}\right) \right] \quad (81a)$$

$$- \frac{2\mu^{1/2}}{\xi_\alpha} \left[ \hat{E}(\xi_\alpha) - E\left(\xi_\alpha, \frac{\pi - \Theta_\alpha}{2}\right) \right]$$

and

$$1 - \delta = (1 - \xi_\beta^2/2) \frac{2\mu^{1/2}}{\xi_\beta} \left[ K(\xi_\beta) - F\left(\xi_\beta, \frac{\pi - \Theta_\beta}{2}\right) \right] \quad (81b)$$

$$- \frac{2\mu^{1/2}}{\xi_\beta} \left[ \hat{E}(\xi_\beta) - E\left(\xi_\beta, \frac{\pi - \Theta_\beta}{2}\right) \right],$$

where

$$\xi^2 = 4\mu / (4\mu + f^2(\delta) - 2\mu(1 - \cos \theta)), \quad (82)$$

and where  $K$ ,  $\hat{E}$ ,  $F$ , and  $E$  denote the complete and incomplete elliptic integrals of first and second kinds, respectively. Equations (81) comprise a

system of two equations in the three unknowns  $f(\mathcal{J})$ ,  $\Theta_\alpha$ , and  $\Theta_\beta$ , and upon elimination of  $f(\mathcal{J})$  yield a relation (henceforth denoted as (†)) between  $\Theta_\alpha$  and  $\Theta_\beta$ . It remains to investigate the system composed of relation (†) and equation (56a), and, in particular, determine the conditions under which real solutions are possible.

It is possible to derive closed-form asymptotic expressions for (†) in the limits of high and low values of  $\mu$ . Thus, with the aid of certain elementary properties of the elliptic integrals, it may be shown that  $\Theta_\alpha = \Theta_\beta$  as  $\mu \rightarrow 0$ . Moreover, as  $\mu \rightarrow \infty$ , (†) is simply given by equation (78). For the intermediate values of  $\mu$  however, (†) must be evaluated numerically.

Relation (†) has been evaluated as a function of  $\mu$  for a range of  $\mathcal{J}$  values. Some typical results are shown in Fig. 4 for  $\mathcal{J} = 0.45$  and 0.55, and in Fig. 5 for  $\mathcal{J} = 0.35$  and 0.65. The quantities  $\Theta_{\text{maj.}}$  and  $\Theta_{\text{min.}}$  are the interface slope angles at the triple point in the majority and minority phase, respectively, i.e.,

$$\Theta_{\min.} = \begin{cases} \Theta_{\alpha} & \text{for } \delta < 0.5 \\ \Theta_{\beta} & \text{for } \delta > 0.5 \end{cases}$$

and

$$\Theta_{\text{maj.}} = \begin{cases} \Theta_{\beta} & \text{for } \delta < 0.5 \\ \Theta_{\alpha} & \text{for } \delta > 0.5 . \end{cases}$$

Also shown in Figs. 4 and 5 is a hypothetical version of equation (56a) with  $\alpha_3 = 1$  and  $\alpha_4 = 1.7$ . Obviously, real solutions are possible for a specified value of  $\mu$  only if the curve corresponding to the (+) relation (the (+) curve) intersects the curve corresponding to equation (56a) (the Y-curve).

The conditions which determine whether or not the (+) and Y-curves intersect are readily ascertained. As before, the case in which  $|\alpha_4(\bar{x}) - \alpha_3| > 1$  can be immediately discounted, because equation (56a) can never be satisfied for any value of  $\mu$ . When  $|\alpha_4(\bar{x}) - \alpha_3| < 1$ , there are two possibilities:

1. If  $\alpha_4(\bar{x}) \leq 1$  and  $\alpha_3 \geq \alpha_4(\bar{x})$ , then, by equations (80), real solutions to equations

Fig. 4 — The triple point angle  $\Theta_{maj}$  as a function of  $\Theta_{min}$  as predicted by the (†) relation (the numbered) curves, and as predicted by a hypothetical version of equation (56a), namely  $\sin \Theta_{maj} + \sin \Theta_{min} = 1.7$ , for  $\delta = 0.45$  and  $0.55$ . In this case  $\delta \in [\delta_{low}, \delta_{up}]$ .

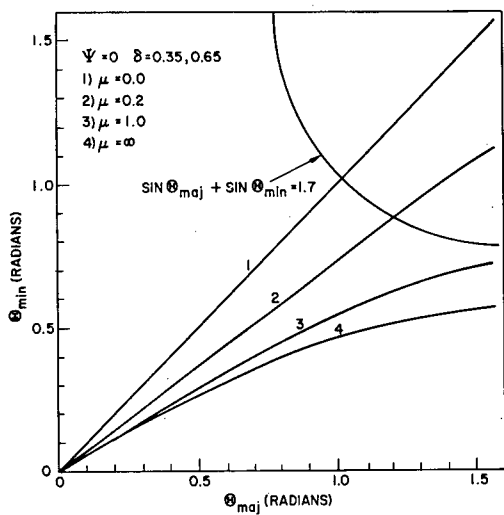
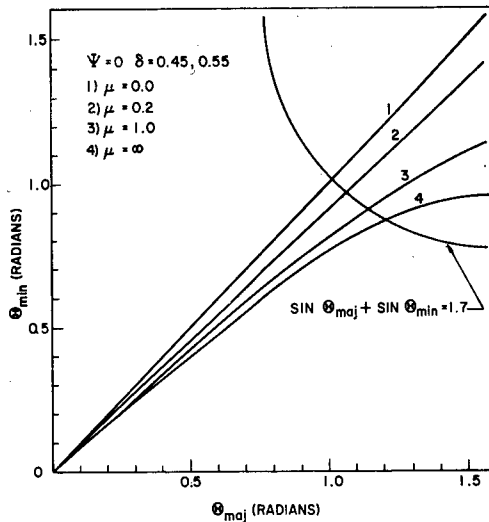


Fig. 5 — The triple point angle  $\Theta_{maj}$  as a function of  $\Theta_{min}$  as predicted by the (†) relation and the hypothetical version of equation (56a)  $\sin \Theta_{maj} + \sin \Theta_{min} = 1.7$  for  $\delta = 0.35$  and  $0.65$ . In this case  $\delta \notin [\delta_{low}, \delta_{up}]$ .

(56a) and (†) exist for large values of  $\mu$  for all values of  $\delta$  in the range  $[0,1]$ . Moreover, since the (†) curves corresponding to  $\mu = 0$  and  $\mu = \infty$  form the upper and lower bounds of an envelope within which all (†) curves must lie, real solutions exist for all values of  $\mu$  for  $\delta \in [0,1]$ .

2. If either  $\alpha_4(\xi) > 1$  or  $\alpha_3 < \alpha_4(\xi)$ , then real solutions exist for all values of  $\mu$  only for a restricted range of  $\delta$  values, i.e.,  $\delta \in [\delta_{low}, \delta_{up}]$ , where  $\delta_{low}$  and  $\delta_{up}$  are given by equation (80). If  $\delta$  lies outside this range, i.e.,  $\delta \notin [\delta_{low}, \delta_{up}]$ , then real solutions exist only when  $\mu$  is less than some maximum value,  $\mu_{max}$ . The cases for which  $\delta \in [\delta_{low}, \delta_{up}]$  and  $\delta \notin [\delta_{low}, \delta_{up}]$  are illustrated in Figs. 4 and 5, respectively.

The values of  $\mu_{max}$ , for any admissible version of equation (56a), may be obtained as a function of  $\delta$  by a simple graphical procedure.

Thus, denoting the value of  $\Theta_{min}$  at which  $\Theta_{maj} = \pi/2$  by  $\hat{\Theta}_{min}$  ( $\hat{\Theta}_{min}^{\dagger}$  for a (†) curve and  $\hat{\Theta}_{min}^Y$  for a Y-curve),  $\hat{\Theta}_{min}^{\dagger}$

for a given value of  $\delta$  may be plotted as a function of  $\mu$ , and  $\mu_{\max.}$  found by locating the point of intersection of the  $\hat{\omega}_{\min.}^{\dagger}$  curve with the horizontal line

$$\hat{\omega}_{\min.}^{\dagger} = \begin{cases} \sin^{-1}[\alpha_4(\frac{\xi}{\lambda}) - \alpha_3] & , \text{ for } \delta < 0.5, \\ \sin^{-1}\left[\frac{\alpha_4(\frac{\xi}{\lambda}) - 1}{\alpha_3}\right] & , \text{ for } \delta > 0.5. \end{cases}$$

Plots of  $\hat{\omega}_{\min.}^{\dagger}$  as a function of  $\mu$  are presented in Fig. 6 for  $0.2 \leq \delta \leq 0.8$  in increments of 0.05.

#### 4.3.3 A physical interpretation of the results

The discussions in Sections 4.3.1 and 4.3.2 were exclusively concerned with the solutions to System I corresponding to  $\omega_{\text{low}} = 0$ . However, if  $\omega_{\text{op}}$  is sufficiently small, then the nonexistence results derived therein should also furnish reasonable approximations to the conditions pertaining to the nonexistence of all solutions to System I for which  $\omega_{\text{low}} \in [0, \omega_{\text{op}}]$ . Assuming this to be the case, and assuming that the relative orientation,  $\xi$ , does not change appreciably with  $\delta$  or  $\mu$  (so that  $\alpha_4(\frac{\xi}{\lambda})$  can be taken as a constant), the aforementioned

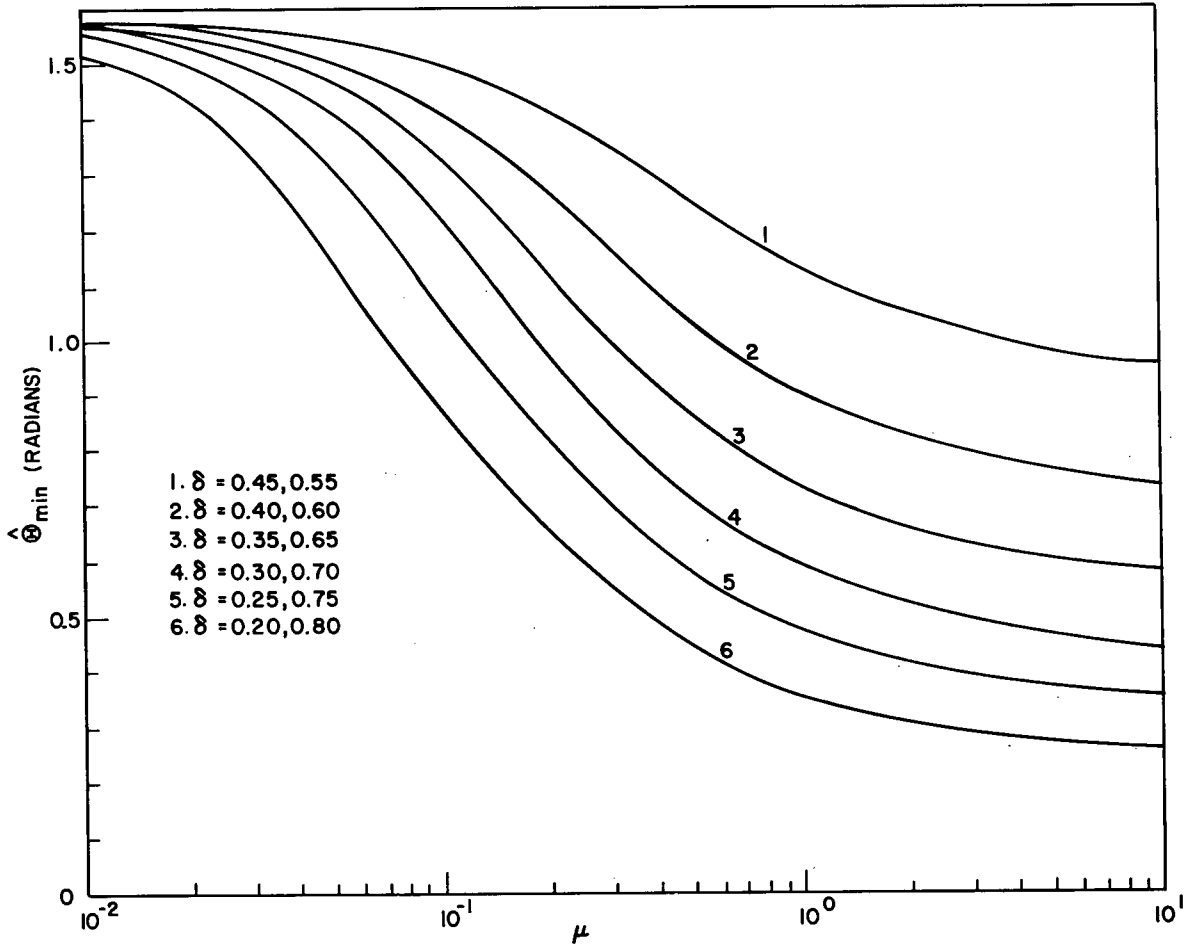


Fig. 6 — The quantity  $\hat{\Theta}_{\min}^{\dagger}$  as a function of  $\mu$  for a range of  $\delta$  values

results, in conjunction with the experimentally observed relation  $V \lambda^2 = \text{constant}$  (this implies that  $\mu \propto V/G$ ), then lead to the following predictions:

1. In systems for which  $|\alpha_4 - \alpha_3| \leq 1$ ,  $\alpha_4 < 1$ ; and  $\alpha_3 \geq \alpha_4$ , lamellar solutions which satisfy equation (63) are possible for all values of  $G/V$  and all volume phase fractions.

2. In systems for which  $|\alpha_4 - \alpha_3| \leq 1$ , and either  $\alpha_4 > 1$  or  $\alpha_3 < \alpha_4$ , lamellar solutions which satisfy equation (63) are possible for all values of  $G/V$  only when the volume fraction lies in the interval  $[\delta_{low}, \delta_{up}]$ , where  $\delta_{low}$  and  $\delta_{up}$  are given by equations (80). When the volume fraction lies outside this range, then lamellar solutions are possible only when  $G/V$  is greater than some critical value,  $(G/V)_c$ . Moreover, the value of  $(G/V)_c$  increases as the volume fraction approaches zero or unity.

The theoretical predictions relating to the impossibility of maintaining a lamellar morphology are in accord with a number of experimental observations of the lamellar-rod transition, e.g., refs. [11,12]. Hence, it is likely that this

transition is simply a physical manifestation of the aforementioned theoretical prediction. If indeed this is the case, then the results presented in this section in effect constitute an approximate theory of the lamellar-rod transition.

#### 4.4 An Approximate Version of System I

##### 4.4.1 The approximate equations

The task of obtaining solutions to System I is computationally formidable; hence, it is reasonable to seek approximations which will simplify the equations, and yet leave the fundamental nature of the solutions unaltered. In this spirit we now invoke the following approximations and assumptions:

1. The solute diffusion length is large compared to the lamellar spacing. This condition, which implies that  $\omega \ll 1$ , is satisfied in the majority of experimental situations.

2. The solid-liquid interface is approximately isothermal. This condition, which implies that  $\mu$  is large, is also frequently satisfied experimentally.

3. The nominal composition,  $c_\infty$ , sufficiently close to the eutectic composition,  $c_E$ , so as to permit a certain term in the expression for  $\tilde{c}_l(x)$  to be safely neglected.

4. The value of  $\omega_{op}$  is small, which implies that the behavior of System I is essentially characterized by the solution corresponding to  $\omega_{low} = 0$ .

5. The system can always adjust the triple-point torque (by selecting a suitable orientation relationship) so as to assure satisfaction of equation (56b) when  $\delta \in [\delta_{low}, \delta_{sup}]$ .

To derive the approximate equations, we first take note that the  $O(\omega)$  term in equation (65) and the  $O(\omega^2)$  term in equation (72) may be neglected as  $\omega$  becomes small with respect to unity. This leads to the following approximate expressions for  $\delta$  and  $\tilde{c}_l(x)$ :

$$\delta = \delta^* = \frac{(c_{\beta E} - c_\infty) \rho_\beta}{\rho_\beta (c_{\beta E} - c_\infty) + \rho_\alpha (c_\infty - c_{\alpha E})} \quad (66)$$

and

$$\tilde{c}_l(x) = \omega \Lambda_1 c_x^*(x), \quad (83)$$

where  $c_{\beta}^*(x)$  (henceforth referred to as the reduced interface concentration) satisfies equation (73) and

$$\Lambda_1 = \frac{c_{\beta E} \rho_{\beta} - c_{\alpha E} \rho_{\alpha}}{d \rho_{\alpha} + (1-d) \rho_{\beta}} . \quad (84)$$

An approximate expression for  $\hat{c}_{\beta}(x)$  can be obtained with the aid of equation (83). Thus, substituting equation (83) into equation (63), expanding the term

$$\int_0^1 A(z, \omega) e^{-2\omega(f(x)-f(z))} dz$$

with respect to  $\omega$ , invoking equation (74), and neglecting terms of  $O(\omega^2)$  gives

$$\begin{aligned} \hat{c}_{\beta}(x) = & \omega \Lambda_1 [c_{\beta}^*(x) + B_1] + c_E \\ & - 2\omega \int_0^1 A(z, 0) (f(x) - f(z)) dz , \end{aligned} \quad (85)$$

where  $B_1$  has no explicit  $\omega$  dependence and is a priori unknown.

Equation (85), together with the condition that the parameter  $\mu$  be large, can now be employed to obtain a simplified form of equation (55). It

is permissible to neglect the terms involving  $\phi_1$  and  $\phi_2$  in equation (55) because, as mentioned at the end of Section 4.3.1, these terms approach zero as  $\mu$  gets large. Therefore, if the term  $A(\zeta, 0)$  is taken to be proportional to  $c_E - c_\infty$  (this choice is consistent with equation (74)), and if it is assumed that  $c_\infty$  is sufficiently close to  $c_E$  to permit the term involving  $A(\zeta, 0)$  in equation (85) to be safely neglected, then substitution of equation (85) into equation (55) (with  $\alpha_1 = 1$ ) results in

$$\frac{f''}{(1+f'^2)^{3/2}} - \frac{f}{\mu} = \Psi [c_2^*(\chi) + B_1] \quad (\chi \in [0, \delta]) \quad (86a)$$

$$\frac{f''}{(1+f'^2)^{3/2}} - \frac{f}{\mu} = -\alpha_2 \Psi [c_2^*(\chi) + B_1] \quad (\chi \in (\delta, 1]), \quad (86b)$$

where

$$\Psi = m_\alpha \left( \frac{V\lambda^2}{2D_e} \right) \left( \frac{\Delta S_{f(\alpha)}}{\delta_{\alpha e}} \right) \Lambda_1. \quad (87)$$

Finally, an explicit expression for  $B_1$  can be derived by employing the condition that  $\Theta_\alpha$  and  $\Theta_\beta$  must be independent of  $\omega$  (and therefore  $\Psi$ ) and using a procedure similar to that used in Sections 4.1.2 and 4.3.1. Thus, with the aid of the approximations used in Section 4.3.1, equations (86a) and (86b) can be integrated out from the triple point to their respective endpoint to give

$$\sin \Theta_\alpha = -\frac{f(d)}{\mu} \delta - \Psi(I_\alpha + B_1 \delta) \quad (88a)$$

and

$$\sin \Theta_\beta = -\frac{f(d)}{\mu} (1-\delta) + \alpha_2 \Psi(I_\beta + B_1 (1-\delta)), \quad (88b)$$

where

$$I_\alpha = \int_0^\delta c_e^*(z) dz \quad (89a)$$

and

$$I_\beta = \int_\delta^1 c_e^*(z) dz. \quad (89b)$$

Eliminating  $f(\delta)$  from equation (88) then yields the relation

$$\begin{aligned} & \delta \sin \Theta_\beta - (1-\delta) \sin \Theta_\alpha \\ &= \Psi [\alpha_2 \delta I_\beta + (1-\delta) I_\alpha + (\alpha_2 + 1) \delta (1-\delta) B_1], \end{aligned} \quad (90)$$

But  $\Theta_\alpha$  and  $\Theta_\beta$  can only be independent of  $\Psi$  if the righthand side of equation (90) vanishes (recall that  $\omega_{low} = \Psi_{low} = 0$ ). Hence, this implies that

$$B_1 = - \frac{(\alpha_2 \delta I_\beta + (1-\delta) I_\alpha)}{(\alpha_2 + 1) \delta (1-\delta)}, \quad (91)$$

and, moreover, that

$$\sin \Theta_\alpha = \frac{\alpha_4 \delta}{\delta + \alpha_3 (1-\delta)} \quad (92a)$$

and

$$\sin \Theta_\beta = \frac{\alpha_4 (1-\delta)}{\delta + \alpha_3 (1-\delta)}, \quad (92b)$$

where equations (92) follow from equation (90) with the righthand side equal to zero and equation (56a).

Equations (73), (86), and (91), together with the boundary conditions

$$f'(0) = f'(1) = 0$$

$$f(\delta_-) = \tan \Theta_\alpha$$

$$f(\delta_+) = -\tan \Theta_\beta,$$

are the soughtafter equations, and comprise a system of three equations (hencefore denoted as System II) for the quantities  $c_{\ell}^*(x)$ ,  $f(x)$ , and  $B_1$  in terms of the parameters  $\mu$  and  $\Psi$  and the known quantities  $\alpha_i$  ( $i=1, \dots, t$ ) and  $\delta$ . Once  $f(x)$  has been obtained,  $\phi_1(x)$ ,  $\phi_2(y)$ , and  $G_{\ell}$  can be found, if desired, by solving equations (50) and (51) for  $\phi_1$  and  $\phi_2$  and substituting the results into equation (59) to obtain  $G_{\ell}$ .

#### 4.4.2 An important property of System II

Before concluding this section, it should be pointed out that the solutions of System II are essentially independent of  $\mu$ . To see why this is so, consider equation (86) and assume that  $c_{\ell}^*(x)$  is independent of  $\mu$ . Then, because  $\Theta_\alpha$ ,  $\Theta_\beta$ ,  $f(\delta)/\mu$ , and  $B_1$  are independent of  $\mu$  by equations (88), (91), and (92), and because  $f(\delta)/\mu \cong f(x)/\mu$ , the relation

$$\frac{f''}{(1+f'^2)^{3/2}} = -\frac{d}{dx} \sin \theta$$

implies that  $f(x)$  is independent of  $\mu$  to within a constant vertical displacement. But the kernels  $C_1$  and  $C_2$  in equation (73) are not functions of  $\mu$ , and, moreover, are invariant with respect to a constant vertical displacement in  $f(x)$ . Therefore,  $c_x^*(x)$  is indeed independent of  $\mu$ , and it follows that the solutions to System II (to within a constant vertical shift in  $f(x)$ ) are functions of the parameter  $\Psi$  alone.

The fact that the solutions depend only on  $\Psi$  leads to an interesting prediction; namely, that the use of virtually any subsidiary condition for the selection of the system operating point must lead to a relation of the form

$$V\lambda^2 = \text{const.},$$

where the constant does not depend on the thermal gradient. This result is in accord with the majority of experimental observations.

## 5. NUMERICAL RESULTS AND COMPARISON WITH EXPERIMENTAL DATA

Having completed the theoretical analysis, it remains to develop and implement a numerical solution, and compare the resulting predictions with experimental data.

### 5.1 Numerical Procedures and Results

#### 5.1.1 A procedure for solving System II

A combination iteration and bootstrap procedure proves effective in obtaining numerical solutions to System II as a function of the parameter  $\Psi$ . To implement this procedure, a step size  $\Delta \Psi$  is specified,  $\Psi$  is set equal to  $\Delta \Psi$ , and an initial guess (iterate 1) for  $f(x)$  is obtained by solving equation (86) with  $\Psi = 0$ . Next, the kernels  $C_1$  and  $C_2$  in equation (73) are evaluated using the initial guess for  $f(x)$  and equation (73) is solved for  $c_e^*(x)$ . This estimate for  $c_e^*(x)$  is then inserted into equations (91) and (86), and equation (86) is resolved with  $\Psi = \Delta \Psi$  to obtain an improved estimate for  $f(x)$  (iterate 2). The kernels  $C_1$  and  $C_2$  are then re-evaluated using the updated

estimate for  $f(x)$ , and the process is repeated until either convergence is obtained (to within a specified tolerance) or until a specified upper bound on the number of iterations is reached. Upon completion of the iteration process,  $\Psi$  is set equal to  $2\Delta\Psi$  and the iteration procedure is repeated taking the last known  $f(x)$  as the initial guess. In this way,  $f(x)$ ,  $c_{\ell}^*(x)$ , and  $B_1$  are ascertained as a function of  $\Psi$  until a specified limit  $\Psi_{up}$  is reached, at which point the calculation is terminated.

A computer program was written to implement the iteration/bootstrap procedure. Equation (86) was solved each time by using a self-starting fifth-order predictor-corrector scheme with an automatic step-size selector to integrate each of the equations out from the triple point. The starting values of  $f$  and  $\theta$ , i.e., the values of these quantities at the triple point, were obtained in each case from equations (88), (91), and (92)

To solve equation (73), an approximate matrix representation was formulated by replacing the integral containing

$C_1$  by a trapezoidal quadrature and those containing  $C_2$  by a quadrature based on product integration (the latter being necessary to properly treat the logarithmic singularity in  $C_2$ ). The relation

$$\lim_{z \rightarrow x} C_1(x, z, f(x), f(z)) = \begin{cases} \frac{f''(x)}{4\pi(1+f'^2(x))} + \frac{1}{2} & (x \neq 0, 1) \\ \frac{f''}{2\pi(1+f'^2(x))} + \frac{1}{2} & (x = 0, 1) \end{cases} \quad (93)$$

was used to evaluate the kernel,  $C_1$ , at the points  $z = x$ . The matrix approximation procedure resulted in a system of linear algebraic equations for the values of  $c_p^*(x)$  at the quadrature points which was then solved by standard techniques; a listing of the program and the accompanying documentation is presented in Appendix D.

### 5.1.2 Validation of the numerical procedures

Because the accuracy of the solutions to System II depends critically on the accuracy of the computed values of  $c_p^*(x)$ , it was deemed necessary to check the convergence of the scheme used to

solve equation (73) before implementing the entire iteration/bootstrap procedure. Thus, equation (73) was successively solved using a 32, 64, and 128 point quadrature. The volume phase fraction was chosen as 0.5 and  $C_1$  and  $C_2$  were evaluated using as  $f(x)$  the solution to equation (86) with  $\Psi = 0$ ,  $\alpha_3 = 0.6218$ , and  $\alpha_4 = 1.3$ . The values of  $c_i^*(x)$  obtained in each case are displayed in Table 1. As can be seen from this table, the convergence is excellent with four-figure agreement achieved in most cases.

Having established the convergence of the interfacial solute concentration calculations, the convergence of the iteration procedure was checked by observing the results of four iterations starting at  $\Psi = 0.5$  and increasing  $\Psi$  in steps of 0.5. The values of  $f-f(\mathcal{J})$  obtained after each iteration for  $\mathcal{J} = 0.5$ ,  $\Psi = 1.0$ ,  $\alpha_2 = 3.855$ ,  $\alpha_3 = 0.6218$ , and  $\alpha_4 = 1.3$  are shown in Table 2.

The first iterate represents the interface shape obtained from the final results of the iteration procedure for  $\Psi = 0.5$ . Subsequent iterations were obtained by solving equation (86)

with  $\Psi = 1.0$ , with  $c_{\chi}^*(x)$  determined from the solution of equation (73), and with  $C_1$  and  $C_2$  evaluated using the interface shape as determined from the previous iteration. As can be seen from the table, convergence is rapid, with four-figure agreement achieved by the fourth iteration. Similar results are displayed in Table 3 for  $\Psi = 3.0$ , where comparable convergence rates are attained.

Finally, it should be mentioned that additional calculations of this type were performed with several other values taken for the  $\Psi$ -step. The rate of convergence of the iteration procedure was found to be relatively insensitive to the particular value chosen.

### 5.1.3 Sensitivity of the solution of equation (73) to interface shape changes and comparison to the Jackson-Hunt solution

Jackson and Hunt [2] obtained solutions to equation (1) which satisfy conditions (4)-(6), (9), and (11) correctly to  $O(\omega)$  for the special case  $f(x) = \text{const.}$ , i.e., a flat interface. Since their solution is widely employed in

TABLE 1

Convergence Check on the Solution to Equation (73)†

$$f = 0.5 \quad \psi = 0 \quad \alpha_1 = 1.0 \quad \alpha_3 = 0.6218 \quad \alpha_4 = 1.3$$

UNCLASSIFIED

x	32-Point Quadrature $c_l^*$	64-Point Quadrature $c_l^*$	128-Point Quadrature $c_l^*$
0.0000E+00	2.9587E-01	2.9591E-01	2.9602E-01
3.1250E-02	2.9387E-01	2.9392E-01	2.9391E-01
6.2500E-02	2.9066E-01	2.9064E-01	2.9062E-01
9.3750E-02	2.8529E-01	2.8526E-01	2.8523E-01
1.2500E-01	2.7769E-01	2.7765E-01	2.7762E-01
1.5625E-01	2.6781E-01	2.6777E-01	2.6774E-01
1.8750E-01	2.5552E-01	2.5548E-01	2.5544E-01
2.1875E-01	2.4071E-01	2.4066E-01	2.4062E-01
2.5000E-01	2.2337E-01	2.2332E-01	2.2328E-01
2.8125E-01	2.0344E-01	2.0339E-01	2.0334E-01
3.1250E-01	1.8065E-01	1.8059E-01	1.8053E-01
3.4375E-01	1.5481E-01	1.5473E-01	1.5467E-01
3.7500E-01	1.2656E-01	1.2647E-01	1.2640E-01
4.0625E-01	9.5502E-02	9.5381E-02	9.5280E-02
4.3750E-01	6.2465E-02	6.2273E-02	6.2114E-02
4.6875E-01	2.9575E-02	2.8998E-02	2.8630E-02
5.0000E-01	1.0805E-06	1.7434E-06	2.7615E-06
5.0000E-01	1.0805E-06	1.7434E-06	2.7615E-06
5.3125E-01	-2.9571E-02	-2.8990E-02	-2.8617E-02
5.6250E-01	-6.2461E-02	-6.2265E-02	-6.2101E-02
5.9375E-01	-9.5497E-02	-9.5373E-02	-9.5267E-02
6.2500E-01	-1.2656E-01	-1.2646E-01	-1.2638E-01
6.5625E-01	-1.5480E-01	-1.5472E-01	-1.5466E-01
6.8750E-01	-1.8064E-01	-1.8058E-01	-1.8052E-01
7.1875E-01	-2.0344E-01	-2.0338E-01	-2.0333E-01
7.5000E-01	-2.2337E-01	-2.2331E-01	-2.2327E-01
7.8125E-01	-2.4070E-01	-2.4065E-01	-2.4061E-01
8.1250E-01	-2.5552E-01	-2.5547E-01	-2.5543E-01
8.4375E-01	-2.6780E-01	-2.6776E-01	-2.6772E-01
8.7500E-01	-2.7768E-01	-2.7764E-01	-2.7760E-01
9.0625E-01	-2.8528E-01	-2.8525E-01	-2.8522E-01
9.3750E-01	-2.9065E-01	-2.9063E-01	-2.9060E-01
9.6875E-01	-2.9386E-01	-2.9391E-01	-2.9389E-01
1.0000E+00	-2.9586E-01	-2.9590E-01	-2.9601E-01

† An E-type format, i.e.  $aE \pm nn = a \times 10^{\pm nn}$ , is used throughout Tables 1-3.

TABLE 2

Iteration Convergence Check for  $\psi = 1.0$ 

$$\alpha_1 = 1.0, \quad \alpha_2 = 3.855, \quad \alpha_3 = 0.6218, \quad \alpha_4 = 1.3, \quad \delta = 0.5$$

x	Iterate 1 f-f( $\delta$ )	Iterate 2 f-f( $\delta$ )	Iterate 3 f-f( $\delta$ )	Iterate 4 f-f( $\delta$ )
.0000E-00	.2471E+00	.2422E+00	.2420E+00	.2420E+00
.3125E-01	.2462E+00	.2413E+00	.2411E+00	.2411E+00
.6250E-01	.2438E+00	.2389E+00	.2388E+00	.2388E+00
.9375E-01	.2398E+00	.2351E+00	.2349E+00	.2349E+00
.1250E+00	.2343E+00	.2297E+00	.2296E+00	.2296E+00
.1563E+00	.2271E+00	.2228E+00	.2227E+00	.2227E+00
.1875E+00	.2183E+00	.2143E+00	.2142E+00	.2142E+00
.2188E+00	.2078E+00	.2041E+00	.2039E+00	.2039E+00
.2500E+00	.1954E+00	.1920E+00	.1919E+00	.1919E+00
.2813E+00	.1810E+00	.1781E+00	.1780E+00	.1780E+00
.3125E+00	.1645E+00	.1620E+00	.1619E+00	.1619E+00
.3438E+00	.1456E+00	.1435E+00	.1435E+00	.1435E+00
.3750E+00	.1240E+00	.1225E+00	.1224E+00	.1224E+00
.4063E+00	.9937E-01	.9833E-01	.9829E-01	.9829E-01
.4375E+00	.7111E-01	.7055E-01	.7052E-01	.7052E-01
.4688E+00	.3841E-01	.3824E-01	.3823E-01	.3823E-01
.5000E+00	.0	.0	.0	.0
.5000E+00	.0	.0	.0	.0
.5313E+00	.3793E-01	.3729E-01	.3727E-01	.3727E-01
.5625E+00	.6956E-01	.6756E-01	.6752E-01	.6752E-01
.5938E+00	.9652E-01	.9287E-01	.9281E-01	.9281E-01
.6250E+00	.1198E+00	.1144E+00	.1143E+00	.1143E+00
.6563E+00	.1400E+00	.1329E+00	.1328E+00	.1328E+00
.6875E+00	.1576E+00	.1488E+00	.1487E+00	.1487E+00
.7188E+00	.1729E+00	.1625E+00	.1624E+00	.1624E+00
.7500E+00	.1862E+00	.1743E+00	.1742E+00	.1742E+00
.7813E+00	.1975E+00	.1844E+00	.1843E+00	.1843E+00
.8125E+00	.2072E+00	.1929E+00	.1928E+00	.1928E+00
.8438E+00	.2153E+00	.2000E+00	.1998E+00	.1999E+00
.8750E+00	.2218E+00	.2057E+00	.2055E+00	.2055E+00
.9063E+00	.2268E+00	.2101E+00	.2099E+00	.2099E+00
.9375E+00	.2304E+00	.2132E+00	.2131E+00	.2131E+00
.9688E+00	.2327E+00	.2151E+00	.2150E+00	.2150E+00
.1000E+01	.2335E+00	.2159E+00	.2158E+00	.2158E+00

TABLE 3

Iteration Convergence Check for  $\psi = 3.0$ 

$$\alpha_1 = 1.0, \quad \alpha_2 = 3.855, \quad \alpha_3 = 0.6218, \quad \alpha_4 = 1.3, \quad \delta = 0.5$$

x	Iterate 1 f-f( $\delta$ )	Iterate 2 f-f( $\delta$ )	Iterate 3 f-f( $\delta$ )	Iterate 4 f-f( $\delta$ )
.0	.2265E+00	.2216E+00	.2213E+00	.2213E+00
.3125F-01	.2257E+00	.2208E+00	.2205E+00	.2205E+00
.6250F-01	.2236E+00	.2188E+00	.2185E+00	.2185E+00
.9375F-01	.2201E+00	.2155E+00	.2152E+00	.2152E+00
.1250F+00	.2153E+00	.2109E+00	.2106E+00	.2106E+00
.1563F+00	.2091E+00	.2049E+00	.2046E+00	.2046E+00
.1875F+00	.2015E+00	.1975E+00	.1972E+00	.1972E+00
.2188F+00	.1922E+00	.1886E+00	.1883E+00	.1883E+00
.2500F+00	.1814E+00	.1781E+00	.1778E+00	.1778E+00
.2813F+00	.1687E+00	.1658E+00	.1656E+00	.1655E+00
.3125F+00	.1540E+00	.1515E+00	.1513E+00	.1513E+00
.3438F+00	.1370E+00	.1350E+00	.1349E+00	.1349E+00
.3750F+00	.1175E+00	.1160E+00	.1159E+00	.1159E+00
.4063F+00	.9498E-01	.9396E-01	.9387E-01	.9387E-01
.4375F+00	.6871E-01	.6815E-01	.6810E-01	.6809E-01
.4688F+00	.3765E-01	.3747E-01	.3746E-01	.3746E-01
.5000F+00	.0	.0	.0	.0
.5000E+00	.0	.0	.0	.0
.5313F+00	.3536E-01	.3478E-01	.3474E-01	.3474E-01
.5625E+00	.6177E-01	.6008E-01	.5995E-01	.5994E-01
.5938F+00	.8254E-01	.7955E-01	.7932E-01	.7931E-01
.6250E+00	.9929E-01	.9492E-01	.9460E-01	.9458E-01
.6563E+00	.1130E+00	.1072E+00	.1068E+00	.1068E+00
.6875F+00	.1243E+00	.1171E+00	.1166E+00	.1166E+00
.7188E+00	.1336F+00	.1251E+00	.1245E+00	.1245E+00
.7500F+00	.1412E+00	.1315E+00	.1308E+00	.1308E+00
.7813F+00	.1475E+00	.1366F+00	.1358E+00	.1358E+00
.8125F+00	.1526E+00	.1406E+00	.1398E+00	.1397E+00
.8438E+00	.1567E+00	.1437E+00	.1429E+00	.1428E+00
.8750F+00	.1599E+00	.1461E+00	.1452E+00	.1452E+00
.9063E+00	.1623E+00	.1479E+00	.1470E+00	.1469E+00
.9375F+00	.1640E+00	.1492E+00	.1482E+00	.1481E+00
.9688F+00	.1651E+00	.1499E+00	.1490E+00	.1489E+00
.1000E+01	.1655E+00	.1503E+00	.1493E+00	.1492E+00

theoretical and experimental studies of eutectic solidification, it was deemed necessary to assess the effect of interface curvature on  $c_{\ell}^*$ .

An investigation of this effect was carried out by solving equation (73) for a series of interface shapes which were obtained by solving equations (86) and (92) with  $\Psi = 0$ ,  $\alpha_3 = 1.0$  (for  $\mathcal{J} = 0.5$ ),  $\alpha_3 = 0.6218$  (for  $\mathcal{J} = 0.65$ ), and values of  $\alpha_4$  ranging from 1.8 to 0.1. The interface shapes employed are shown in Figs. 7a and 8a for  $\mathcal{J} = 0.5$  and  $\mathcal{J} = 0.65$ , respectively.

The values of  $c_{\ell}^*(x)$  obtained from the solution of equation (73) with a 68-point quadrature (this is used in all subsequent work), along with the Jackson-Hunt result, are shown in Figs. 7b and 8b for  $\mathcal{J} = 0.5$  and  $\mathcal{J} = 0.65$ , respectively. It is apparent that the present results encompass Jackson and Hunt's results as the interface curvature decreases (indeed, this serves as an additional check on the numerical solution to equation (73)). However, as the interface curvature increases, the solutions of equation (73) change considerably, leading to significant

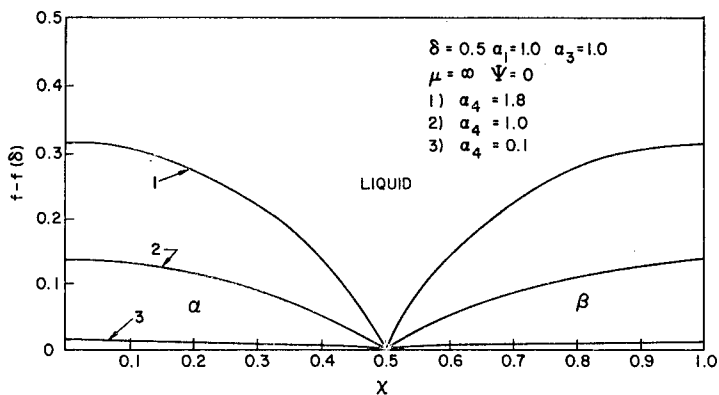


Fig. 7a — Interface shapes employed in the comparison of the present theory with the Jackson-Hunt theory for  $\delta = 0.5$

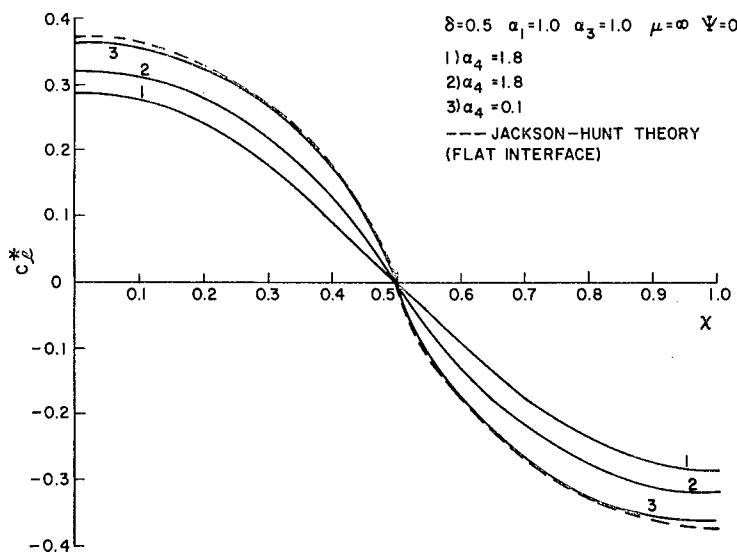


Fig. 7b — The reduced interfacial solute concentrations  $c_2^*$  predicted by the present theory for the interface shapes shown in Fig. 7a compared with the Jackson-Hunt prediction

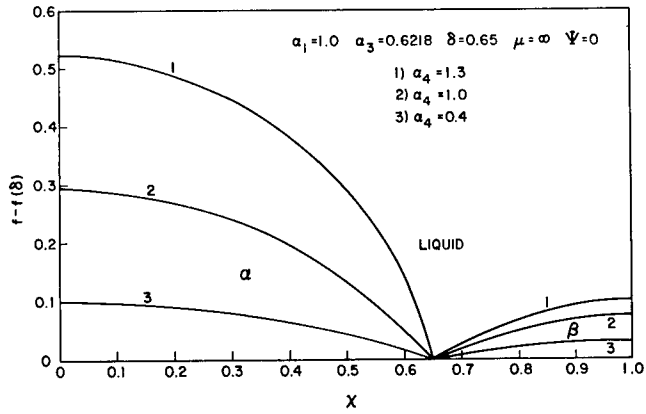


Fig. 8a — Interface shapes employed in the comparison of the present theory with the Jackson-Hunt theory for  $\delta = 0.65$

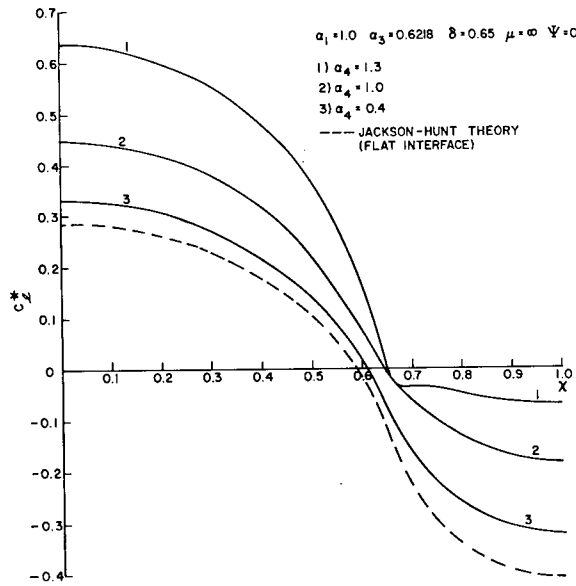


Fig. 8b — The reduced interfacial solute concentrations  $c_2^*$  predicted by the present theory for the interface shapes shown in Fig. 8a compared with the Jackson-Hunt prediction

departures from Jackson and Hunt's theory, which are particularly pronounced in the unsymmetric case, i.e.,  $f = 0.65$ .

#### 5.1.4 Some typical numerical results

To illustrate the behavior of the solutions as a function of  $\Psi$ , the iteration/bootstrap procedure was implemented for two values of  $f$ , namely  $f = 0.4$  and  $0.7$ , with  $\alpha_2 = 3.855$ ,  $\alpha_3 = 0.6218$ , and  $\alpha_4 = 1.2$ . A  $\Psi$ -step of 0.5 was used and four iterations per  $\Psi$ -step were performed. The computed interface shapes are shown in Figs. 9a and 10a for  $f = 0.4$  and  $f = 0.7$ , respectively, for values of  $\Psi$  ranging from 0 to 5.0 in increments of 1.0. The reduced interfacial concentrations corresponding to these interface shapes are shown in Figs. 9b and 10b.

#### 5.2 Comparison with Experimental Data and Previous Theoretical Results

If suitable subsidiary conditions were available for the selection of the system operating point,  $\Psi_{op}$ , and if all the thermodynamic and transport properties required by the theory were known, then the theory could be critically compared with experiment in

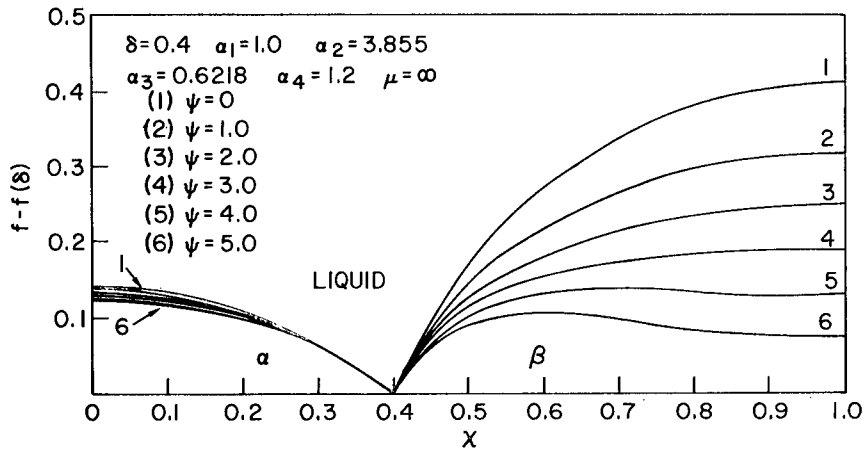


Fig. 9a — Variation of the interface shape with  $\psi$  for  $\delta = 0.4$

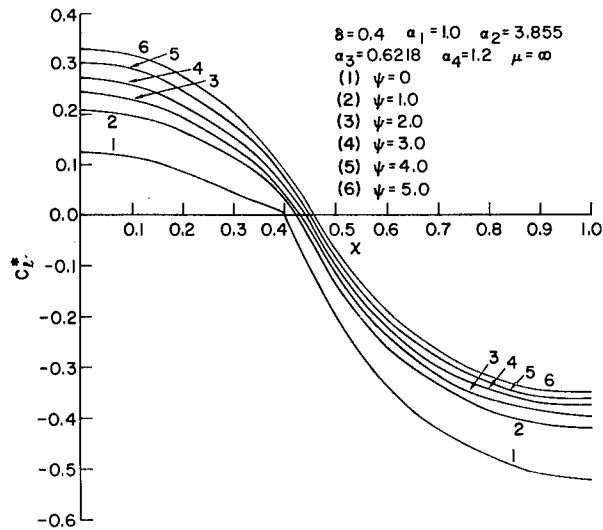


Fig. 9b — The reduced interfacial solute concentrations  $c_{\delta}^*$  corresponding to the interface shapes shown in Fig. 9a

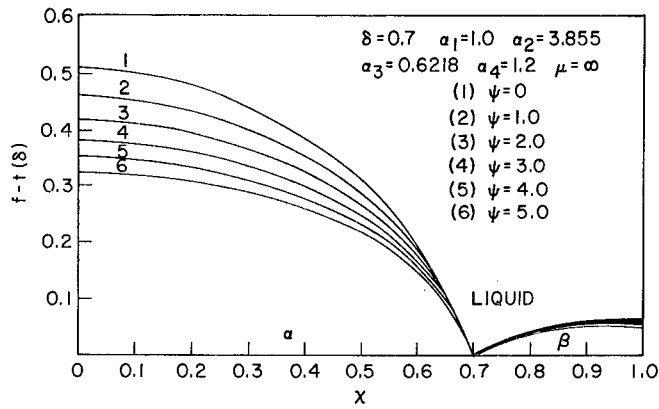


Fig. 10a — Variation of the interface shape with  $\psi$  for  $\delta = 0.7$

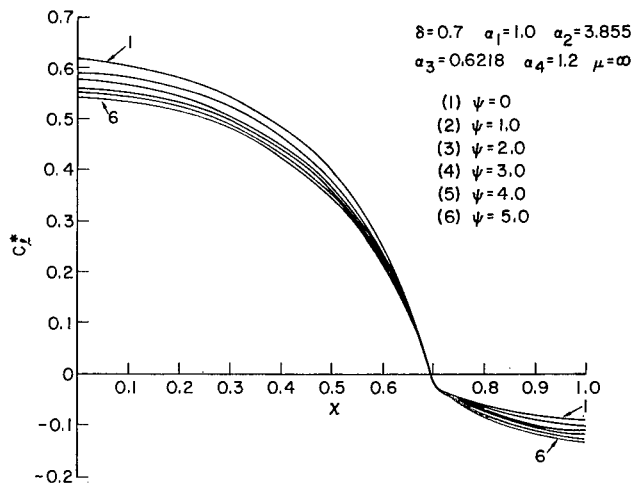


Fig. 10b — The reduced interfacial solute concentrations  $c_i^*$  corresponding to the interface shapes shown in Fig. 10a

a relatively routine fashion. Unfortunately, neither of these requirements is currently satisfied, even for the simplest eutectic systems. In particular, very little is known regarding the chemical diffusivities,  $D_L$ , and even less is known about the interfacial energies  $\gamma_{ae}$ ,  $\gamma_{pe}$ , and  $\gamma_{\alpha\beta}$ . Moreover, the stability analysis and/or variational principle required for the selection of  $\psi_{op}$  are still awaiting development. Hence, it does not appear possible at this stage to utilize the available experimental results to critically evaluate the theory and the assumptions therein. Rather, we must be content to make comparisons which are essentially qualitative in nature, and then hope that meaningful results can be extracted.

#### 5.2.1 A procedure for assessing the theory

With these considerations in mind, the following procedure was formulated to check the consistency of the theoretical predictions with experiment:

1. The quantities  $f$  and  $\alpha_2$  are calculated using data obtained from the phase diagram, presuming one is available.

2. The quantities  $\alpha_1$ ,  $\alpha_3$ , and  $\alpha_4$  (which depend on the interfacial energies) are estimated using procedures to be discussed shortly.

3. The iteration/bootstrap procedure is implemented and  $\psi_{op}$  is selected using Tiller's [1] "minimum supercooling hypothesis."

4. Equation (87), with  $\psi = \psi_{op}$ , is utilized in conjunction with experimental information concerning the  $V-\lambda$  relation to obtain an expression for the quantity ( $N_{\alpha\ell} D_{\ell}$ ).

5.  $N_{\alpha\ell}$  is estimated, thereby yielding an estimate for  $D_{\ell}$ .

6. The resulting value of  $D_{\ell}$  is compared with values obtained by independent measurements (when such values are available), or with the rule of thumb that  $D_{\ell} \cong 1 \times 10^{-5} \text{ cm}^2 \text{ sec}$ .

#### 5.5.2 Estimation of $\alpha_1$ , $\alpha_3$ , $\alpha_4$ , and $\psi_{op}$

To estimate  $\alpha_1$  and  $\alpha_3$ , we note that for a pure material the Gibbs-Thomson coefficient,  $a$ , can be approximated by the relation

$$a = \left( \frac{\gamma_{SL}}{\Delta S_f} \right) \approx K \left( \frac{M}{\rho N_0} \right)^{1/3} T_m, \quad (94)$$

where  $\gamma_{sl}$  is the solid/liquid interfacial energy,  $M$  is the molecular weight,  $N_0$  is Avagadro's number,  $T_m$  is the melting temperature,  $\rho$  is the density, and  $K$  is a constant such that  $0 < K \leq 1$ . Then assuming that equation (94) can be applied to each solid phase in a binary eutectic system with  $T_m$  taken as  $T_E$  and  $K_{\alpha} = K_{\beta}$ , the required expressions for  $\alpha_1$  and  $\alpha_2$  follow immediately. Hence,

$$\alpha_1 = \frac{\alpha_{\beta}}{\alpha_{\alpha}} = \left( \frac{M_{\beta} \rho_{\alpha}}{M_{\alpha} \rho_{\beta}} \right)^{1/3} \approx 1 \quad (95)$$

and (with  $\alpha_1 = 1$ )

$$\alpha_2 = \frac{\gamma_{\beta l}}{\gamma_{\alpha l}} \approx \frac{\Delta S_{f\beta}}{\Delta S_{f\alpha}} = \frac{\rho_{\beta} L_{\beta}}{\rho_{\alpha} L_{\alpha}}, \quad (96)$$

where  $L_{\epsilon}$  ( $\epsilon = \alpha, \beta$ ) is the latent heat of fusion of the appropriate phase.

The quantity  $\alpha_4$  can be obtained from equations (80) when the limiting volume fractions  $f_{low}$  and  $f_{up}$  are known. The limiting volume fractions can be estimated from either lamellar-rod transition data, or by an educated guess when such data is unavailable, thus providing the required estimate of  $\alpha_4$ .

As mentioned in Section 5.2.1, the system operating point,  $\Psi_{op}$ , is estimated using Tiller's "minimum supercooling hypothesis," which states that for a prescribed value of  $V$  the system will select a value of  $\lambda$  such that the average interfacial supercooling,  $\Delta T_{av}$ , is minimized.

For large values of  $\mu$ , the solid/liquid interface is approximately isothermal. Therefore, the interfacial supercooling,  $\Delta T(x)$ , is approximately equal to  $\Delta T_{av}$ , and is given by

$$\Delta T = T_E - \hat{T}(x) = -\lambda G_S f(x) \cong -\lambda G_S f(\delta) \cong \Delta T_{av},$$

which, with the aid of the relations

$$\mu = \frac{\gamma_{\alpha\ell}}{\lambda^2 G_S \Delta S_{f\alpha}},$$

$$\Psi = m_\alpha \left( \frac{V\lambda^2}{2D_\alpha} \right) \left( \frac{\Delta S_{f\alpha}}{\gamma_{\alpha\ell}} \right) \Lambda_1,$$

and

$$\Lambda_1 = \frac{c_{\beta E} \rho_\beta - c_{\alpha E} \rho_\alpha}{\delta \rho_\alpha + (1-\delta) \rho_\beta},$$

can be written as

$$\Delta T_{av} \cong -\lambda G_s \frac{f(\delta)}{\mu} \mu = -\frac{\Lambda_2}{\Psi^{1/2}} \frac{f(\delta)}{\mu},$$

where

$$\Lambda_2 = \left[ \frac{V m_\alpha \gamma_{\alpha e}}{2 D_e \Delta S_{fd}} \Lambda_1 \right]^{1/2},$$

and is a constant when  $V$  is fixed. Hence, the determination of  $\Psi_{op}$  essentially reduces to obtaining the quantity  $-f(\delta)/\mu$  as a function of  $\Psi$  with the iteration/bootstrapping procedure (recall that  $f(\delta)/\mu$  is independent of  $\mu$ ), and then minimizing  $\Delta T_{av}$  with respect to  $\Psi$ .

It will subsequently be shown that the quantity  $f(\delta)/\mu$  can usually be approximated by a simple linear relation in  $\Psi$ , i.e.,

$$-\frac{f(\delta)}{\mu} \cong a_0 + a_1 \Psi,$$

where  $a_0$  and  $a_1$  are constants determined from the iteration/bootstrap procedure. Hence, the system operating point,  $\Psi_{op}$ , is given by

$$\Psi_{op} = \frac{a_0}{a_1},$$

which, with the aid of equation (87), leads to the following expression for the  $V$ - $\lambda$  relation:

$$V\lambda^2 = \left( \frac{a_0}{a_1} \right) \left( \frac{2D_\alpha \gamma_{\alpha\beta}}{M_\alpha \Delta S_{f\alpha} \Lambda_1} \right) = \Lambda_3 \gamma_{\alpha\beta} D_\alpha = \text{const.} \quad (97)$$

### 5.2.3 Comparison of theory with experiment

The procedure described in Section 5.2.1 was implemented for six alloy systems in which regular lamellar structures are known to form; namely the systems Sn-Pb, Pb-Cd, Cd-Zn, Al-CuAl<sub>2</sub>, Ag-Cu, and Sn-Cd (the phase arbitrarily labeled  $\alpha$  is always listed first). The phase-diagram data for these systems was obtained from Hansen [13] and is listed in Table 4.

The interfacial energies,  $\gamma_{\alpha\beta}$ , were estimated using equation (94) with  $\Delta S_f = \Delta S_{fA} = L_A/T_E$ ,  $M = M_A$ ,  $\rho = \rho_A$ ,  $T_m = T_E$ , and  $K \in [1/3, 1]$ , where the subscript A denotes the principle constituent of the  $\alpha$  phase. These properties are tabulated in Table 5, and, with the exception of the solid/liquid interfacial energy,  $\gamma_{s\ell}$ , were obtained from Smithells [14]. The values of the

quantities  $\alpha_2$ ,  $\alpha_3$ ,  $\alpha_4$ , and  $\delta$  used in the calculations are shown in Table 6. Also shown are the  $\delta$ -ranges,  $[\delta_{low}, \delta_{up}]$ , which were used to obtain  $\alpha_4$ .

The quantity,  $-f(\delta)/\mu$ , as obtained from the iteration/bootstrap procedure, is displayed as a function of  $\Psi$  for several representative alloy systems in Fig. 11. As is evident from the figure,  $f(\delta)/\mu$  varies approximately linearly with  $\Psi$ , thus justifying the use of equation (97).

The calculated values of  $\Psi_{op}$  and  $\Lambda_3$  are listed in Table 7 along with experimentally determined values of the quantity  $V\lambda^2$ . Also shown are the estimated values of  $D_\ell$  which were calculated by substituting the experimental values of  $V\lambda^2$  and the estimates of  $\gamma_{\alpha\ell}$  (Table 5) into equation (97).

Finally, the values of  $D_\ell$  provided by the theory are tabulated in Table 8 along with corresponding experimental values for the four alloy systems for which such data is available; namely the systems Sn-Pb, Pb-Cd, Al-CuAl<sub>2</sub>, and Sn-Cd.

TABLE 4  
Phase Diagram Data for Selected Eutectic Alloy Systems

System	$M_{\alpha}$ (°K/wt.fract.)	$M_{\beta}$ (°K/wt.fract.)	$T_E$ (°K)	$c_E$ (wt.fract.)	$c_{\alpha E}$ (wt.fract.)	$c_{\beta E}$ (wt.fract.)
Sn-Pb	100	285	456	0.381	0.025	0.81
Pb-Cd	250	315	521	0.174	0.033	1.0
Cd-Zn	175	365	539	0.174	0.03	0.98
Al-CuAl <sub>2</sub>	420†	300†	821	0.33†	0.055†	0.54†
Ag-Cu	400	490	1052	0.281	0.088	0.92
Sn-Cd	100	165	450	0.323	0.056	0.998

† Wt. fract. Cu

TABLE 5  
Relevant Physical Properties of Selected Pure Materials

Material	Latent Heat (cal/g)	Density (g/cm <sup>3</sup> )	Atomic Wt. (g)	$\gamma_{sl}$ (erg/cm <sup>2</sup> )
Pb	5.74	11.68	207.2	30 - 90
Sn	14.2	7.3	118.7	40 - 130
Cd	13.6	8.64	112.4	45 - 140
Zn	26.3	7.14	65.4	70 - 210
Ag	25.3	10.5	107.9	95 - 290
Al	92.7	2.70	26.98	90 - 270
Cu	48.9	8.96	63.54	140 - 420
CuAl <sub>2</sub>	76.5	3.25	-----	-----

TABLE 6

Values of the Parameters Used in the Calculations

System	$\alpha_2$	$\alpha_3$	$\alpha_4$	$\delta$	$\delta$ -range
Sn-Pb	2.9	0.65	1.16	0.658	0.35 - 0.8
Pb-Cd	1.25	1.75	1.2	0.812	0 - 0.9
Cd-Zn	2.0	1.6	1.18	0.822	0 - 0.9
Al-CuAl <sub>2</sub> <sup>†</sup>	0.7	1.0	1.55	0.5	0.35 - 0.65
Ag-Cu	1.22	1.65	1.1	0.74	0 - 0.95
Sn-Cd	1.6	1.15	1.2	0.75	0.06 - 0.85

<sup>†</sup>  $\delta$  is not the volume fraction corresponding to the eutectic composition for this system.

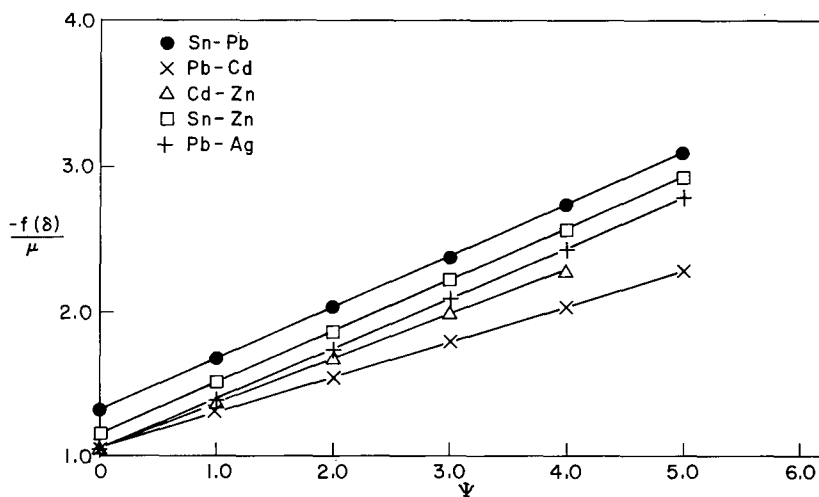


Fig. 11 — The quantity  $-f(\delta)/\mu$  as a function of  $\psi$  for representative alloy systems

TABLE 7

The Results of the Present Theory and the Jackson-Hunt Theory

System	$V\lambda^2$ (experiment) ( $\text{cm}^3/\text{sec}$ )	$\psi_{\text{op}}$	$\Lambda_3$ (present theory) ( $\text{cm}^3/\text{cal}$ )	$\Lambda_3$ (J-H theory) ( $\text{cm}^3/\text{cal}$ )	Calc. values of $D_f$ ( $\text{cm}^2/\text{sec}$ )
Sn-Pb	$8.25 \times 10^{-12}$ (a)	3.73	0.318	0.302	$0.84 - 2.7 \times 10^{-5}$
Pb-Cd	5.26 (b)	4.30	0.358	0.466	0.68 - 2.1
Cd-Zn	6.93 (c)	3.47	0.224	0.289	0.93 - 2.8
Al-CuAl <sub>2</sub>	27.5 (d)	7.5	0.217	0.200	2 - 6
Ag-Cu	3.7 (e)	3.8	0.103	0.107	0.52 - 1.6
Sn-Cd	<del>5.7-18</del> (f)	4.02	0.385	0.458	0.73 - 4.9

(a) obtained from ref. 15.

(b) obtained from ref. 16.

(c) obtained from ref. 17.

(d) obtained from ref. 18.

(e) obtained by fitting the data in ref. 19 (crudely) to a  $V\lambda^2 = \text{const.}$  relation.

(f) low value obtained from ref. 19 -- high value obtained from ref. 20.

TABLE 8

Calculated and Experimental Solute Diffusivities

System	$D_f$ (calc.) ( $\text{cm}^2/\text{sec}$ )	$D_f$ (experiment) ( $\text{cm}^2/\text{sec}$ )	Remarks
Sn-Pb	$0.84-2.7 \times 10^{-5}$	$0.67 \times 10^{-5}$ (a) 1. (b) 0.63 (c) 0.62 (d)	Eutectic composition-extrapolated to $T_E$ Eutectic composition- extrapolated to $T_E$ Eutectic composition-extrapolated to $T_E$ Eutectic composition and temperature
Pb-Cd	$0.68-2.1 \times 10^{-5}$	$1.-1.5 \times 10^{-5}$ (e)	Eutectic composition at 623°K
Al-CuAl <sub>2</sub>	$2.-6. \times 10^{-5}$	$3.26 \times 10^{-5}$ (d)	Eutectic composition and temperature
Sn-Cd	$0.73-4.9 \times 10^{-5}$	$3.6 \times 10^{-5}$ (f)	Eutectic composition at 673°K

(a) obtained from ref. 21.

(b) obtained from ref. 22.

(c) obtained from ref. 23.

(d) obtained from ref. 18.

(e) obtained from ref. 24.

(f) obtained from ref. 25.

Reasonable agreement is achieved in all cases, thus lending some credence to the  $V-\lambda$  relation predicted by the theory. Moreover, the calculated values of  $D_e$  for the remaining systems appear viable on the basis of the data in Table 8.

#### 5.2.4 Comparison with the theory of Jackson and Hunt

As a final item, it is of interest to compare the  $V-\lambda$  relations predicted by the present theory with those predicted by the Jackson-Hunt [2] analysis.

Utilizing the current notation and employing the assumption used in ref. 2, i.e.

$$\gamma_{\alpha\ell} \sin \Theta_\alpha = \gamma_{\beta\ell} \sin \Theta_\beta = \frac{1}{2} \gamma_{\alpha\beta},$$

it can be readily shown that equation (17a) in the aforementioned reference assumes the form

$$V\lambda^2 = \left[ \frac{1+\delta + \delta/(\alpha_3\alpha_2)}{4m_\alpha \Delta S_{j\alpha} \Lambda_1 P} \right] \gamma_{\alpha\beta} D_e = \bar{\Lambda}_3 \gamma_{\alpha\ell} D_e, \quad (98)$$

where

$$\bar{\Lambda}_3 = \frac{[1+\delta + \delta/(\alpha_3\alpha_2)] \alpha_4}{4m_\alpha \Delta S_{j\alpha} \Lambda_1 P} \quad (99a)$$

and

$$P = \sum_{n=1}^{\infty} \left( \frac{1}{n\pi} \right)^3 \sin^2 n\pi\delta. \quad (99b)$$

Hence, the desired comparison can be made simply by comparing the values of  $\Lambda_3$  and  $\bar{\Lambda}_3$  obtained from equations (97) and (99a), respectively.

The values of these quantities for the six alloy systems are displayed in Table 7. Despite the large disparities in the interfacial solute concentration distributions (see Section 5.1.3), good agreement is achieved, with the relative differences in  $\Lambda_3$  ranging from 5% for the Sn-Pb system to 30% for Pb-Cd. Whether or not such good correlations can be maintained when the operating point,  $\bar{\psi}_{cp}$ , is established by criteria other than the "minimum supercooling hypothesis," however, remains an open question.

## 6. SUMMARY AND CONCLUSIONS

1. A general treatment of the free-boundary problem associated with the growth of a lamellar eutectic solid from its melt was presented. The analysis served to decouple the calculation of the interfacial quantities from the computation of the bulk temperature and solute distributions, and led to a system of nonlinear integro-differential equations for the shape of the solid/liquid interface and quantities defined on the interface.

2. The behavior of the integro-differential equations was critically examined, and it was shown that:

- The thermodynamic equilibrium requirements at the  $\alpha/\beta$ /liquid triple point must be compatible with constraints imposed by the diffusion equation in order for lamellar solutions to exist.

- When lamellar solutions are possible, the solutions generally admit to a relatively narrow range of possible crystallographic orientation relationships between the two solid phases.

3. The behavior of particular solutions to the integro-differential equations was analyzed

and the information thus obtained was used to formulate an approximate theory of the lamellar rod transition.

4. Simplified versions of the integro-differential equations were derived by assuming that (1) the solute diffusion length is large compared to the lamellar spacing and (2) the solid/liquid interface is approximately isothermal. In particular, it was shown that the solutions to these equations are function of only a single parameter,  $\Psi$ , which is proportional to  $V\lambda^2$ , thus implying that the use of virtually any subsidiary condition for the selection of the system operating point must lead to the familiar relation  $V\lambda^2 = \text{constant}$ .

5. The simplified theory was used to investigate the effect of interface curvature on the interfacial solute distribution and the results were compared to the predictions of Jackson and Hunt, who assumed the interface to be planar. It was found that the present results encompassed those of Jackson and Hunt as the interface curvature decreased. However, as the interface curvature

increased, the interfacial solute distributions changed considerably, leading to significant departures from the Jackson-Hunt theory, which were particularly pronounced in the unsymmetric case ( $f = 0.65$ ).

6. A procedure was formulated to check the consistency of the theoretical predictions with experiment, and was implemented for six alloy systems which were known to solidify with a regular lamellar microstructure. Good correlation between theory and experiment was achieved in all cases.

7. The lamellar spacing-freezing rate relations predicted by the new theory were compared with those predicted by the Jackson-Hunt analysis. Good agreement was achieved in spite of the large disparities in the predicted interfacial solute concentration distributions, thus implying that the  $V-\lambda$  relations obtained with the "minimum supercooling hypothesis" are relatively insensitive to the solid/liquid interface shape and the detailed solute concentration distribution on the interface.

8. Recommendations for further work include:

- A detailed stability analysis of the steady-state solutions and/or development of a suitable variational principle in order to establish a definitive  $V-\lambda$  relation.

- Interface stability studies to determine the onset of dendritic growth.

- Studies of cell formation and colony growth due to third-element additions.

- Extension of the theory to include interfacial molecular attachment kinetics and faceting.

## REFERENCES

1. W. A. Tiller, "Polyphase Solidification" in Liquid Metals and Solidification, Cleveland, Ohio: American Society for Metals, 1958.
2. K. A. Jackson and J. D. Hunt, Trans. AIME 236 (1966) 1129.
3. M. Colin, G. Lesoult, M. Turpin, and J. Zeyons, J. Crystal Growth 28, (1975) 103.
4. M. E. Glicksman and R. J. Schaefer, Private communication concerning their work on determining the equilibrium shape of a grain-boundary groove in a temperature gradient.
5. S. Strässler and W. R. Schneider, "Stability of Lamellar Eutectics," Brown-Bovari Research Report KLR-73-02 (Feb. 1973).
6. G. E. Nash, "Capillarity-Limited Steady-State Dendritic Growth, Part I - Theoretical Development," NRL Report 7679 (May 1974).
7. G. E. Nash and M. E. Glicksman, Phil. Mag. 24 (1971) 577.
8. J. D. Hunt and K. A. Jackson, Trans. AIME 236 (1966) 843.

9. L. M. Hogan, R. W. Kraft, and F. D. Lemkey, "Eutectic Grains," in Advances in Materials Research, Vol. 5, H. Herman, Editor, New York: Wiley-Interscience, 1971.
10. H. W. Reddick and F. H. Miller, Advanced Mathematics for Engineers (3rd edition), New York: John Wiley and Sons, 1960, p. 139.
11. F. R. Mollard and M. C. Flemings, Trans, AIME 239 (1967) 1534.
12. S. A. David and H. D. Brody, Met. Trans. 5 (1974) 2309.
13. M. Hansen, Constitution of Binary Alloys, New York: McGraw-Hill, 1958, p. 1107.
14. C. J. Smithells, Metals Reference Book (4th edition), New York: Plenum Press, 1967.
15. J. D. Hunt and J. P. Chilton, J. Inst. Metals 92 (1963) 21.
16. G. A. Chadwick, J. Inst. Metals 92 (1963) 18.
17. W. A. Tiller and R. Mrdjenovich, J.A.P. 34 (1963) 3639.
18. R. M. Jordan and J. D. Hunt, Met. Trans. 3 (1972) 1385.

19. D. J. S. Cooksey, D. Munson, M. P. Wilkinson, and A. Hellawell, *Phil. Mag.* 10 (1964) 745.
20. A. Moore and R. Elliot, "Eutectic Solidification," in *Proceedings of the Conference on Solidification of Metals*, Brighton, U.K. (1967).
21. J. M. Lommel and B. Chalmers, *Trans. AIME* 215 (1959) 499.
22. K. G. Davis, *Canad. Met. Quart.* 5 (1966) 245.
23. P. A. Savintsev and V. I. Rogov, *Zavod. Lab.* 35 (1969) 195 (in Russian).
24. L. E. Trimble, W. L. Pieper, and F. B. Canfield, *Met. Trans.* 2 (1971) 1669.
25. S. Sugino, A. Onishi, and H. Hagiwara, *Bull. Osaka Univ. Prefect. Ser. A* 17 (1968) 175 (in English).
26. P. M. Morse and H. Feshback, Methods of Theoretical Physics, Part 1, New York: McGraw-Hill, 1953, Chap. 7.

APPENDIX ADerivation of the Explicit Form of the Single-Layer Potential  $U_{\omega}^v[h](x, y)$ 

The single-layer potential

$$U_{\omega}^v[h](x, y) = \frac{1}{2\omega} \int_0^1 \tilde{K}(x, z, y, v(z), \omega) h(z) \frac{dz}{\cos \theta(z)} \quad (\text{A.1})$$

introduced in Section 3.1.2 essentially represents the concentration field due to a distribution of point sources of strength  $h(x)$  acting on the surface  $v(x)$  in the strip  $[0, 1]$ . This implies that the kernel

$$\frac{1}{2\omega} \tilde{K}(x, z, y, v(z), \omega) \equiv G(x, z, y, v(z), \omega)$$

satisfies the equation

$$\frac{\partial^2 G}{\partial x^2} + \frac{\partial^2 G}{\partial y^2} + 2\omega \frac{\partial G}{\partial y} = -\delta(x-z) \delta(y-v(z)) \quad (\text{A.2})$$

in the strip  $[0, 1]$  with boundary conditions

$$\frac{\partial G}{\partial x} = 0, \quad x = 0, 1, \quad (\text{A.3a})$$

$$\lim_{y \rightarrow -\infty} G < \infty \quad (\text{A.3b})$$

$$\lim_{y \rightarrow \infty} G = 0, \quad (\text{A.3c})$$

where  $\delta(s-t)$  is the Dirac delta function. Thus, the required expression for  $U_{\omega}^V[h](x, y)$  can be obtained once a suitable solution to equations (A.2) and (A.3) is found.

An eigenfunction expansion approach probably affords the simplest and most direct method for solving equations (A.2) and (A.3). To implement this technique, we assume that

$$G = \sum_{n=0}^{\infty} f_n(y) \cos n\pi x, \quad (\text{A.4})$$

thus insuring that boundary conditions (A.3a) are satisfied. Then substituting equation (A.4) into equation (A.2) and expanding the term  $\delta(x-z)$  in a Fourier cosine series, i.e.

$$\delta(x-z) = 1 + 2 \sum_{n=1}^{\infty} \cos n\pi x \cos n\pi z,$$

results in

$$\begin{aligned}
 & f_0''(y) + 2\omega f_0'(y) + \delta(y - v(z)) \\
 & + \sum_{n=1}^{\infty} \left[ -f_n(y) n^2 \pi^2 + f_n''(y) + 2\omega f_n'(y) \right. \\
 & \left. + 2 \cos n\pi z \delta(y - v(z)) \right] \cos n\pi x = 0.
 \end{aligned} \tag{A.5}$$

But the basis functions  $\{1, \cos \pi x, \cos 2\pi x, \dots\}$  are linearly independent, which implies that equation (A.5) can be satisfied only if

$$f_0''(y) + 2\omega f_0'(y) + \delta(y - v(z)) = 0 \tag{A.6a}$$

and

$$\begin{aligned}
 & f_n''(y) + 2\omega f_n'(y) - n^2 \pi^2 f_n(y) \\
 & + 2 \cos n\pi z \delta(y - v(z)) = 0 \quad (n=1, 2, \dots).
 \end{aligned} \tag{A.6b}$$

Hence, G will satisfy equations (A.2) and (A.3), provided that the functions  $f_n(y)$  satisfy equations (A.6) along with the boundary conditions

$$\lim_{y \rightarrow \infty} f_n(y) = 0 \tag{A.7a}$$

and

$$\lim_{y \rightarrow -\infty} f_n(y) < \infty. \tag{A.7b}$$

Equation (A.6a) can be solved in a routine fashion by transforming it into a first-order equation with the substitution  $p_0(y) = f_0'(y)$ , and then integrating the resulting equation twice using the relations

$$\int_0^y \int(\xi-t) g(\xi) d\xi = \begin{cases} \text{const. for } y < t \\ \text{const.} + g(t) \text{ for } y > t \end{cases}$$

and

$$p_0' + 2\omega p_0 = e^{-2\omega y} \frac{d}{dy} (p_0 e^{2\omega y}).$$

This results in

$$\begin{aligned} p_0(y) &= f_0'(y) \\ &= C_1 e^{-2\omega y} - H(y-v(z)) e^{-2\omega(y-v(z))} \end{aligned}$$

and

$$\begin{aligned} f_0(y) &= -\frac{C_1}{2\omega} e^{-2\omega y} + \frac{1}{2\omega} \\ &+ \frac{1}{2\omega} H(y-v(z)) [e^{-2\omega(y-v(z))} - 1] + C_2, \end{aligned}$$

where  $H$  denotes the Heaviside unit step function and  $C_i$  ( $i=1, 2$ ) are arbitrary functions of

$z$  and  $\omega$ . But  $C_1$  and  $C_2$  must vanish if equations (A.7) are to be satisfied. Hence,

$$f_0(y) = \frac{1}{2\omega} + \frac{1}{2\omega} H(y-v(z)) \left[ e^{-2\omega(y-v(z))} - 1 \right]. \quad (\text{A.8})$$

To solve equations (A.6b), it is convenient to take

$$f_n(y) = u_n(y) e^{-\omega y}. \quad (\text{A.9})$$

Then substituting equation (A.9) into equation (A.6b) gives

$$u_n'' - (\omega^2 + n^2\pi^2) u_n = -2 \cos n\pi z e^{2\omega y} \delta(y-v(z)),$$

or equivalently,

$$u_n'' - (\omega^2 + n^2\pi^2) u_n = 0 \quad \text{for } y \neq v(z) \quad (\text{A.10a})$$

and

$$\lim_{\gamma \rightarrow v^+(\zeta)} u_n' - \lim_{\gamma \rightarrow v^-(\zeta)} u_n' = -2 \cos \kappa \pi \zeta e^{2\omega v(\zeta)}, \quad (\text{A.10b})$$

where the jump condition (A.10b) results from integrating equation (A.10a) from  $\gamma = v(\zeta) - \epsilon$  to  $\gamma = v(\zeta) + \epsilon$  and then taking the limit as  $\epsilon \rightarrow 0$ .

A general solution to equation (A.10a) which permits satisfaction of conditions (A.7) and (A.10b) is given by

$$u_n = D_{1n} e^{-(\omega^2 + \kappa^2 \pi^2)^{1/2} (\gamma - v(\zeta))} + D_{2n} e^{-(\omega^2 + \kappa^2 \pi^2)^{1/2} \gamma}, \quad (\text{A.11})$$

where  $D_{1n}$  and  $D_{2n}$  are arbitrary functions of  $\zeta$  and  $\omega$ . But  $D_{2n}$  must vanish if equation (A.7b) is to be satisfied. Hence, using equation (A.10b) to evaluate  $D_{1n}$  and substituting equation (A.11) back into equation (A.9) gives for  $f_n(\gamma)$  :

$$f_n(y) = \frac{\cos \pi k z \exp \left\{ -(\omega^2 + \kappa^2 \pi^2)^{1/2} |y - v(z)| - \omega(y - v(z)) \right\}}{(\omega^2 + \kappa^2 \pi^2)^{1/2}} \quad (\text{A.12})$$

With  $f_n(y)$  ( $n=0,1,2,\dots$ ) now determined, an explicit expression for  $G$  could, in principle, be obtained simply by substituting equations (A.8) and (A.12) back into equation (A.4). However, the resulting expression for  $G$  will not be well suited for numerical evaluation, primarily because the resulting series converges very slowly for points  $(x,y)$  in the neighborhood of the point  $(z, v(z))$ . Hence, to complete the solution, we must incorporate into the analysis a device to accelerate the convergence of the aforementioned series.

Such a device was formulated by Morse and Feshbach [26] in their treatment of a related class of problems, and simply consists of adding and subtracting to equation (A.4) the solution to equation (A.2) with  $\omega = 0$ , i.e.

$$J = \sum \frac{1}{\kappa \pi} \cos \pi k x \cos \pi k z e^{-\pi \kappa |y - v(z)|}$$

Thus, upon noting that

$$J = -\frac{1}{4\pi} \ln [2 \cosh \pi (y - v(z)) - 2 \cos \pi (x - z)]$$

(A.13)

$$-\frac{1}{4\pi} \ln [2 \cosh \pi (y - v(z)) - 2 \cos \pi (x + z)]$$

$$+ \frac{1}{2} |y - v(z)|$$

(see ref. 26 for a derivation of equation (A.13)),  
the Morse and Feshbach procedure furnishes the  
following expression for G:

$$G(x, z, y, v(z), \omega) = \frac{1}{2\omega} \tilde{K}(x, z, y, v(z), \omega)$$

$$= -\frac{1}{4\pi} \ln [2 \cosh \pi (y - v(z)) - 2 \cos \pi (x - z)]$$

$$-\frac{1}{4\pi} \ln [2 \cosh \pi (y - v(z)) - 2 \cos \pi (x + z)]$$

$$+ \frac{1}{2} |y - v(z)| + \frac{1}{2\omega}$$

$$+ \frac{1}{2\omega} H(y - v(z)) [e^{-2\omega(y - v(z))} - 1]$$

$$+ \sum_{n=1}^{\infty} \cos n\pi x \cos n\pi z [(\omega^2 + n^2\pi^2)^{-1/2}$$

(A.14)

$$\cdot \exp \left\{ -(\omega^2 + n^2\pi^2)^{1/2} |y - v(z)| - \omega(y - v(z)) \right\}$$

$$- (n\pi)^{-1} \exp \left\{ -n\pi |y - v(z)| \right\} ] .$$

It can be shown that the series in equation (A.14) converges rapidly for all values of  $x$ ,  $y$ ,  $z$ , and  $v(z)$  in the strip  $[0, 1]$ . Hence, substitution of equation (A.14) into equation (A.1) yields the required expression for  $U_{\omega}^v[h](x, y)$ .

## APPENDIX B

### The Indeterminacy Associated with the Solute Concentration Field

It was asserted in Section 2.2 that the system composed of equations (1), (4)-(6), (9), and (11) does not generally provide a unique concentration field,  $c_x$ , even when the interface shape, freezing rate, and lamellar spacing are specified. In this Appendix, we establish the validity of this assertion.

We consider first the limiting case  $\eta_\alpha = \eta_\beta = \infty$ . In this case the nondimensional versions of equations (1), (4)-(6), (9), and (11) become

$$\nabla^2 c_x + 2w \frac{\partial c_x}{\partial y} = 0 \quad (\text{B.1})$$

and

$$\lim_{y \rightarrow \infty} c_x = c_\infty \quad (\text{B.2})$$

$$\frac{\partial c_x}{\partial x} = 0, \quad x = 0, 1, \quad (\text{B.3})$$

$$-g_x^c = 2\omega \cos \theta \left( \hat{C}_x - \frac{\rho_\alpha}{\rho_x} C_{\alpha E} \right), \quad x \in [0, \delta), \quad (\text{B.4a})$$

$$-g_x^c = 2\omega \cos \theta \left( \hat{C}_x - \frac{\rho_\beta}{\rho_x} C_{\beta E} \right), \quad x \in (\delta, 1], \quad (\text{B.4b})$$

where

$$g_x^c = \sin \theta(x) \frac{\partial C_x}{\partial x} + \cos \theta(x) \frac{\partial C_x}{\partial y} \Big|_{y=f(x)}, \quad (\text{B.5})$$

$$J = J^* = \frac{(C_{\beta E} - C_{\infty}) \rho_\beta}{\rho_\beta (C_{\beta E} - C_{\infty}) + \rho_\alpha (C_{\infty} - C_{\alpha E})}, \quad (\text{B.6})$$

and the remaining symbols are the same as in the main text. Now let  $C_x^1 = C_x^0 + I(y, \omega)$ , where  $C_x^0$  is any solution to equations (B.1)-(B.4) and

$$I(y, \omega) = \int_0^1 A(z, \omega) e^{-2\omega(y-f(z))} dz. \quad (\text{B.7})$$

Then, because  $I(y, \omega)$  satisfies equation (B.1) and

$$\frac{dI}{dn} = \cos \theta \left. \frac{\partial I}{\partial y} \right|_{y=f(x)} = -2\omega I(f(x), \omega) \cos \theta(x),$$

$c_2^1(x, y)$  also satisfies equations (B.1)-(B.4).

Hence, the solute concentration field is unique only to within a term of the form  $I(y, \omega)$ , where the function  $A(z, \omega)$  is arbitrary, thus verifying the assertion for this case.

A proof of the assertion for the general case  $n_\alpha$  and  $n_\beta < \infty$  is not as straightforward as in the preceding case.

For the general case, it is convenient to utilize the results of Section 3.3; namely that the solute concentration on the solid/liquid interface,  $\hat{c}_2(x)$ , is given by

$$\hat{c}_2(x) = \tilde{c}_2(x) + I(f(x), \omega) + c_\infty, \quad (\text{B.8})$$

where  $\tilde{c}_2(x)$  is found by solving

$$-\frac{1}{2} \tilde{c}_2(x) + \int_0^1 K_1(x, z, f(x), f(z), \omega) \tilde{c}_2(z) dz + \int_0^1 K_2(x, z, f(x), f(z), \omega) S_1(z) dz = 0, \quad (\text{B.9})$$

with

$$S_1(x) = c_{\infty} - \frac{\rho_{\alpha}}{\delta \rho_{\alpha} + (1-\delta)\rho_{\beta}} \left\{ c_{\alpha E} \right. \quad (\text{B.10a})$$

$$\left. + \frac{m_{\alpha}}{n_{\alpha}} \left[ \tilde{c}_2(x) + (c_{\infty} - c_E) + I(f(x), \omega) \right] \right\}, \quad x \in [0, \delta)$$

$$S_1(x) = c_{\infty} - \frac{\rho_{\beta}}{\delta \rho_{\alpha} + (1-\delta)\rho_{\beta}} \left\{ c_{\beta E} \right. \quad (\text{B.10b})$$

$$\left. + \frac{m_{\beta}}{n_{\beta}} \left[ \tilde{c}_2(x) + (c_{\infty} - c_E) + I(f(x), \omega) \right] \right\}, \quad x \in (\delta, 1],$$

and where  $\delta$  is found from the solution of

$$c_{\infty} [\delta \rho_{\alpha} + (1-\delta)\rho_{\beta}] = c_{\alpha E} \delta \rho_{\alpha} + c_{\beta E} (1-\delta)\rho_{\beta}$$

$$+ \rho_{\alpha} \int_0^{\delta} \frac{m_{\alpha}}{n_{\alpha}} \left[ \tilde{c}_2(z) + (c_{\infty} - c_E) + I(f(z), \omega) \right] dz$$

$$+ \rho_{\beta} \int_{\delta}^1 \frac{m_{\beta}}{n_{\beta}} \left[ \tilde{c}_2(z) + (c_{\infty} - c_E) + I(f(z), \omega) \right] dz. \quad (\text{B.11})$$

In order to prove that the concentration field,  $c_j$ , is not unique, it is sufficient to demonstrate that a change in  $I(y, \omega)$  implies a change in  $\hat{c}_j(x)$  and/or  $\mathcal{J}$ .

By utilizing a perturbation analysis of equation (B.9) similar to that employed in Section 4.2, it is readily shown that changes in the  $O(\omega^n)$  terms in  $I(y, \omega)$  can only induce corresponding changes in the  $O(\omega^{n+1})$  terms in  $\hat{c}_j(x)$ . Hence, it is evident that changes in  $I(y, \omega)$  do indeed induce changes in  $\hat{c}_j(x)$  and  $\mathcal{J}$ . Therefore, the assertion is affirmed for the general case as well.

## APPENDIX C

Derivation of Equation (62)

By equation (28) in the main text, the interfacial solute concentration,  $\hat{c}_2(x)$ , is given by

$$\hat{c}_2(x) = \tilde{c}_2(x) + c_\infty + \int_0^1 A(z, \omega, \mu) e^{-2\omega(f(x)-f(z))} dz, \quad (\text{C.1})$$

where  $\tilde{c}_2(x)$  and the volume phase fraction,  $\delta$ , are found by solving equations (33) and (57), respectively. If it is assumed that  $n_\alpha$  and  $n_\beta$  are large, then a perturbation analysis of equation (33) reveals that

$$\tilde{c}_2(x) = \omega \left[ \frac{c_{\beta E} \rho_\beta - c_{\alpha E} \rho_\alpha}{\delta \rho_\alpha^* + (1-\delta) \rho_\beta} \right] c_2^*(x) + O(\omega^2), \quad (\text{C.2})$$

where  $\tilde{c}_2(x)$  is the solution to equation (73), and  $\delta^*$  is given by

$$\delta^* = \frac{(c_{\beta E} - c_\infty) \rho_\beta}{(c_{\beta E} - c_\infty) \rho_\beta + (c_\infty - c_{\alpha E}) \rho_\alpha}. \quad (\text{C.3})$$

Moreover,  $\delta \approx \delta^*$  . Thus, expanding the term

$$\int_0^1 A(z, \omega, \mu) e^{-2\omega(f(x) - f(z))} dz$$

with respect to  $\omega$  and substituting equation (C.2) into equation (C.1) yields

$$\hat{G}_2(x) = B_0(\mu) + C_E + O(\omega), \quad (C.4)$$

where

$$B_0(\mu) = \int_0^1 A(z, 0, \mu) dz + C_\infty - C_E, \quad (C.5)$$

and is a priori unknown.

The quantity  $B_0(\mu)$  is determined from the condition that equations (55) and (56) in the main text are to be satisfied simultaneously to  $O(1)$  with respect to  $\omega$  . In the analysis to follow, this condition will be used to obtain explicit expressions for  $B_0(\mu)$  for the two limiting cases of small and large values of  $\mu$  .

For simplicity, we shall consider the case of equal thermal conductivities, i.e.,  $k_\alpha = k_\beta = k_\ell$  .

In this case, by utilizing equation (C.4) and the definition of  $\mu$ , i.e.,  $\mu = \gamma_{\alpha, \beta} / G \Delta S_{\beta} \lambda^2$ , equations (55) (correct to  $O(1)$ ) can be written as

$$\frac{f''}{(1+f'^2)^{3/2}} - \frac{f}{\mu} = \frac{\Phi}{\mu^{1/2}} B_0, \quad \chi \in [0, \delta) \quad (\text{C.6a})$$

$$\frac{f''}{(1+f'^2)^{3/2}} - \frac{f}{\mu} = -\alpha_2 \frac{\Phi}{\mu^{1/2}} B_0, \quad \chi \in (\delta, 1] \quad (\text{C.6b})$$

where  $\Phi$  is a dimensionless parameter given by

$$\Phi = \frac{m_{\alpha}}{(a_{\alpha} G)^{1/2}}, \quad (\text{C.7})$$

$\alpha_2 = m_{\beta} / m_{\alpha}$ , and where  $\alpha_1 = a_{\alpha} / a_{\beta}$  was assumed equal to unity. Assuming that there exists a range of relative orientation relations such that real values of  $\Theta_{\alpha}$  and  $\Theta_{\beta}$  can be found which satisfy equations (56a) and (56b),  $B_0$  is determined by solving equation (C.6) subject to subsidiary conditions given by equations (56c) and (56d), i.e.,

$$f(\delta_-) = f(\delta_+) \quad , \quad (C.8a)$$

and

$$f'(0) = f'(1) = 0, \quad (C.8b)$$

Solution for small values of  $\mu$

Let

$$g(x) = f(x) + \mu^{1/2} \Phi B_0 \quad , \quad x \in [0, \delta), \quad (C.9a)$$

$$g(x) = f(x) - \alpha_2 \mu^{1/2} \Phi B_0 \quad , \quad x \in (\delta, 1]. \quad (C.9b)$$

Then, substituting equations (C.9) into equations (C.6)

and noting that

$$\frac{g''}{(1+g'^2)^{3/2}} = -\frac{d}{dg} \cos \theta$$

gives

$$\frac{d}{dg} \cos \theta + \frac{g}{\mu} = 0 \quad , \quad x \in [0, 1]. \quad (C.10)$$

If equation (C.10) is now integrated from  $q = q(0)$  to  $q(\delta_-)$ , and from  $q = q(1)$  to  $q(\delta_+)$ , then, with the aid of equation (C.8b), which implies that

$$\cos \theta \Big|_{q=q(0)} = \cos \theta \Big|_{q=q(1)} = 0,$$

we obtain

$$\cos \theta_\alpha - 1 + \frac{1}{\mu} \int_{q(0)}^{q(\delta_-)} \xi \, d\xi = 0 \quad (\text{C.11a})$$

and

$$\cos \theta_\beta - 1 + \frac{1}{\mu} \int_{q(0)}^{q(\delta_+)} \xi \, d\xi = 0. \quad (\text{C.11b})$$

The quantities  $q(0)$  and  $q(1)$  are not known in general, and are difficult to obtain for arbitrary values of  $\mu$ . However, as  $\mu \rightarrow 0$ ,  $q(x)$  must approach zero except, perhaps, in a very small region in the neighborhood of the triple-point groove; i.e., the solution for small values of  $\mu$  (large values of  $\lambda$ ) must be the plane-front solution with a perturbation in the neighborhood of the groove.

Thus,

$$g(0) = g(1) \approx 0 \quad \text{for } \mu \text{ small.} \quad (\text{C.12})$$

With the aid of equation (C.12), the quantity  $B_0$  is now readily determined. Thus, substituting equation (C.12) into equation (C.11), integrating, and substituting the results into equation (C.9) gives

$$f(\delta_-) = (2\mu)^{1/2} (1 - \cos \Theta_\alpha)^{1/2} - \mu^{1/2} \Phi B_0 \quad (\text{C.13a})$$

and

$$f(\delta_+) = (2\mu)^{1/2} (1 - \cos \Theta_\beta)^{1/2} + \alpha_2 \mu^{1/2} \Phi B_0. \quad (\text{C.13b})$$

Hence, by virtue of equation (C.8a),

$$B_0 = \frac{[2(1 - \cos \Theta_\alpha)]^{1/2} - [2(1 - \cos \Theta_\beta)]^{1/2}}{(\alpha_2 + 1) \Phi} \quad (\text{C.14})$$

(for small values of  $\mu$  ).

This result is equivalent to that expressed by equation (62b) in the main text.

Solution for large values of  $\mu$

As was mentioned in Section 4.3.1, when the parameter  $\mu$  is sufficiently large,

$$\int_0^{\delta} f(\beta) d\beta \approx \delta f(\delta)$$

and

(C.15)

$$\int_{\delta}^1 f(\beta) d\beta \approx (1-\delta) f(\delta).$$

Thus, with the aid of equations (C.15), the relation

$$\frac{f''}{(1+f'^2)^{3/2}} = -\frac{d}{dx} \sin \theta,$$

and equation (C.8b), equations (C.6) can be integrated out from the triple point to their respective end-points in a straightforward manner to give

$$\frac{\delta f(\delta_-)}{\mu} = -\sin \theta_{\alpha} - \frac{\Phi}{\mu^{1/2}} B_0 \delta \quad (\text{C.16a})$$

and

$$\frac{(1-\delta) f(\delta_+)}{\mu} = -\sin \theta_{\beta} + \alpha_2 \frac{\Phi}{\mu^{1/2}} B_0 (1-\delta). \quad (\text{C.16b})$$

Therefore, again by virtue of equation (C.8a),

$$B_0 = \frac{[\delta \sin \Theta_\beta - (1-\delta) \sin \Theta_\alpha] \mu^{1/2}}{\Phi(\alpha_2+1) \delta(1-\delta)} \quad (\text{C.17})$$

(for large values of  $\mu$ ).

This result is equivalent to that expressed by equation (62c). Moreover, as discussed at the end of Section 4.3.1, this result is asymptotically valid, even when  $k_\alpha \neq k_\beta \neq k_L$ .

APPENDIX DA Description of the Computer Program for Solving System II

Language: Fortran Extended Version 3,

Computer: CDC 6600.

Operating System: SCOPE 3.3.

Program Input: Each set of input data consists of four logical records. The first record consists of a 0-80-character title. The contents of the remaining records are tabulated in Table D.1. The data sets may be stacked; the run will terminate when the program reads an END OF FILE.

Program Output: The program output consists of tabulated values of  $f(x)$ ,  $\tan\theta(x)$ ,  $\kappa(x)$  (interface curvature),  $f(x)-f(d)$ ; and  $c_p^*(x)$  (denoted as ACOL in the program), which are printed at the end of each iteration. A sample output is included at the end of this Appendix.

Program Listing: The program listing follows on page 147.

TABLE D.1  
INPUT DATA REQUIRED

Variable Name	Type	Definition	Comments
Record 2			
BETA3	Floating point	$\alpha_1$	1. BETA3 is always taken as unity. 2. RMU is usually taken as 15. 3. To insure real values for $\alpha$ and $\beta$ , DELTA must lie in the range $(j_{L,N}, j_{U,L})$ , where $j_{L,N}$ and $j_{U,L}$ are given by equations (80a) and (80b).
BETA4	↓	$\alpha_3$	
BETA5		$\alpha_4$	
BETA9		$\alpha_2$	
DELTA		$j$	
RMU		$\mu$	
Record 3			
M N MMAX NMAX	Fixed point  ↓	These variables are used to control the number of quadrature points in the integrals in equation (73).	1. MMAX and NMAX should usually be set equal to 1024. 2. The values of M and N are $j$ -dependent. For $0.25 < j < 0.75$ take $M = N = 32$ ; for $0 < j < 0.25$ take $M = 16, N = 32$ ; for $0.75 < j < 1.0$ take $M = 32, N = 16$ .
Record 4			
ISKIP1 ISKIP2 ITER1 ISTPLIM PSISTEP PSIHI	Fixed point  ↓ Floating point "	1. ISKIP1 and ISKIP2 are used for debugging purposes.  2. ITER1 is the number of iterations to be done per $\psi$ -step.  3. ISTPLIM is an upper limit on the number of $\psi$ -steps to be taken.  4. PSISTEP = $\lambda \psi$ (the amount by which $\psi$ is incremented per step).  5. PSIHI is a upper limit on $\psi$ .	1. ISKIP1 and ISKIP2 can be taken as any nonzero integer.  2. ITER1 iterations are done per step, unless convergence is obtained. A conservative value of ITER1 is 4.  3. The calculation terminates when either $\psi = \text{PSIHI}$ or $\psi = \text{PSISTEP} * \text{ISTPLIM}$ , whichever is less.

```

10 PROGRAM SPIROT3(INPUT,OUTPUT,TAPE1=INPUT)
20 COMMON/F5PACK/UGH1,UGH2,UGH3
30 COMMON/WGHTPAC/MP1,MPNP1
40 COMMON/BLK1/PI
50 COMMON/IMOD/IMOD
60 COMMON/ISIM/ISIM
70 COMMON/TRIG/QCM,QCF,QTM,QTP
80 COMMON/INRDFLG/INRDFLG
90 DIMENSION STOP1(130)
100 DIMENSION XX(2050),FF0(2050),X(130),F0(130),ACOL(70),CAPF2(130)
110 DIMENSION ATEST(130,4),AMAT(70,70)
120 DIMENSION STOPF(2050),COSARY(130),TANARY(130),BKAPARY(130)
130 DIMENSION TITLF(8),FN(11),FLAST(70)
140 EXTERNAL FUNCT1,FUNCT2,FUNCT3,FUNCT4
150 1    FORMAT(6F10.1)
160 2    FORMAT(4I5)
170 3    FORMAT(10X,4F13.4)
180 4    FORMAT(40X,F13.4)
190 5    FORMAT(/)
200 6    FORMAT(7F10.1)
210 7    FORMAT(I10,F13.4)
220 8    FORMAT(10X,2F13.4)
230 9    FORMAT(10X,2I10)
240 10   FORMAT(5X,6I8,4F13.4)
250 11   FORMAT(10X,6F13.4)
260 12   FORMAT(10X,6F13.4)
270 13   FORMAT(10X,4I6)
280 14   FORMAT(1H1)
290 15   FORMAT(80A1)
300 16   FORMAT(25X,8A10)
310 17   FORMAT(10X,3F13.4)
320 18   FORMAT((10F13.4))
330 19   FORMAT(4I5,2F10.1)
340 20   FORMAT(16X,**X*.11X.*FF0*)
350 21   FORMAT(17X.**X*.11X.*ACOL*)
360 22   FORMAT(10X,5F13.4)
370 23   FORMAT(26X.*INTERFACE SOLUTION*/18X.*ITERATE*,I3,11X.*PSI=*,
380+*F11.4/18X.*THETA=*.F11.4,5X,
390+*THETA+*.F11.4/18X.*R1=*.F11.4/)
400 26   FORMAT(17X.**X*.12X.*F*,8X.*TAN THETA*,6X.*KAPPA*,6X,
410+*F-F(DELTA)*)
420 27   FORMAT(20X.*SOLUTION OF THE INTEGRAL EQUATION*/28X,
430+*DET=*.F11.4/20X.*I1=*.F11.4,5X.*I2=*.F11.4/)
440**C   IN SPIROT3,THE GROOVE ANGLES ARE TAKEN TO BE
450**C   INDEPENDENT OF PSI
460**C   HIGH MU APPROXIMATION
470**C   M,MMAX,N,NMAX MUST BE GIVEN AS 2 TO AN INTEGER POWER
480**C   THIS VERSION OF SPIROT3 CAN ONLY BE RUN ON SCOPE
490 DO 800 J4X=1,100
500 READ(1)(TITLE(I),I=1,8)
510 IF(EOF(1))880,890
520 890   CONTINUE
530 READ(1)BETA3,BETA4,BETA5,      BETA9,DELTA,RMU
540 READ(1)M,N,MMAX,NMAX
550 READ(1)ISKIP1,ISKIP2,ITER1,ISTPLM,PSISTEP,PSIHI
560 O1=1.-DELTA $ O2=-DELTA $ RTMU=SQRT(RMU)
570 PI=3.14159      $ F1=DELTA/MMAX $ H2=(1.-DELTA)/NMAX $ TOL=1.F-3
580 NMAXP1=NMAX+1 $ MMAXP1=MMAX+1 $ MMAXP2=MMAX+2
590 MNTOTP1=MMAX+NMAX+1 $ NP1=N+1 $ MP1=M+1 $ MPNP1=M+N+1 $ MP2=M+2
600 HOLD1=H1 $ HOLD2=H2

```

```

610 QSP=(BETA5*(1.-DELTA))/(BETA3*DELTA+(1.-DELTA)*BETA4)
620 QSM=BETA5-BETA4*QSP
630 FODLTA=BETA3*BETA5/(BETA3*DELTA+(1.-DELTA)*BETA4)
640 FODLTA=-PMU*FODLTA
650 THTAPL=ASIN(QSP) & THTAMI=ASIN(QSM)
660 BETA6=BETA7=1.
670 MPN=M+N
680 MM1=M-1 & MPNM1=M+N-1
690 ICH=1
700 MPRINT =M/16 & NPRINT=N/16
710 IF(MPRINT.EQ.0) MPRINT=1
720 IF(NPRINT.FQ.0) NPRINT=1
730 TOL8=1.E-3
740 TOLERR=1.E-3
750 INRDFLG=0
760 PRINT 16,(TITLE(I),I=1,8)
770 PRINT 5
780 PRINT 3,BETA3,BETA4,BETA5,BETA9
790 PRINT 12, DELTA,THTAPL,THTAMI,PMU,FODLTA
800+.PSISTEP
810 PRINT 13,M,MMAX,N,NMAX
820 PRINT 5
830 QCM=COS(THTAMI) & QCP=COS(THTAPL)
840 QSM=SIN(THTAMI) & QSP=SIN(THTAPL)
850 QTM=TAN(THTAMI) & QTP=TAN(THTAPL)
860 Y7=FODLTA**2-2.*PMU*(1.-QCM)
870 FCONST=0.
880 R1XX=0.
890 IF(Y7.GT.0.) FCONST=-SQRT(Y7)
900 CALL F7FRO(H1,ICH,MMAXP1,PMU,FODLTA,FCONST,STORF,TOL8)
910 IF(INRDFLG.EQ.1) GO TO 850
920 DO 90 I=1,MMAXP1
930 FF0(I)=STORF(MMAXP2-I)
940 90 CONTINUE
950 XYZ=PMU*BETA3
960 Y7=FODLTA**2-2.*XYZ*(1.-QCP)
970 FCONST=0.
980 IF(Y7.GT.0.) FCONST=-SQRT(Y7)
990 CALL F7FRO(H2,MMAXP1,MNTOTP1,XYZ,FODLTA,FCONST,FF0,TOL8)
1000 IF(INRDFLG.FQ.1) GO TO 850
1010 DO 100 I=1,MMAXP1
1020 XX(I)=(I-1)*H1
1030 100 CONTINUE
1040 DO 110 I=MMAXP2,MNTOTP1
1050 XX(I)=DELTA+(I-MMAXP1)*H2
1060 110 CONTINUE
1070 H1=DELTA/M & H2=(1.-DELTA)/N
1080 DO 120 I=1,MP1
1090 X(I)=XY(1+(I-1)*MMAX/M)
1100 F0(I)=FF0(1+(I-1)*MMAX/M)
1110 120 CONTINUE
1120 DO 130 I=MP2,MPNF1
1130 X(I)=XY(MMAXP1+(I-MP1)*NMAX/N)
1140 F0(I)=FF0(MMAXP1+(I-MP1)*NMAX/N)
1150 130 CONTINUE
1160 RKAPM1=F0(MP1)/PMU & RKAPM1=F0(MP1)/PMU/BETA3
1170 COSAPY(MP1)=TANAPY(MP1)=RKAPARY(MP1)=0.
1180 DO 310 I=1,M
1190 COSARY(I)=1.-(F0(I)**2-F0(1)**2)/2./PMU
1200 Y1=COSAPY(I)

```

```

1210 TANARY(I)=SQRT(1./Y1**2-1.) $ RKAPARY(I)=F0(I)/RMU
1220 310 CONTINUE
1230 DO 320 I=MP2,MPNP1
1240 COSARY(I)=1.-(F0(I)**2-F0(MPNP1)**2)/2./RMU/BETA3
1250 Y1=COSARY(I)
1260 TANARY(I)=-SQRT(1./Y1**2-1.)
1270 RKAPARY(I)=F0(I)/RMU/BETA3
1280 320 CONTINUE
1290 IF(ISKIP1.NE.0) GO TO 655
1300 PRINT 20
1310 DO 300 I=1,MNTOTP1,8
1320 PRINT 8,XX(I),FF0(I)
1330 300 CONTINUE
1340 PRINT 5
1350 655 CONTINUE
1360 PSI=0.
1370 ISTEP=0
1380 825 CONTINUE
1390 IFLGEPF=1
1400 ITCNT1=0
1410 PSI=PSI+PSISTEP
1420 ISTEP=ISTEP+1
1430 IF(ISTEP.GT.ISTPLJM) GO TO 850
1440 IF(PSI.GT.PSTHI) GO TO 850
1450 DO 810 K107=1,ITER1
1460 ITCNT1=ITCNT1+1
1470 PRINT 23,ITCNT1,PSI , THTAMI,THTAPL,R1XX
1480 PRINT 26
1490 DO 380 I=1,MP1,MPRINT
1500 Y1=TANARY(I) $ Y2=RKAPARY(I)
1510 IF(I.EQ.MP1) Y1=QTM
1520 IF(I.EQ.MP1) Y2=RKAPM1
1530 Y3=F0(I)-F0(MP1)
1540 PRINT 22,X(I),F0(I),Y1,Y2,Y3
1550 380 CONTINUE
1560 DO 420 J=MP1,MPNP1,NPRINT
1570 Y1=TANARY(I) $ Y2=RKAPARY(I)
1580 IF(I.EQ.MP1) Y1=-QTP
1590 IF(I.EQ.MP1) Y2=RKAPP1
1600 Y3=F0(I)-F0(MP1)
1610 PRINT 22,X(I),F0(I),Y1,Y2,Y3
1620 420 CONTINUE
1630 IF(K107.EQ.ITER1) GO TO 825
1640 IF(IFLGEPF.EQ.0) GO TO 825
1650 DO 140 I=1,MP1
1660 Y1=COSARY(I) $ Y2=X(I) $ Y3=X(I)
1670 IF(I.EQ.MP1) Y1=CCM
1680 Y4=F0(I) $ Y1=PI/Y1
1690 CALL MOD TRAP(FUACT1,XX,FF0,1,MMAXP1,Y1,Y2,Y3,Y4,TOL,ANS1)
1700 IF(I.EQ.1) ANS1=2.*ANS1
1710 IQ1=IMOD
1720 Y1=QCP $ Y1=PI/Y1
1730 CALL MOD TRAP(FUACT1,XX,FF0,MMAXP1,MNTOTP1,Y1,Y2,Y3,Y4,TOL,ANS2)
1740 IF(I.EQ.1) ANS2=2.*ANS2
1750 IQ2=IMOD
1760 ACQ1(I) =2.*Q1*ANS1+2.*Q2*ANS2
1770 CAPE2(I)=RTMU*BETA7*(ANS1+BETA6*ANS2)
1780 ATEST(I,1)=ANS1 $ ATEST(I,2)=ANS2
1790 IF(ISKIP2.NE.0) GO TO 140
1800 PRINT 9,IQ1,IQ2
1810 140 CONTINUE

```

```

1820 DO 150 I=MP2,MPNP1
1830 Y1=OCM          $ Y1=PI/Y1 $ Y2=X(I) $ Y3=X(I) $ Y4=F0(I)
1840 CALL MOD TRAP(FUNCT1,XX,FF0,1,MMAXP1,Y1,Y2,Y3,Y4,TOL,ANS1)
1850 IF(I.EQ,MPNP1) ANS1=2.*ANS1
1860 IQ1=IMOD
1870 Y1=COSAPY(I) $ Y1=PI/Y1
1880 CALL MOD TRAP(FUNCT1,XX,FF0,MMAXP1,MNTOTP1,Y1,Y2,Y3,Y4,TOL,ANS2)
1890 IF(I.EQ,MPNP1) ANS2=2.*ANS2
1900 IQ2=IMOD
1910 ACQ1(I) =2.*Q1*ANS1+2.*Q2*ANS2
1920 CAPF2(I)=PTMU*BETA7*(ANS1+BETA6*ANS2)
1930 ATEST(I,1)=ANS1 $ ATEST(I,2)=ANS2
1940 IF(ISKIP2.NE.0) GO TO 150
1950 PRINT 9,IQ1,IQ2
1960 150 CONTINUE
1970 PRINT 5
1980 DO 160 I=1,MPNP1
1990 Y1=PI $ Y2=0. $ Y3=X(I) $ Y4=F0(I)
2000 ANS1=ANS2=0.
2010 IQ1=IQ2=0
2020 IF(I.EQ,1.OR.I.EQ,MPNP1) GO TO 640
2030 CALL SIM(FUNCT2,XX,FF0,1,MMAXP1,Y3,Y4,TOL,ANS1)
2040 IQ1=ISIM
2050 CALL SIM(FUNCT2,XX,FF0,MMAXP1,MNTOTP1,Y3,Y4,TOL,ANS2)
2060 IQ2=ISIM
2070 640 CALL SIM(FUNCT3,XX,FF0,1,MMAXP1,Y3,Y4,TOL,ANS3)
2080 IQ3=ISIM
2090 CALL SIM(FUNCT3,XX,FF0,MMAXP1,MNTOTP1,Y3,Y4,TOL,ANS4)
2100 IQ4=ISIM
2110 ACQ1(I) =ACQ1(I) +2.*Q1*(ANS1+ANS3) +2.*Q2*(ANS2+ANS4)
2120 CAPF2(I)=CAPF2(I)+PTMU*BETA7*(ANS1+ANS3 +BETA6*(ANS2+ANS4))
2130 ATEST(I,1)=ATEST(I,1)+ANS1+ANS3
2140 ATEST(I,2)=ATEST(I,2)+ANS2+ANS4
2150 IF(ISKIP2.NE.0) GO TO 160
2160 CALL SIM(FUNCT4,XX,FF0,1,MMAXP1,Y3,Y4,TOL,ANS1)
2170 IQ5=ISIM
2180 CALL SIM(FUNCT4,XX,FF0,MMAXP1,MNTOTP1,Y3,Y4,TOL,ANS2)
2190 IQ6=ISIM
2200 ATEST(I,3)=ANS1 $ ATEST(I,4)=ANS2
2210 PRINT 10,IQ1,IQ2,IQ3,IQ4,IQ5,IQ6 ,ATEST(I,1),ATEST(I,3),
2220+ATEST(I,2),ATEST(I,4)
2230 160 CONTINUE
2240 PRINT 5
2250 DO 170 I=1,MPNP1
2260 DO 170 J=1,MPNP1
2270 IF(J.LT,MP1) 600,605
2280 600 UGH1=COSAPY(J) $ UGH2=TANAPY(J) $ UGH3=BKAPARY(J)
2290 AMAT(I,J)=-H1*WGHT(J)*FUNCT5(X(I),X(J),F0(I),F0(J))
2300 GO TO 620
2310 605 IF(J.GT,MP1) 610,615
2320 610 UGH1=COSAPY(J) $ UGH2=TANAPY(J) $ UGH3=BKAPARY(J)
2330 AMAT(I,J)=-H2*WGHT(J)*FUNCT5(X(I),X(J),F0(I),F0(J))
2340 GO TO 620
2350 615 AMAT(I,J)=-FUNCT6(X(I),X(J),F0(I),F0(J),H1,H2,
2360+BKAPMT,BKAPPL)*WGHT(J)
2370 620 IF(I.EQ,J) AMAT(I,J)=AMAT(I,J)+1.
2380 170 CONTINUE
2390 NROW=70 $ NCOL=1 $ IDONT=0
2400 CALL MATALG(AMAT,ACQ1,MPNP1,NCOL,IDONT,DETINT,NROW)
2410 ANS42=0.

```

```

2420 DO 430 I=1,MP1
2430 FLAST(I)=F0(I)
2440 ANS42=ANS42+ACOL(I)*H1*WGHT2(I)
2450 430 CONTINUE
2460 ANS43=0.
2470 DO 440 I=MP1,MPNP1
2480 ANS43=ANS43+ACOL(I)*H2*WGHT2(I)
2490 FLAST(I)=F0(I)
2500 440 CONTINUE
2510 R1XX=RFTA9*DELTA*ANS43+(1.-DELTA)*ANS42
2520 R1XX=-R1XX/((RFTA9+1.)*DELTA*(1.-DELTA))
2530 Y1=RFTA3*DELTA+(1.-DELTA)*RFTA4
2540 Y2=RFTA3*ANS42-RFTA4*RFTA9*ANS43
2550 Y2=Y2+R1XX*(RFTA3*DELTA-RFTA4*RFTA9*(1.-DELTA))
2560 F0(MP1)=PSI*Y2+RFTA3*RFTA5
2570 F0(MP1)=-F0(MP1)*RMU/Y1
2580 FN(1)=0. $ FN(2)=QTM $ FN(3)=F0(MP1) $ FN(4)=RMU
2590 FN(5)=0. $ FN(6)=DELTA $ FN(7)=-1.
2600 FN(8)=PMU*PSI $ FN(9)=FN(10)=0.
2610 FN(11)=R1XX
2620 MRAT=MMAX/M
2630 CALL FNEW(HOLD1,1,MP1,1,MMAXP1,MRAT,FN,CAPF2,ACOL,X,STORF,STOR1)
2640 IF(INPDLG.EQ.1) GO TO 850
2650 DO 390 J=1,MMAXP1
2660 FF0(I)=STORF(MMAXP2-I)
2670 390 CONTINUE
2680 DO 400 I=1,MP1
2690 TANARY(I)=STOR1(MP2-I)
2700 F0(I)=FF0(1+(I-1)*MRAT)
2710 Y1=TANARY(I)**2
2720 COSARY(I)=SQRT(1./(1.+Y1))
2730 Y1=F0(I)
2740 Y1=Y1+PMU*PSI*(ACOL(I)+R1XX)
2750 RKAPARY(I)=Y1/PMU
2760 IF(I.EQ.MP1) RKAPMI=RKAPARY(I)
2770 400 CONTINUE
2780 FN(1)=DELTA $ FN(2)=QTP $ FN(4)=RFTA3*RMU
2790 FN(6)=0. $ FN(7)=1. $ FN(8)=-RFTA9*RMU*PSI
2800 NRAT=MMAX/N
2810 CALL FNEW(HOLD2,MP1,MPNP1,MMAXP1,MNTOTP1,NRAT,FN,CAPF2,ACOL,X,
2820+FF0,TANARY)
2830 IF(INPDLG.EQ.1) GO TO 850
2840 DO 410 J=MP1,MPNP1
2850 TANARY(J)=-TANARY(J)
2860 F0(J)=FF0(MMAXP1+(J-MP1)*NRAT)
2870 Y1=TANARY(J)**2
2880 COSARY(J)=SQRT(1./(1.+Y1))
2890 Y1=F0(J)
2900 Y1=Y1-RFTA9*PMU*PSI*(ACOL(J)+R1XX)
2910 RKAPARY(J)=Y1/PMU/RFTA3
2920 IF(J.EQ.MP1) RKAPPL=RKAPARY(J)
2930 410 CONTINUE
2940 TANARY(MP1)=COSARY(MP1) =RKAPARY(MP1)=0.
2950 F0(MP1)=F0(MP1)
2960 CALL TFRP(FLAST,F0,MPNP1,TOLERR,IFLGERR)
2970 PRINT 27,DETINT,ANS42,ANS43
2980 PRINT 21
2990 DO 230 I=1,MP1,MPRINT
3000 PRINT 8 ,X(I),ACOL(I)
3010 230 CONTINUE

```

```

3020 DO 350 I=MP1,MPNF1,NPRINT
3030 PRINT 8 ,X(I),ACCL(T)
3040 350 CONTINUE
3050 PRINT 5
3060 PRINT 5
3070 810 CONTINUE
3080 850 CONTINUE
3090 PRINT 14
3100 800 CONTINUE
3110 880 CONTINUE
3120 END
3130 SUBROUTINE SPLINE(X,Y,M,XINT,YINT)
3140 DIMENSION X(300),Y(300),C(4,300)
3150 IF (X(1)+Y(M)-ATEP)10,3,10
3160 10 CALL SPLICCN(X,Y,M,C)
3170 ATEP=X(1)+Y(M)
3180 K=1
3190 3 IF (XINT-X(K)) 70,1,2
3200 70 K=1
3210 GO TO 7
3220 1 YINT=Y(1)
3230 RETURN
3240 2 IF (XINT-X(K+1))6,4,5
3250 4 YINT=Y(K+1)
3260 RETURN
3270 5 K=K+1
3280 IF (M-K) 71,71,3
3290 71 K=M-1
3300 GO TO 7
3310 6 IF (XINT-X(K))13,12,11
3320 12 YINT=Y(K)
3330 RETURN
3340 13 K=K-1
3350 GO TO 6
3360 11 YINT=(X(K+1)-XINT)*(C(1,K)*(X(K+1)-XINT)**2+C(3,K))
3370 YINT=YINT+(XINT-X(K))*(C(2,K)*(XINT-X(K))**2+C(4,K))
3380 RETURN
3390 7 CONTINUE
3400 101 FORMAT(8H0XINT = E18.9,32H. OUT OF RANGE FOR INTERPOLATION)
3410 GO TO 11
3420 END
3430 SUBROUTINE SPLICCN(X,Y,M,C)
3440 DIMENSION X(300),Y(300),C(4,300),D(300),P(300),E(300),A(300,3),B(3
3450+00),7(300)
3460 MM=M-1
3470 DO 2 K=1,MM
3480 D(K)=X(K+1)-X(K)
3490 P(K)=D(K)/6.
3500 2 F(K)=(Y(K+1)-Y(K))/D(K)
3510 DO 3 K=2,MM
3520 3 B(K)=E(K)-F(K-1)
3530 A(1,2)=-1.-D(1)/D(2)
3540 A(1,3)=D(1)/D(2)
3550 A(2,3)=P(2)-P(1)*A(1,3)
3560 A(2,2)=2.*(P(1)+F(2))-P(1)*A(1,2)
3570 A(2,3)=A(2,3)/A(2,2)
3580 R(2)=R(2)/A(2,2)
3590 DO 4 K=3,MM
3600 4 A(K,2)=2.*(P(K-1)+P(K))-P(K-1)*A(K-1,3)
3610 B(K)=B(K)-P(K-1)*B(K-1)

```

```

3620 A(K,3)=P(K)/A(K,2)
3630 4 R(K)=R(K)/A(K,2)
3640 Q=D(M-2)/D(M-1)
3650 A(M,1)=1.+Q+A(M-2,3)
3660 A(M,2)=-Q-A(M,1)*A(M-1,3)
3670 R(M)=R(M-2)-A(M,1)*R(M-1)
3680 7(M)=R(M)/A(M,2)
3690 MN=M-2
3700 DO 6 I=1,MN
3710 K=M-I
3720 6 7(K)=R(K)-A(K,3)*7(K+1)
3730 7(1)=-A(1,2)*7(2)-A(1,3)*7(3)
3740 DO 7 K=1,MM
3750 Q=1./(6.*D(K))
3760 C(1,K)=7(K)*Q
3770 C(2,K)=7(K+1)*Q
3780 C(3,K)=Y(K)/D(K)-7(K)*P(K)
3790 7 C(4,K)=Y(K+1)/D(K)-Z(K+1)*P(K)
3800 FND
3810 FUNCTION FUNCT 10(X,G,7,M)
3820 DIMENSION G(130),Z(130)
3830 CALL SPLINE(7,G,M,X,Y)
3840 FUNCT10=Y
3850 END
3860 SUBROUTINE F NEW(H,ILO,IHI,JLO,JHI,NRATIO,A,R,C,D,F,TN)
3870 DIMENSION A(11),Y(2),DY(2),SCRATCH(20),P(130),C(130),D(130)
3880 DIMENSION BN(130),CN(130),DN(130)
3890 DIMENSION F(2050),TN(130)
3900 ERR=1.E-7 $ NEQ=2 $ II=ILO $ X=A(1) $ Y(1)=A(2) $ Y(2)=A(3)
3910 M=IHI-ILO+1 $ HH=H/2. $ NTL=1 $ NPL=0 $ TL=H+A(1)
3920 JJ=JLO
3930 F(JJ)=A(3) $ TN(II)=0.
3940 DO 10 I=1,M
3950 BN(I)=R(I+ILO-1)
3960 CN(I)=C(I+ILO-1)
3970 DN(I)=D(I+ILO-1)
3980 10 CONTINUE
3990 KK=0
4000 110 CALL NOPDSF(KK,X,HH,NEQ,Y,DY,ERR,SCRATCH,NTL,TL,NPL,0.)
4010+,PRTURNS(140)
4020 GO TO (120,110,130)KK
4030 120 DY(1)=SQRT(1.+Y(1)**2)**3/A(4)*(Y(2)+A(5)*FUNCT10(A(6)+A(7)*X
4040+,
4050+BN,DN,M)+A(8)*(FUNCT10(A(6)+A(7)*X,CN,DN,M)+A(9)*(EXP(-A(10)*Y(2)
4060+)-1.)+A(11)))
4070 DY(2)=Y(1) $ GO TO 110
4080 130 JJ=JJ+1
4090 F(JJ)=Y(2)
4100 IF((JJ-JLO)/NRATIO*NRATIO.NE.JJ-JLO) GO TO 20
4110 II=II+1
4120 TN(II)=Y(1)
4130 20 IF(JJ.EQ.JHI) GO TO 140
4140 TL=TL+H $ GO TO 110
4150 140 CONTINUE
4160 END
4170 SUBROUTINE FZERO(H,ILO,IHI,Q,YZERO,YCONST,YARRAY,TOL8)
4180 DIMENSION YARRAY(2050),SCRATCH(10)
4190 ERR=1.E-7 $ NEQ=1 $ II=ILO $ HH=H/2. $ NTL=1 $ NPL=0
4200 TL=H $ Y=YZERO $ X=0. $ YARRAY(II)=YZERO
4210 KK=0

```

```

4220 110 CALL NORDSET(KK,X,HH,NEQ,Y,DY,ERR,SCRATCH,NTL,TL,NPL,0.)
4230+,RETURN(140)
4240 GO TO (120,110,130)KK
4250 120 DY=FUNCTR(Y,YCONST,0) $ GO TO 110
4260 130 II=II+1
4270 YARRAY(II)=Y
4280 IF(II,FO,IHI) GO TO 140
4290 AR=FUNCTR(Y,YCONST,0)
4300 AR=ARS(AR)
4310 IF(AR,LT,TOLR) GO TO 150
4320 TL=TL+H $ GO TO 110
4330 150 JL=II+1
4340 DO 160 J=JL,IHI
4350 YARRAY(J)=Y
4360 160 CONTINUE
4370 140 CONTINUE
4380 END
4390 SUBROUTINE MOD TRAP(F,7,F07,NLO,NHI,C,A,X,F0X,TOL,ANS)
4400 DIMENSION Z(2050),F0Z(2050),AF(2050),ALN(2050)
4410 COMMON/IMOD/IMOD
4420 INC=(NHI-NLO)/2 $ ANS=0. $ ASQ=A**2
4430 IMOD=1
4440 DO 10 I=NLO,NHI,INC
4450 Y1=Z(I) $ Y2=F07(I)
4460 AF(I)=F(X,Y1,F0X,Y2,A,C)
4470 ALN(I)=0.
4480 IF(Y1,NE,A) ALN(I)=ALOG(ABS(Y1-A)*C)
4490 10 CONTINUE
4500 50 NUP=NHI-INC
4510 ANSLAST=ANS
4520 ANS=0.
4530 DO 20 I=NLO,NUP,INC
4540 Y1=AF(I) $ Y2=AF(I+INC)-AF(I) $ Y3=Z(I+INC)-Z(I) $ Y4=Y2/Y3
4550 Y5=((Y1-Y2/Y3*Z(I))*(Z(I+INC)-A)+Y2/Y3/2.*(Z(I+INC)**2-ASQ))
4560+*ALN(I+INC)
4570 Y6=((Y1-Y2/Y3*Z(I))*(Z(I)-A)+Y2/Y3/2.*(Z(I)**2-ASQ))*ALN(I)
4580 Y7=Y1*Y3 $ Y8=Y2/Y3/4.*((Z(I)+A)**2-(Z(I+INC)+A)**2)
4590 Y9=Y2*Z(I)
4600 ANS=ANS+Y5-Y6-Y7+Y8+Y9
4610 20 CONTINUE
4620 IF(INC,FO,(NHI-NLO)/2) GO TO 30
4630 FRR=ARS(ANS-ANSLAST)
4640 IF(ANSLAST,NE,0.) FRR=FRR/ARS(ANSLAST)
4650 IF(NUP,FO,NHI-1,CR,ERR,LE,TOL) GO TO 60
4660 30 NROT=NLO+INC/2
4670 NTOP=NHI-INC/2
4680 IMOD=IMOD+1
4690 DO 40 I=NROT,NTOP,INC
4700 Y1=Z(I) $ Y2=F0Z(I)
4710 AF(I)=F(X,Y1,F0X,Y2,A,C)
4720 ALN(I)=0.
4730 IF(Y1,NE,A) ALN(I)=ALOG(ABS(Y1-A)*C)
4740 40 CONTINUE
4750 INC=INC/2
4760 GO TO 50
4770 60 CONTINUE
4780 END
4790 SUBROUTINE SIM(F,Z,F07,NLO,NHI,X,F0X,TOL,ANS)
4800 DIMENSION Z(2050),F0Z(2050),AF(2050)
4810 COMMON/ISIM/ISIM

```

```

4820 INC=(NHI-NLO)/2 & ANS=0. & H=(7(NHI)-Z(NLO))/2.& HOVR3=H/3.
4830 ISIM=1
4840 DO 10 I=NLO,NHI,INC
4850 AF(I)=F(X,Z(I),FOX,F0Z(I))
4860 10 CONTINUE
4870 50 ANSLAST=ANS
4880 ANS=0. & J=1
4890 DO 20 I=NLO,NHI,INC
4900 W=HOVR3
4910 IF(I.EQ.NLO.OR.I.EQ.NHI) GO TO 25
4920 W=4.*HOVR3
4930 IF(J/2*2.EQ.J) GO TO 25
4940 W=2.*HOVR3
4950 25 ANS=ANS+W*AF(I)
4960 J=J+1
4970 20 CONTINUE
4980 IF(INC.EQ.(NHI-NLO)/2) GO TO 30
4990 FRP=ARS(ANS-ANSLAST)
5000 IF(ANSLAST.NE.0.) FRP=FRP/ARS(ANSLAST)
5010 IF(INC.EQ.1.OR.FRP.LE.TOL) GO TO 60
5020 30 NROT=NLO+INC/2
5030 NTOP=NHI-INC/2
5040 ISIM=ISIM+1
5050 DO 40 I=NROT,NTOP,INC
5060 AF(I)=F(X,Z(I),FOX,F0Z(I))
5070 40 CONTINUE
5080 INC=INC/2 & HOVR3=HOVR3/2.
5090 GO TO 50
5100 60 CONTINUE
5110 END
5120 FUNCTION WGHT(J)
5130 COMMON/WGHTPAC/MP1,MPNP1
5140 WGHT=.5
5150 IF(J.EQ.1.OR.J.EQ.MP1.OR.J.EQ.MPNP1) RETURN
5160 WGHT=1.
5170 END
5180 FUNCTION WGHT2(J)
5190 COMMON/WGHTPAC/MP1,MPNP1
5200 WGHT2=1./3.
5210 IF(J.EQ.1.OR.J.EQ.MP1.OR.J.EQ.MPNP1) RETURN
5220 WGHT2=4./3.
5230 IF(J/2*2.EQ.J) RETURN
5240 WGHT2=2./3.
5250 END
5260 FUNCTION FUNCT1(X,Z,FOX,F0Z,A,C)
5270 COMMON/BLK1/PI
5280 FUNCT1=-1./PI
5290 IF(X.EQ.Z) RETURN
5300 Y1=2.*COSHF(PI*(FOX-F0Z)) & Y2=2.*COS(PI*(X-Z))
5310 Y3=-1./2./PI*ALOG(Y1-Y2)
5320 FUNCT1=Y3/ALOG(APS(Z-A)*C)
5330 END
5340 FUNCTION FUNCT2(X,Z,FOX,F0Z)
5350 COMMON/BLK1/PI
5360 Y1=2.*COSHF(PI*(FOX-F0Z)) & Y2=2.*COS(PI*(X+Z))
5370 Y3=-1./2./PI*ALOG(Y1-Y2)
5380 FUNCT2=Y3
5390 END
5400 FUNCTION COSHF(X)
5410 COSHF=(EXP(X)+EXP(-X))/2.
5420 END

```

```

5430 FUNCTION SINHF(X)
5440 SINHF=(EXP(X)-EXP(-X))/2.
-----
5450 FND
5460 FUNCTION FUNCT3(X,Z,F0X,F0Z)
5470 FUNCT3=F0Z-F0X
-----
5480 END
5490 FUNCTION FUNCT4(X,Z,F0X,F0Z)
5500 COMMON/RLK1/PI
5510 FUNCT4=F0Z-F0X
5520 IF(Z.F0.0..AND.X.EQ.0.) RETURN
5530 IF(Z.F0.1..AND.X.EQ.1.) RETURN
5540 Y1=2.*COSHF(PI*(F0X-F0Z)) $ Y2=2.*COS(PI*(X+Z))
5550 FUNCT4=FUNCT4-1./2./PI*ALOG(Y1-Y2)
5560 IF(X.EQ.Z) RETURN
5570 Y3=2.*COS(PI*(X-Z))
5580 FUNCT4=FUNCT4-1./2./PI*ALOG(Y1-Y3)
5590 FND
-----
5600 FUNCTION FUNCT5(X,Z,F0X,F0Z)
5610 COMMON/RLK1/PI
5620 COMMON/FSPACK/CS,TN,BK
5630 FUNCT5=1./PI/CS*PK+1.
5640 IF(Z.F0.0..AND.X.EQ.0.) RETURN
5650 IF(Z.F0.1..AND.X.EQ.1.) RETURN
5660 Y1=SINHF(PI*(F0X-F0Z)) $ Y2=TN*SIN(PI*(X+Z))
5670 Y3=COSHF(PI*(F0X-F0Z)) $ Y4=COS(PI*(X+Z))
5680 FUNCT5=1./PI/2./CS*PK+1.+(Y1-Y2)/(Y3-Y4)/2.
5690 IF(X.EQ.Z) RETURN
5700 Y5=TN*SIN(PI*(X-Z)) $ Y6=COS(PI*(X-Z))
5710 FUNCT5=(Y1-Y2)/(Y3-Y4)/2.+(Y1+Y5)/(Y3+Y6)/2.+1.
5720 FND
5730 FUNCTION FUNCT6(X,Z,F0X,F0Z,H1,H2,PKAPM1,BKAPPL)
5740 COMMON/TRIG/QCM,GCP,QTM,QTP
5750 COMMON/RLK1/PI
5760 Y1=SINHF(PI*(F0X-F0Z)) $ Y2=SIN(PI*(X+Z))
5770 Y3=QTM $ Y4=-QTP $ Y5=COSHF(PI*(F0X-F0Z))
5780 Y6=COS(PI*(X+Z))
5790 FMI=(Y1-Y3*Y2)/(Y5-Y6)/2.+1
5800 FPL=(Y1-Y4*Y2)/(Y5-Y6)/2.+1.
5810 IF(X.NE.Z) GO TO 10
5820 Y7=1./2./PI/QCM*PKAPM1
5830 Y8=1./2./PI/QCP*BKAPPL
5840 FMI=FMI+Y7 $ FPL=FPL+Y8
5850 FUNCT6=H1*FMI+H2*FPL
5860 RETURN
5870 10 Y7=SIN(PI*(X-Z)) $ Y8=COS(PI*(X-Z))
5880 FMI=FMI+(Y3*Y7+Y1)/(Y5-Y8)/2.
5890 FPL=FPL+(Y4*Y7+Y1)/(Y5-Y8)/2.
5900 FUNCT6=H1*FMI+H2*FPL
5910 FND
5920 FUNCTION FUNCT8(Y,YC,0)
5930 A1=(1.-1./2./0*(Y**2-YC**2))**2
5940 IF(A1.GT.1.) A1=1.
5950 FUNCT8=SQRT(1./A1-1.)
5960 FND
5970 SUBROUTINE NORDSET (K,T,H,N,Y,F,DELTAY,R,NTL,TL,NPL,PL)
5980+.RETURNS(ASP1)
-----
5990**C
6000**C K CONTROL INTEGER FOR USER STATEMENTS INTEGE
6010**C T INDEPENDENT VARIABLE REAL
6020**C H INTEGRATION STEP SIZE REAL

```



```

6630 3001 ASSIGN 3002 TO KFLIP
6640 GO TO 1002
6650 3002 CONTINUE
6660 T LEFT=T
6670 IF(NPL.EQ.0) GO TO 5050
6680 DO 3004 J=1,NPL
6690 PLFFT(J)=PL(J)
6700 IF(PL(J).EQ.0.)3003,3004
6710 3003 ASSIGN 3004 TO KFLIP
6720 GO TO 1003
6730 3004 CONTINUE
6740 5050 CONTINUE
6750 DO 3010 I=1,N
6760 3010 R(9,I)=Y(I)
6770 D1=-1.
6780 ASSIGN 3100 TO ISFCUR
6790 GO TO 1400
6800 3020 I=STEP.AND.3
6810 IF(I.NE.0) GO TO 2000
6820 I=STEP/4
6830 GO TO (3030,3050,3030,3080,3030,3040) I
6840 3030 D1=-1.
6850 ASSIGN 2000 TO ISFCUR
6860 GO TO 1400
6870 3040 D1=2.
6880 HMAX=HMIN=-H
6890 ASSIGN 3050 TO ISFCUR
6900 GO TO 1400
6910 3050 DO 3060 I=1,N
6920 Y(I)=R(9,I)
6930 3060 R(10,I)=0.0
6940 3070 ASSIGN 3030 TO KFLIP
6950 GO TO 1000
6960 3080 D1=.5
6970 ASSIGN 3090 TO ISFCUR
6980 GO TO 1400
6990 3090 IF(HALVE)3100,3050
7000 3100 STEP=0
7010 DO 3110 I=1,N
7020 3110 R(1,I)=R(2,I)=R(3,I)=R(4,I)=0.0
7030 GO TO 3050
7040**C
7050**C CONTROL SECTION FOR TIME INTERRUPTS DURING NORMAL INTEGRATION
7060**C STATEMENT 1700 INTEGRATES FORWARD,RETURNING TO
7070**C
7080 1700 GO TO 1600
7090 1701 DO 1702 I=1,N
7100 R(6,I)=Y(I)
7110 1702 R(8,I)=F(I)
7120 TSAVE=T
7130 1703 Z=2.*TSAVE
7140 DO 1705 I=1,NTL
7150 IF (TL(I).LT.Z) 1704,1705
7160 1704 Z=TL(I)
7170 J=I
7180 1705 CONTINUE
7190 IF (Z.GF.TSAVE) GO TO 1707
7200 ASSIGN 1706 TO KFLIP
7210 RTEST=TSAVE/Z
7220 RTEST=RTEST.AND..NOT.3

```

```

7230 IF (RTEST.FO.1.0) 17051,17053
7240 17051 DO 17052 I=1,N
7250 17052 Y(I)=B(6,I)
7260 T=TSAVE
7270 GO TO 1001
7280 17053 HP=Z-TSAVE
7290 ASSIGN 1001 TO ISTWO
7300 GO TO 1200
-----
7310 1706 ASSIGN 1703 TO KFLIP
7320 ASSIGN 1002 TO ISTHREE
7330 GO TO 1300
-----
7340 1707 DO 1708 I=1,N
7350 F(I)=R(8,I)
7360 1708 Y(I)=R(6,I)
-----
7370 T=TSAVE
7380 ASSIGN 1300 TO KFLIP
7390 ASSIGN 1709 TO ISTHREE
7400 GO TO 1001
7410 1709 RTEST=Z/T
7420 RTEST=RTEST.AND..NOT.3
-----
7430 IF (RTEST.EQ.1.0) 1710,1711
7440 1710 ASSIGN 1711 TO KFLIP
7450 GO TO 1002
7460 1711 IF(NPL.EQ.0) GO TO 5060
7470 DO 1712 I=1,NPL
7480 1712 FIND(I)=.FALSE.
7490 5060 CONTINUE
7500 GO TO 1700
7510**C
7520**C      INTEGRATE ONE STEP
7530**C
7540**C      SAVE CONDITIONS AT START OF STEP
7550**C
7560 2000 DO 2010 I=1,N
7570 R(6,I)=Y(I)
7580 R(7,I)=R(10,I)
7590 2010 R(8,I)=F(I)
7600 TSTART=T
7610**C
7620**C      ENTRY FOR HALVED STEP
7630**C
7640 2020 T=T+H
7650 DO 2030 I=1,N
7660 Z=0
-----
7670 Y(I)=R(6,I)+DELY(I)
7680 2030 R(5,I)=F(I)+(2.*R(1,I)+(3.*R(2,I)+(4.*R(3,I)+5.*R(4,I))))
7690**C
7700**C      ITERATE TWICE,DEVELOP TEST PARAMETERS
7710**C
7720 HALVF=.FALSE.
7730 DOURLF=.TRUE.
7740 TEST(1)=TEST(2)=0.
7750 DO 2070 J=1,2
7760 ASSIGN 2040 TO KFLIP
7770 GO TO 1000
7780 2040 DO 2070 I=1,N
7790 Z=F(I)-R(5,I)
7800 IF(J.FO.2) 2050,2060
7810 2050 Z7=ABS(Z*H)
7820 RTEST=DELTAY*ABS(Y(I))

```

```

7830 IF (Z.GT.RTEST) HALVF=.TRUE.
7840 IF (Z.GT.RTEST*.015625) DOURLF=.FALSE.
7850 2060 DPTA(1)=B(6,I)
7860 DPTA(2)=R(7,I)
7870 Z=Z*.329861111111
7880 DPTFMA=DPTFMA+DELY(I)
7890 Z=ABS(DPTA(1)-Y(I))
7900 IF (Z.GT.TEST(J)) TEST(J)=Z
7910 Y(I)=DPTA(1)
7920 R(10,I)=DPTA(2)
7930 2070 CONTINUE
7940**C
7950**C CHECK TEST PARAMETERS,BUMP COUNT OF INTEGRATION STEPS
7960**C
7970 STEP=STEP+1
7980 IF (STEP.GT.1.AND.STEP.LT.25) GO TO 1100
7990 IF (R.*TEST(2).GT.TEST(1).AND..NOT.DOUBLE) GO TO 1500
8000 IF (R.*TEST(2).GT.TEST(1)) DOURLF=.FALSE.
8010 IF (STEP.EQ.1) GO TO 1100
8020 IF (HALVF) 1500,1100
8030**C
8040**C UPDATE POLTIME,RETURNS TO 3020 IF STARTING - 1701 OTHERWISE
8050**C
8060 1100 DO1101 I=1,N
8070 Z=F(I)-R(5,I)
8080 R(1,I)=R(1,I)+(3.*R(2,I)+(6.*R(3,I)+(10.*R(4,I)+Z/.96)))
8090 R(2,I)=R(2,I)+(4.*R(3,I)+(10.*R(4,I)+Z*.4861111111))
8100 R(3,I)=R(3,I)+(5.*R(4,I)+Z/.6)
8110 1101 R(4,I)=R(4,I)+Z/120.
8120 IF (STEP.LE.24) GO TO 3020
8130 IF (F.GT.HMAX) HMAX=F
8140 IF (F.LT.HMIN) HMIN=F
8150 GO TO 1701
8160**C
8170**C ROUTINE TESTPHI,FALSE EXIT IS 1300,TRUE EXIT IS 1800
8180**C
8190 1300 IF (NPL.EQ.0) GO TO 5070
8200 DO 1301 I=1,NPL
8210 IF (FIND(I)) GO TO 1301
8220 IF (PL(I)*PLEFT(I).LT.0) GO TO 1303
8230 1301 CONTINUE
8240 5070 CONTINUE
8250 IF (NPL.EQ.0) GO TO 5080
8260 DO 1302 I=1,NPL
8270 1302 PLEFF(I)=PL(I)
8280 5080 CONTINUE
8290 TLEFT=T
8300 GO TO Isthree(1002,1709,1800)
8310 1303 IF (NPL.EQ.0) GO TO 5090
8320 DO 1304 I=1,NPL
8330 1304 PRITE(I)=PL(I)
8340 5090 CONTINUE
8350 TRITE=T
8360 GO TO 1800
8370**C
8380**C DEPENDENT VARIABLE SEARCH PROCEDURE,ENTERED IF PL(I) CHANGES
8390**C
8400 1800 Z=0.0
8410 IF (NPL.EQ.0) GO TO 5100
8420 DO 1802 I=1,NPL

```

```

0430 IF (FIND(I)) GO TO 1802
0440 IF (PRITE(I).FO.0) PLFFT(I)=0
0450 ZZ=PLFFT(I)/PRITE(I)
0460 IF (ZZ.LE.Z) 1801,1802
0470 1801 Z=ZZ
0480 J=I
0490 1802 CONTINUE
0500 S100 CONTINUE
0510 HP=(TRITE-TSAVE)-(TRITE-TLFFT)/(I.-Z)
0520 IF ((TSAVE+HP).FG.T.OR.Z.FO.0) 1803,1804
0530 1803 ASSIGN 1703 TO KFLIP
0540 FIND(J)=.TRUE.
0550 GO TO 1003
0560 1804 ASSIGN 1001 TO ISTWO
0570 ASSIGN 1300 TO KFLIP
0580 ASSIGN 1800 TO IS THRE
0590 GO TO 1200
0600**C
0610**C CHECK FOR DOUBLE OF STEP SIZE
0620**C
0630 1600 IF(DOUBLE) 1601,2000
0640 1601 N1=2.
0650 ASSIGN 2000 TO ISFOUR
0660 GO TO 1400
0670**C
0680**C SUBROUTINE CALLS, ASSUMES KFLIP SET PRIOR TO ENTRY
0690**C
0700 1000 K=1
0710 IDER=IDER+1
0720 RETURN
0730 1001 K=2
0740 IFOS=IFOS+1
0750 RETURN
0760 1002 K=J+2
0770 ILL=ILL+1
0780 RETURN
0790 1003 K=J+NTL+2
0800 IPL=IPL+1
0810 RETURN
0820**C
0830**C SUBROUTINE TO CHANGE STEP SIZE
0840**C
0850 1400 H=H*D1
0860 N2=N1*D1
0870 N3=D2*D1
0880 N4=D3*D1
0890 N0 1401 I=1,N
0900 R(1,I)=R(1,I)*D1
0910 R(2,I)=R(2,I)*D2
0920 R(3,I)=R(3,I)*D3
0930 1401 R(4,I)=R(4,I)*D4
0940 GO TO ISFOUR(3100,2000,3050,3090,2020)
0950**C
0960**C ROUTINE TO PREDICT INTERMEDIATE VALUES OF Y(I)
0970**C
0980 1200 T=TSAVE+HP
0990 D1=HP/H
0900 N2=D1*D1
0910 N3=D2*D1
0920 N4=D3*D1

```

```

9030 DO 1201 I=1,N
9040 1201 Y(I)=R(6,I)+I*P*(R(8,I)+(D1*R(1,I)+(D2*R(2,I)+(D3*R(3,I)+D4*R(
9041)+4
9050+,I
9060+))))))
9070 GO TO ISTWO(1001)
9080**C
9090**C RESTORE I,Y,F. HALVE STEP SIZE, TRY STEP AGAIN
9100**C
9110 1500 RTEST=H/2
9120 IF(T.FO.(T+RTEST)) 5030,5040
9130 5030 PRINT 55020
9140 INRDFLG=1
9150 RETURN ASP1
9160 5040 CONTINUE
9170 STEP=STEP-1
9180 T=TSTART
9190 DO 1501 I=1,N
9200 Y(I)=R(6,I)
9210 R(10,I)=R(7,I)
9220 1501 F(I)=R(8,I)
9230 D1=.5
9240 ASSIGN 2020 TO ISFOUR
9250 GO TO 1400
9260 FND .
9270 SUBROUTINE MATALG (A,X,NR,NV,IDO,DET,NACT)
9280 DIMENSION A(NACT,NACT),X(NACT,NACT)
9290 IF(IDO) 1,2,1
9300 1 DO 3 I=1,NR
9310 DO 4 J=1,NR
9320 4 X(I,J)=0.0
9330 3 X(I,I)=1.0
9340 NV=NR
9350 2 DET=1.0
9360 NR1=NR-1
9370 DO 5 K=1,NR1
9380 IR1=K+1
9390 PIVOT=0.0
9400 DO 6 I=K,NR
9410 7=A(6,I,K)
9420 IF(7-PIVOT) 6,6,7
9430 7 PIVOT=7
9440 IPP=I
9450 6 CONTINUE
9460 IF(PIVOT) 8,9,8
9470 9 DET=0.0
9480 RETURN
9490 8 IF(IPR-K) 10,11,10
9500 10 DO 12 J=K,NR
9510 7=A(IPR,J)
9520 A(IPR,J)=A(K,J)
9530 12 A(K,J)=7
9540 DO 13 J=1,NV
9550 7=X(IPR,J)
9560 X(IPR,J)=X(K,J)
9570 13 X(K,J)=7
9580 DET=-DET
9590 11 DET=DET*A(K,K)
9600 PIVOT=1.0/A(K,K)
9610 DO 14 J=IR1,NR

```

```

0620 A(K,J)=A(K,J)*PIVOT
0630 DO 14 I=IR1,NR
0640 14 A(I,J)=A(I,J)-A(I,K)*A(K,J)
0650 DO 5 J=1,NV
0660 IF(X(K,J)) 15,5,15
0670 15 X(K,J)=X(K,J)*PIVOT
0680 DO 16 J=IR1,NR
0690 16 X(I,J)=X(I,J)-A(I,K)*X(K,J)
0700 5 CONTINUE
0710 IF(A(NR,NR)) 17,9,17
0720 17 DET=DET*A(NR,NR)
0730 PIVOT=1./A(NR,NR)
0740 DO 18 J=1,NV
0750 X(NR,J)=X(NR,J)*PIVOT
0760 DO 18 K=1,NR1
0770 J=NR-K
0780 SUM=0.0
0790 DO 19 L=I,NR1
0800 19 SUM=SUM+A(I,L+1)*X(L+1,J)
0810 18 X(I,J)=X(I,J)-SUM
0820 END
0830 SUBROUTINE TERR(A,P,N,TOL,TERR)
0840 DIMENSION A(70),P(70)
0850 IERR=0
0860 DO 10 I=1,N
0870 Y1=ABS(A(I)-P(I))
0880 IF(A(I).NE.0) Y1=Y1/ABS(A(I))
0890 IF(Y1.GT.TOL) GO TO 20
0900 10 CONTINUE
0910 RETURN
0920 20 IERR=1
0930 END

```

